universität wien

DISSERTATION

Titel der Dissertation

„FACS purification and transcriptome analysis of *Drosophila* neural stem cells reveals a role for Klumpfuss in self-renewal“

Verfasserin

Heike Harzer, Diplombiochemikerin

angestrebter akademischer Grad

Doktorin der Naturwissenschaften (Dr.rer.nat.)

Wien, 2012

Studienkennzahl lt. Studienblatt:	A 091 490
Dissertationsgebiet lt. Studienblatt:	Dr.-Studium der Naturwissenschaften Molekulare Biologie
Betreuerin / Betreuer:	Dr. Jürgen A. Knoblich

Table of Contents

1 SUMMARY

Stem cells need to control the balance between self-renewal and differentiation in order to generate correct lineages. Defects in this balance can lead to either tissue degeneration or formation of tumors. Asymmetrically dividing *Drosophila* larval neuroblasts have emerged as a model to study how stem cells maintain their self-renew capacity and give rise to their specific lineages.

Drosophila larval neuroblasts are ideal for genetic analysis but are limited by the lack of cell-type specific gene expression data. Here, we describe methodology to isolate large numbers of neuroblasts and their differentiated neuronal progeny by fluorescence-activated cell sorting (FACS). With immunofluorescent stainings and gene expression analysis for known neuroblast and neuronal markers we prove the identity and purity of the sorted cell populations. We show that neuroblasts retain both cell cycle and lineage characteristics with live-imaging experiments and determine the transcriptional profiles of neuroblasts and neurons by mRNA sequencing. We identify 28 predicted neuroblast specific transcription factors and arrange them in a network based on their co-expression in numerous *Drosophila* tissues. The network contains hubs for Notch-signaling, growth control and chromatin regulation, and all these processes have been shown to be involved in neuroblast identity.

Over-expression experiments for the neuroblast specific transcription factors identify Klumpfuss as a new regulator of self-renewal. Klumpfuss is expressed in primary type I and type II neuroblasts and in mature intermediate neural progenitors (INPs) in type II lineages, but not in immature INPs and ganglion mother cells (GMCs). Continued expression of Klumpfuss in immature INPs results in their de-differentiation into type II neuroblast-like cells and formation of transplantable brain tumors. Presence of Klumpfuss protein in GMCs does not cause their reversion into ectopic neuroblasts. Loss of Klumpfuss function causes shrinkage and loss of almost all type II and to some extend type I neuroblasts.

To elucidate how cell fate determinants establish a differentiation cell fate in GMCs we separated type I neuroblasts and their daughter cells at different time-points of GMC maturation by FACS. We analyzed expression levels of the 28 neuroblast specific transcription factors in a time-course ranging from neuroblasts, GMCs during different stages of maturation to terminally differenitiated neurons. For some transcription factors we observe an increase of transcript levels in GMCs just after neuroblast division, while known neuroblast fate determinants show a decrease of expression in GMCs only at the time-point of the second neuroblast division. Identification of downstream targets of cell fate and neuroblast fate determinants in neuroblasts and GMCs by loss of function experiments will enable us to build a transcriptional network aiding to explain self-renewal maintenance in neuroblasts and establishment of differentiation in GMCs.

2 ZUSAMMENFASSUNG

Stammzellen sind in der Lage, differenzierende und regenerierende Tochterzellen zu produzieren, wobei das Gleichgewicht zwischen Selbsterneuerung und Differenzierung strikt kontrolliert werden muss. Jede Störung kann entweder zur Degeneration von Geweben oder zur Entstehung von Tumoren führen. Aus diesem Grund ist es wichtig, jene grundlegenden Mechanismen zu verstehen, welche die Balance zwischen Stammzellregeneration und Differenzierung kontrollieren. Dafür nutzen wir in dieser Studie neuronale Stammzellen, sogenannte Neuroblasten, aus dem larvalen Nervensystem der Fruchtfliege *Drosophila melanogaster*.

Neuroblasten teilen sich asymmetrisch in eine größere, sich selbst erneuernde Stammzelle und eine kleinere differenzierende Zelle, die Ganglion-Mutterzelle (GMC). Während der Zellteilung akkumulieren Zellschicksaldeterminanten an einer Seite der Stammzelle und werden ausschließlich in die GMC segregiert, wo sie ein Differenzierungsprogramm einleiten.

Larvale Neuroblasten sind gut geeignet, um genetische Interaktionen zwischen verschiedenen Proteinen zu untersuchen, allerdings ist nicht viel darüber bekannt, welche spezifischen Proteine in den unterschiedlichen neuronalen Zelltypen exprimiert sind. In dieser Studie beschreiben wir eine Methode, um eine große Anzahl von Neuroblasten sowie ihre differenzierten neuronalen Tochterzellen mittels Fluorescence-activated cell sorting (FACS) aus larvalen Gehirnen zu isolieren. Wir zeigen mit Hilfe von Immunfluoreszenz sowie Expressionsanalysen, dass die sortierten Zellen die korrekte Identität besitzen und die Zellpopulationen nicht mit anderen neuronalen Zelltypen kontaminiert sind. Desweiteren teilen sich die isolierten Neuroblasten in Kultur entsprechend ihrem Verhalten *in vivo* asymmetrisch und mit ähnlicher Zellzyklusdauer. Die Transkriptomanalyse von Neuroblasten und Neuronen mittels mRNA Sequenzierung ergibt 28 Transkriptionsfaktoren, die im Vergleich zu Neuronen stark in Neuroblasten exprimiert sind. Diese Transkriptionsfaktoren können in einem Netzwerk angeordnet werden, welches auf deren Co-expression in verschiedenen *Drosophila* Geweben basiert. Dieses Netzwerk enthält Knotenpunkte mit Genen, die wichtige Prozesse in der Stammzelle steuern, wie den Notch Signaltransduktionsweg, die Kontrolle des Wachstums und Chromatinremodellierung.

Die Überexpression dieser Neuroblasten-spezifischen Transkriptionsfaktoren identifiziert Klumpfuss als bisher unbekannten Regulator für die Selbsterneuerung von Neuroblasten. Klumpfuss ist in primären Typ I und II Neuroblasten sowie in gereiften intermediären Vorläufernervenzellen der Typ II Zelllinie exprimiert. Das Protein kann nicht in den direkten Nachkommen der Typ I und II Neuroblasten, den GMCs sowie unreifen intermediären Vorläufernervenzellen, detektiert werden. Wenn Klumpfuss in unreifen intermediären Vorläufernervenzellen dauerhaft exprimiert bleibt, differenzieren diese Zellen zurück zu Typ II Neuroblasten. Dies hat die Entstehung von Hirntumoren zur Folge, aus denen Teile entnommen und in andere Gewebe der Fliege transplantiert werden können wo sie erneut Tumore bilden. Dieses Phänomen kann nicht beobachtet werden, wenn Klumpfuss weiterhin in GMCs vorhanden bleibt. Ein Verlust von Klumpfuss in Neuroblasten hat den Verlust sowie das Schrumpfen von fast allen Typ II und einigen Typ I Neuroblasten zur Folge.

Um herauszufinden, wie die Zellschicksaldeterminanten ein Differenzierungsprogramm etablieren, indem sie Stammzellfaktoren wie beispielsweise Klumpfuss herunter regulieren und Differenzierungsfaktoren anschalten, separierten wir Neuroblasten und GMCs zu unterschiedlichen Zeitpunkten ihres Reifungsprozesses mittels FACS. Wir analysierten die Expression der 28 Neuroblasten-spezifischen Transkriptionsfaktoren in einer Zeitreihe von Neuroblasten, unterschiedlich alten Ganglion-Mutterzellen sowie terminal differenzierten Neuronen. Für einige dieser Transkriptionsfaktoren konnten wir einen Anstieg ihrer Expression in GMCs bereits kurz nach der Zellteilung beobachten, während die Expression bekannter Neuroblastenfaktoren erst um den Zeitpunkt der zweiten Neuroblastenteilung herum stark sinkt. Die Identifizierung der Zielgene der Zellschicksal- und Neuroblastendeterminanten mittels knock down Experimenten wird es uns ermöglichen, ein transkriptionelles Netzwerk zu erstellen, welches helfen kann zu erklären, wie Selbsterhaltung der Neuroblasten sowie Differenzierung in GMCs funktionieren.

3 GENERAL INTRODUCTION

3.1 STEM CELLS AND ASYMMETRIC CELL DIVISION

Stem cells play an important role during development, when an entire organism with a vast number of different cell types is generated. Stem cells also replace damaged or dying cells during tissue homeostasis in the adult. For this, stem cells have to remain in an undifferentiated state and maintain their identity over a series of cell divisions. At the same time, stem cells need to generate more differentiated daughter cells that ultimately undergo terminal differentiation (Figure 1A).

In order to generate different cell types, stem cells have to divide in an asymmetric fashion giving rise to a self-renewing cell, as well as a daughter cell that differs from the stem cell in for example gene expression, morphology or developmental potential (Horvitz and Herskowitz, 1992). Asymmetric cell division can be initiated by either extrinsic or intrinsic mechanisms (Horvitz and Herskowitz, 1992). For the extrinsic mechanism, stem cells receive self-renewal signals from the surrounding cells, the so-called stem cell niche (Figure 1B). These signals keep the stem cell in a self-renewing state and set up the axis of polarity and cell division. The daughter cell intended for differentiation then divides away and looses contact with the stem cell niche, and will therefore receive less self-renewing signaling cues allowing it to differentiate. The extrinsic mechanism is more commonly used in adult stem cells, for example as a response to environmental stress or diseases, since it can be adapted by changing the angle of cell division. This would lead to two daughter cells that stay in contact with the niche and will become stem cells (reviewed in (Knoblich, 2008)). For the intrinsic mechanism (Figure 1C), cell fate determinants get segregated asymmetrically into only one of the two daughter cells, and the cell receiving these determinants undergoes differentiation. A pre-defined developmental program usually regulates this mechanism, and thereby confers a high level of rigidity.

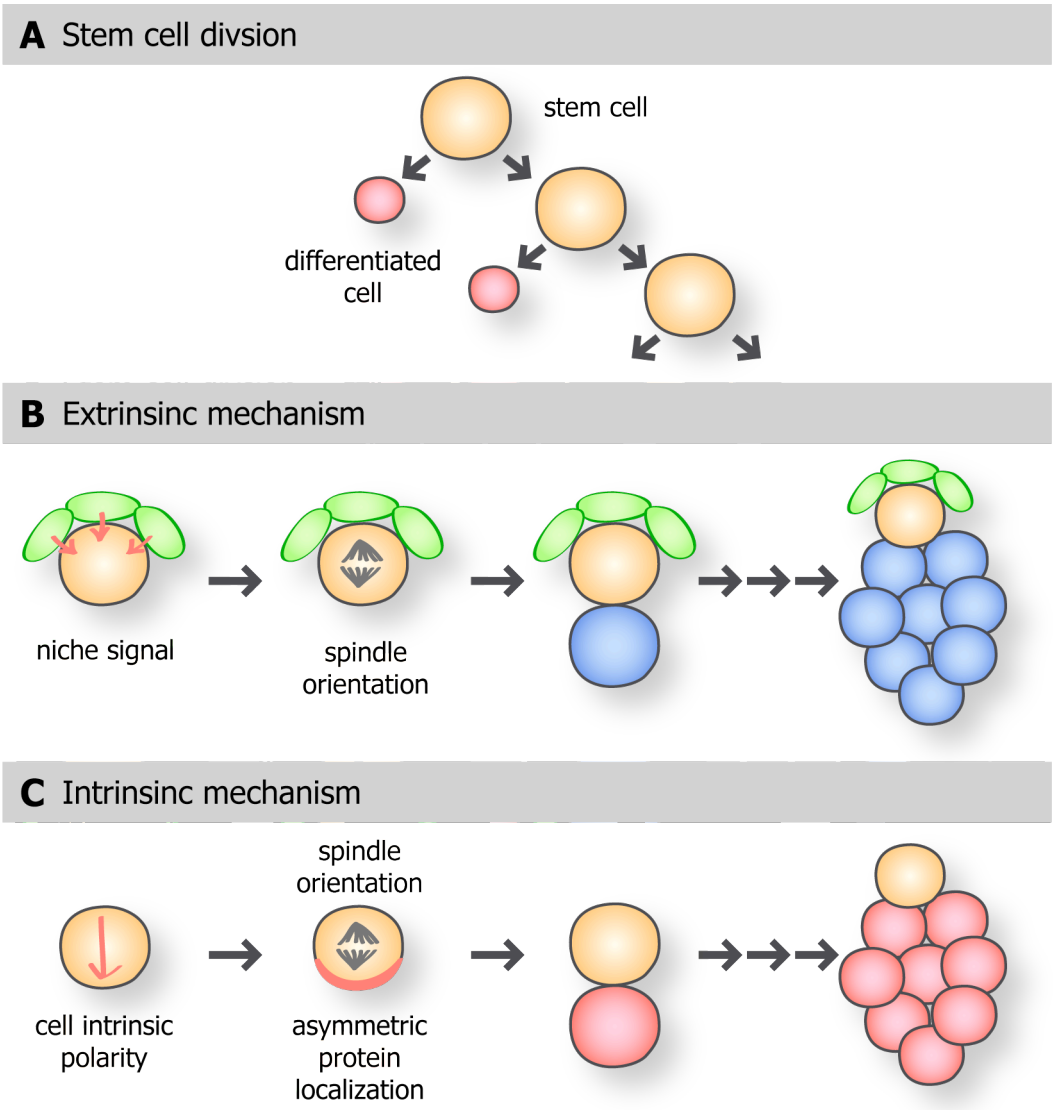

Figure 1. Stem cell division and modes of asymmetric cell division
(A) Stem cells divide asymmetrically giving rise to a more differentiated and a self-renewing daughter cell. **(B)** In an extrinsic mechanism, the stem cell (green) receives a signal from the surrounding niche (yellow) to maintain its self-renewal capacity and establish an axis of polarity. The daughter cell destined to differentiate (blue) has to divide away from the stem cell niche to establish a different fate. **(C)** Cells that divide via an intrinsic mechanism set up an axis of polarity during interphase. During mitosis the intrinsic polarity causes orientation of the spindle and asymmetric localization of certain proteins. Only one of the two daughter cells will receive these fate determinants and will adopt a different fate. (Figure 1B and C adapted from (Knoblich, 2008))

The fruitfly *Drosophila melanogaster* is one of the best-understood model systems for asymmetric cell division. Several stem cell populations, some dividing by an extrinsic (germ line stem cells, reviewed for example in (Spradling *et al.*, 2011)), others by an intrinsic mechanism (neuroblasts (NBs), reviewed for example in (Knoblich, 2008)), have been identified and studied in great detail. Embryonic and especially larval NBs, which give rise to all the different cell types found in a *Drosophila* brain, have proven to be a great model system to study stem cell biology (reviewed in (Knoblich, 2010; Technau *et al.*, 2006; Wu *et al.*, 2008; Doe, 2008)).

3.2 *DROSOPHILA* NEUROBLASTS – ORIGEN AND TYPES

3.2.1 *Drosophila* brain development

During early development the embryonic ectoderm is determined by early patterning genes to be either neurogenic or non-neurogenic. Within the neuroectoderm, future NBs are selected by lateral inhibition, a process involving Notch/Delta signaling that specifies the expression of proneural genes in individual cells (reviewed in (Skeath and Thor, 2003; Technau *et al.*, 2006)). NBs delaminate, and start to divide asymmetrically giving rise to a self-renewing NB and a ganglion mother cell (GMC). The GMC divides once more to produce neurons or glia. Embryonic NBs can divide up to 18 times. NBs decrease in size after each division and by the end of embryonic development either die, or become quiescent. Quiescent NBs start re-growing and dividing again from late first and second instar larval stages ((Ito and Hotta, 1992), reviewed in (Wu *et al.*, 2008)). Re-entering the cell cycle is orchestrated by a series of events. In larval stages the animal starts feeding, and amino acid intake activates Target of rapamycin (TOR) signaling in the fat body, the *Drosophila* equivalent to the mammalian liver. The fat body then releases a signal, possibly the cytokine Unpaired 2 (Rajan and Perrimon, 2012), which is sensed by glia cells and activates Phosphatidylinositol 3-kinase (PI3K) and TOR signaling and causes Insulin-like peptide (ILP) secretion. ILPs then trigger PI3K and TOR signaling in quiescent NBs, which results in re-activation of their cell cycle (Sousa-Nunes *et al.*, 2011; Chell and Brand, 2010). Unlike embryonic NBs, larval NBs re-grow to their original size after each cell division and can divide hundreds of times.

NBs undergo a series of temporal identities governed by the presence of certain TFs during embryonic and larval stages. Different identities lead to the generation of specific progeny from each NB at a specific time point during development (Isshiki *et al.*, 2001; Maurange *et al.*, 2008). It was shown that thoracic NBs cease to divide and differentiate terminally at 20-30 hours after puparium formation (APF) (Ito and Hotta, 1992; Maurange *et al.*, 2008). Therefore, two waves of neurogenesis, one during embryogenesis and one during larval and early pupa stages, generate all the neurons found in the adult *Drosophila* central nervous system.

3.2.2 *Drosophila* larval neuroblasts

The larval brain can be subdivided into three parts: the optic lobes, the central brain and the VNC. Two types of central brain NBs can be distinguished based on their division mode (Bello *et al.*, 2008; Bowman *et al.*, 2008; Boone and Doe, 2008) (Figure 2A). Approximately 180 type I NBs can be found in the larval central brain (Urbach and Technau, 2003). They are characterized by the expression of the transcription factors (TFs) Deadpan (Dpn), Asense (Ase) (Bowman *et al.*, 2008) and Prospero (Pros), which is retained in the cytoplasm (Figure 2B, left). Like embryonic NBs, type I NBs divide into a larger cell that maintains NB properties and into a smaller GMC, which shows nuclear localization of the TF Pros, and generates two Pros positive postmitotic neurons and/ or glia.

The 16 type II NBs, which are located in the dorsoposterior region of the brain, do not express Ase and Pros, but also divide asymmetrically into a self-renewing NB and a smaller intermediate neural progenitor (INP) cell (Figure 2B, right) (Bowman *et al.*, 2008). The INP undergoes a maturation phase and first turns on Ase, followed by the re-expression of Dpn, and cytoplasmic Pros. INPs have the capacity to divide asymmetrically multiple times generating Ase and Pros positive GMCs, which then give rise to Pros positive neurons and/ or glia cells through a terminal division (Izergina *et al.*, 2009; Boone and Doe, 2008; Bowman *et al.*, 2008). This modified lineage allows type II NBs to produce up to 450 neurons, whereas a type I NB typically generates only 110 neurons (Bello *et al.*, 2008).

Apart from NBs in the central brain, type I NBs can be found in the VNC, and specialized types of NBs exist in the optic lobes and mushroom bodies (Knoblich, 2010).

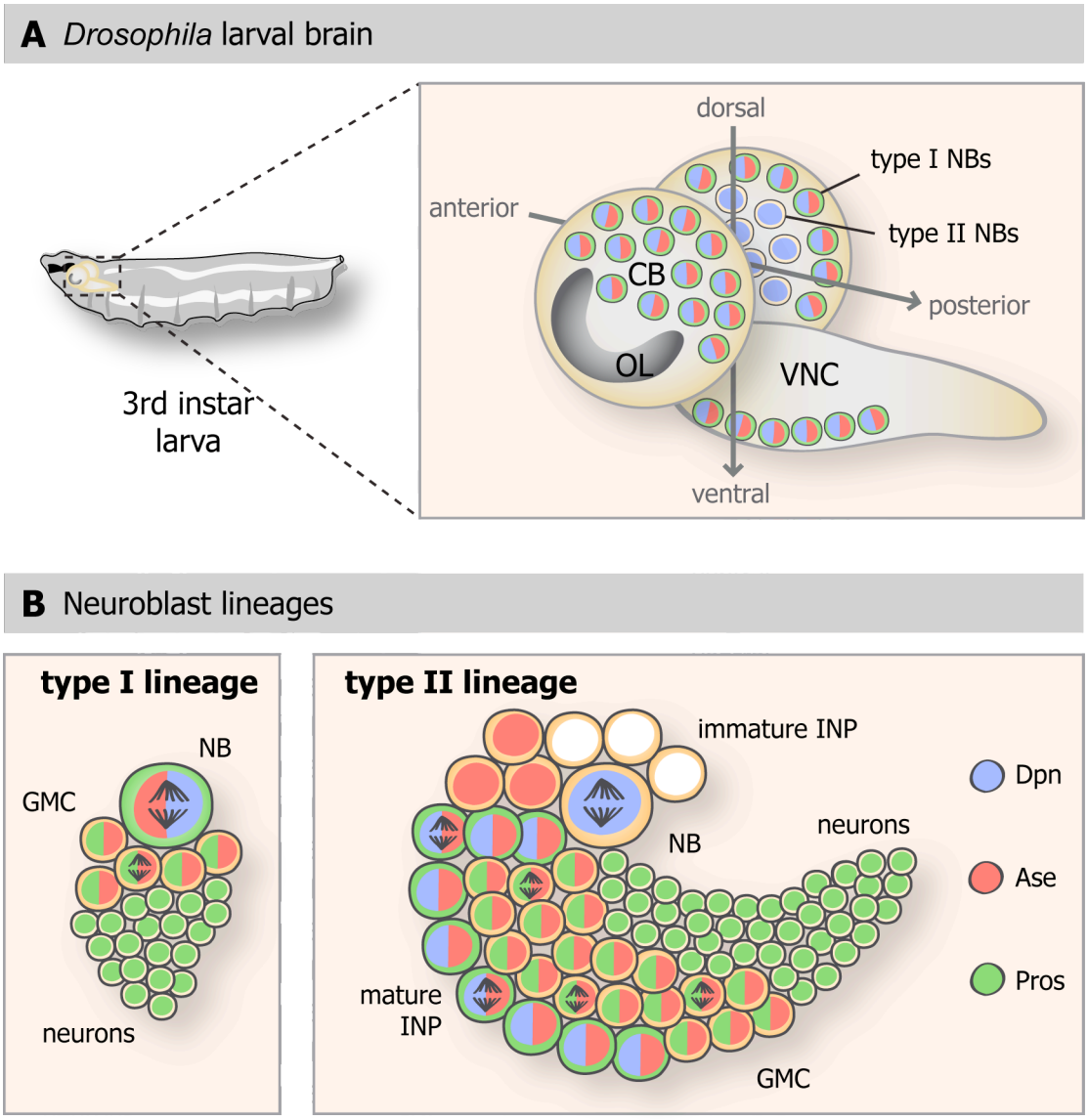

Figure 2. The *Drosophila* larval brain
(A) The third instar *Drosophila* larval brain can be divided into three parts: the central brain (CB), the ventral nerve cord (VNC) and the optic lobes (OL). Type I neuroblasts (NBs) on the anterior and posterior, and the 16 II NBs on the posterior side reside in the CB. Only type I NBs exist in the VNC, and optic lobe NBs, a specialized type of NBs, can be found in the OLs. **(B)** Two types of NB lineages can be distinguished – type I NBs are marked by the presence of Deadpan (Dpn), Asense (Ase) and cytoplasmic Prospero (Pros), and divide asymmetrically giving rise to Ase and Pros positive ganglion mother cells (GMCs). GMCs divide terminally into Pros positive neurons or glia cells. Type II NBs express only Dpn and also divide asymmetrically into immature intermediate neural progenitors (iINPs). iINPs undergo a maturation phase and first turn on Ase, followed by Dpn and cytoplasmic Pros. Mature INPs divide several times and produce GMCs and ultimately neurons or glia.

3.3 ASYMMETRIC CELL DIVISION OF *DROSOPHILA* NEUROBLASTS

3.3.1 Cell fate determinants

In all types of *Drosophila* NBs different cell fates are established via unequal distribution of a set of specific proteins called cell fate determinants. Known cell fate determinants are the Notch repressor Numb, the TF Pros and the translational repressor Brain tumor (Brat) (reviewed in (Doe, 2008; Knoblich, 2008; Chia *et al.*, 2008)). During mitosis (late prometaphase), the cell fate determinants locate in a cortical crescent on the basal side of the NB or INP, and upon cytokinesis segregate into the smaller daughter cell (Bello et al., 2006; Lee *et al.*, 2006b; Betschinger *et al.*, 2006; Spana *et al.*, 1995; Knoblich *et al.*, 1995) (Figure 3A).

Numb was first found to segregate asymmetrically in sensory organ precursor cells (SOPs), the precursors of the peripheral nervous system. Loss of *numb* causes defects in cell fate specification of SOP daughter cells – instead of two inner (neuron and sheath) and two outer cells (socket and hair), only outer cells are generated (Rhyu *et al.*, 1994). Numb is a membrane associated protein (Qin *et al.*, 2004; Benetka *et al.*, 2008) and acts as a repressor of Notch signaling. It is postulated to execute its function by asymmetrically localizing α-Adaptin, a subunit of the endocytic AP-2 complex, and linking it with Notch via its phospho-tyrosine-binding (PTB) domain. This triggers degradation of Notch and an unequal Notch/Delta signal in the daughter cells (Guo *et al.*, 1996; Santolini *et al.*, 2000; Berdnik *et al.*, 2002). In type II NBs, Numb and α-Apaptin also interact to antagonize Notch signaling by internalizing the Notch pathway member Sanpodo and the Notch receptor in the INP, however different protein domains of α-Apaptin compared to other cells (*e.g.* SOPs) seem to be required (Song and Lu, 2012). Mutating *numb* in larval NBs leads to an excess of NBs at the expense of differentiated progeny, due to elevated Notch signaling in both daughter cells (Wang *et al.*, 2006). Asymmetric distribution of Numb was shown to be facilitated Partner of Numb (Pon) (Lu *et al.*, 1998) (Figure 3A). However, Pon is not absolutely crucial for Numb localization, because in *pon* mutants Numb crescents, with some delay, still form (Lu *et al.*, 1998).

Pros, a homeodomain TF (Chu-Lagraff *et al.*, 1991), is synthesized and retained in the cytoplasm of the NB, and relocates into the nucleus of the GMC after cell division (Spana and Doe, 1995; Hirata *et al.*, 1995; Knoblich *et al.*, 1995). In embryos, mutations in *pros* lead to a decrease in neuronal progeny (Doe *et al.*, 1991) and to an excess of NB like cells due to the transformation of GMCs into self-renewing cells (Choksi *et al.*, 2006). In larval NBs, the lack of Pros causes severe over-proliferation phenotypes and results in brains consisting almost entirely of ectopic NBs at the expense of their differentiated progeny (Bello *et al.*, 2006; Betschinger *et al.*, 2006). Pros can act both as a repressor and activator of gene expression, with target genes being involved in self-renewal and terminal differentiation, respectively (Choksi *et al.*, 2006). Pros is bound by the adaptor protein Miranda (Mira), which facilitates its basal localization in the NB during mitosis (Shen *et al.*, 1997; Ikeshima-Kataoka *et al.*, 1997).

A tumor-like neoplasm in larval brains upon *brat* knock out (Arama *et al.*, 2000), as well as the function of Brat in embryos as a translational repressor (Sonoda and Wharton, 2001) had already been described before Brat was discovered to be a cell fate determinant (Betschinger *et al.*, 2006; Lee *et al.*, 2006b; Bello *et al.*, 2006). In contrast to *pros* mutants, where tumors arise from misspecified GMCs from type I and type II NBs, mutating *brat* causes an over-proliferation of only type II NBs due to de-differentiation of INPs (Bowman *et al.*, 2008). The molecular function of Brat in larval NBs remains elusive, and a role for the translation inhibition complex described in embryos has not been shown yet. However, some hints come from related protein family members, the NHL proteins Mei-P26 and the mouse homolog TRIM32. Both proteins were shown to be involved in cell growth and proliferation and act by inhibiting the TF Myc (Betschinger *et al.*, 2006; Neumuller *et al.*, 2008; Schwamborn *et al.*, 2009). In addition, Brat has a described role in growth control and ribosome biogenesis in epithelial cells (Frank *et al.*, 2002). The adaptor protein Mira also binds Brat and allows its localization to the basal cortex during NB division (Shen *et al.*, 1997; Ikeshima-Kataoka *et al.*, 1997; Betschinger *et al.*, 2006; Lee *et al.*, 2006b). Mira gets degraded in the GMC and releases Pros and Brat (Hirata *et al.*, 1995; Ikeshima-Kataoka *et al.*, 1997). In *mira* mutants, Brat and Pros localization becomes cytoplasmic and both get distributed equally into the daughter cells (Shen *et al.*, 1997; Ikeshima-Kataoka *et al.*, 1997; Betschinger *et al.*, 2006; Lee *et al.*, 2006b) (Figure 3A).

The brain tumors caused by mutations in the cell fate determinants *pros*, *numb* and *brat* can be transplanted into the abdomen of wild type host flies, and can be propagated indefinitely by serial injections. Transplanted NBs become aneuploid and start invading other tissues, which ultimately results in the death of the host fly (Caussinus and Gonzalez, 2005; Gonzalez, 2007).

3.3.2 Locating cell fate determinants basally

The basal localization of Brat, Pros and Numb, facilitated by their respective adaptor proteins, depends on a protein complex that accumulates on the apical membrane before mitosis. This complex contains atypical Protein Kinase C (aPKC), as well as the PDZ domain proteins partitioning defective-3 (Par-3, also known as Bazooka, Baz) and Par-6 (Petronczki and Knoblich, 2001; Schober *et al.*, 1999; Wodarz *et al.*, 1999; Wodarz *et al.*, 2000; Rolls *et al.*, 2003) (Figure 3A).

Initially, an apical-basal polarity is inherited by embryonic NBs, because the apical Par-complex localization is maintained when NBs delaminate from the neuroepithelium (Yoshiura *et al.*, 2012). In all subsequent embryonic and larval NB divisions, the orientation of division is aligned relative to the axis of the previous cell division (Rusan and Peifer, 2007; Rebollo *et al.*, 2007; Rebollo *et al.*, 2009). Centrosomes were described to provide a reference point for the localization of the Par-complex at the apical side of the cell, thereby creating an apical-basal axis of polarity within the cell (Rebollo *et al.*, 2009). It is still not clear however, how cortical polarity is linked and oriented relative to the centrosome.

The mechanism by which the Par-complex localizes the basal cell fate determinants has recently been solved (Wirtz-Peitz *et al.*, 2008) (Figure 3B). During interphase, aPKC forms a complex with Par6 and the cytoskeleton protein lethal (2) giant larvae (Lgl). This inactive complex gets activated upon entry into mitosis by the kinase Aurora A (AurA). AurA phosphorylates Par-6, which leads to autophosphorylation and hence activation of aPKC, and subsequent phosphorylation of Lgl by aPKC. Phosphorylated Lgl gets released from the complex and is replaced by Par-3. The complex consisting of Par-3, Par-6 and aPKC can use Numb as a substrate, which gets phosporylated by aPKC, and released from the apical cortex. It was shown that aPKC-dependent phosphorylation is a general mechanism for asymmetric localization of proteins during

mitosis, and for example also localization of Mira can be directed by phosphorylation by aPKC (Wirtz-Peitz *et al.*, 2008; Atwood and Prehoda, 2009).

3.3.3 Coupling asymmetric cell division and spindle orientation

For correct inheritance of cell fate determinants by the GMC, the mitotic spindle has to be aligned with the axis of polarity (Figure 3C). The Par-complex functions to couple basal localization of cell fate determinants with spindle orientation, by interacting via Par-3 with the apically localized adaptor protein Inscuteable (Insc) (Kraut *et al.*, 1996; Kraut and Campos-Ortega, 1996; Wodarz *et al.*, 1999; Schober *et al.*, 1999). This interaction results in stabilization of the Par-complex (Wodarz *et al.*, 1999; Wodarz *et al.*, 2000; Petronczki and Knoblich, 2001), and links the complex to the adaptor protein Partner of Inscuteable (Pins) (Yu *et al.*, 2000; Schaefer *et al.*, 2000) and to the heterotrimeric G-protein α_i-subunit ($G\alpha_i$) (Schaefer *et al.*, 2001), which attaches the complex to the plasma membrane. Pins and $G\alpha_i$ form a complex together with the Nuclear Mitotic Apparatus (NuMA)-related Mushroom body defect (Mud) (Siller *et al.*, 2006; Izumi *et al.*, 2006; Bowman *et al.*, 2006). Mud recruits the minus-end directed microtubule motor proteins Dynein/ Dynactin (Siller and Doe, 2008) and connects the complex to the mitotic spindle.

Correct alignment of the mitotic spindle with the axis of polarity is crucial for correct asymmetric cell division. When spindle orientation is randomized, such as in *mud* mutants, the fate of both daughters is ultimately determined by the ratio of apical and basal determinants that get inherited by the daughter cells (Cabernard and Doe, 2009).

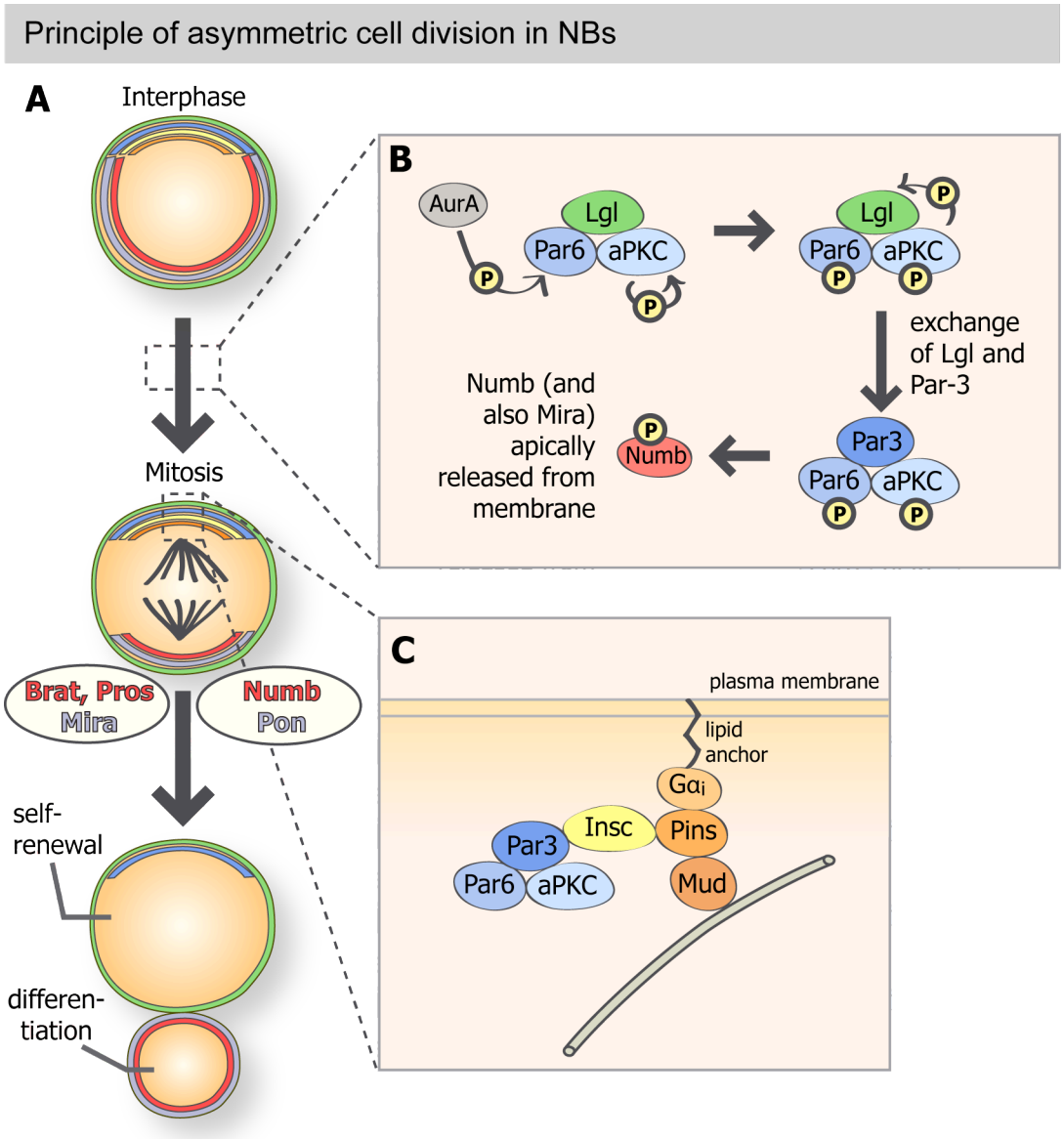

Figure 3. Principle of asymmetric cell division
(A) The apical complex consisting of the Par-complex (blue), Inscuteable (Insc, yellow) and the spindle complex (orange) accumulate on the apical membrane before mitosis. This directs the cell fate determinants Brat, Pros and Numb (red) via their respective adapter proteins (purple) to the basal cortex. Upon asymmetric division of the NB, the self-renewing daughter cell retains the apical complex, while the cell fate determinants are segregated into the differentiating GMC. **(B)** A phosphorylation cascade directs the cell fate determinant Numb to the basal membrane. Aurora A activates the inactive interphase complex consisting of Lgl, Par6 and aPKC via a phosphorylation cascade. Following a subunit exchange, the active Par-complex can phosphorylate downstream targets like Numb, which then gets released from the apical cortex (Adapted from Wirtz-Peitz *et al.*, 2008). **(C)** For alignment of the spindle along the apical/ basal axis, the active Par-complex connects via Insc with the Gαi/Pins/Mud complex, which allows connection with the apical membrane and microtubule attachment.

3.4 SELF-RENEWAL VERSUS DIFFERENTIATION AND TUMOR FORMATION

3.4.1 Relationship between cancer, Notch signaling and cell growth

The recently developed "cancer stem cell (CSC) hypothesis" states that a small population of stem cell like cancer cells can form and sustain a tumor (Reya *et al.*, 2001). CSCs are thought to be responsible for metastasizing of tumors and relapse after cancer therapy, and thus need to be eliminated for a successful treatment. Notch signaling was shown to regulate stem cell behavior in many tissues and species (Pellegrinet *et al.*, 2011; Lefort *et al.*, 2007; Ohlstein and Spradling, 2007; Luo *et al.*, 2005), and was linked to CSC-based cancers (Harrison *et al.*, 2010; Varnum-Finney *et al.*, 2000).

Also in NBs is the Notch signaling pathway the major pathway for NB lineage decisions ((Wang *et al.*, 2006; Bowman *et al.*, 2008), for a Notch pathway review see (Bray, 2006)). Over-activation of an active form of Notch (N_{intra}) causes strong NB neoplasia, and most ectopic NBs do not express Ase and seem to be of type II origin (Bowman *et al.*, 2008). Some type I lineages are also sensitive to elevated Notch levels and over-proliferate (Zacharioudaki *et al.*, 2012). Knock down of *Notch* results in a reduction of total NB numbers (Wang *et al.*, 2006), and in a complete loss of type II lineages (Bowman *et al.*, 2008). Opposite phenotypes from *Notch* loss- and gain-of-function were expected from the cell fate determinant Numb, a negative regulator of Notch signaling (see also 3.3.1). Indeed, mutating *numb* causes the formation of brain tumors made up almost entirely of type II NBs (Bowman *et al.*, 2008), with some type I lineages also contributing to the phenotype (Lin *et al.*, 2010). Conversely, *numb* over-expression causes loss of type II lineages (Bowman *et al.*, 2008), however it has not been investigated whether type I NB numbers are also affected.

It was shown that Notch is involved in the regulation of NB growth (Song and Lu, 2011). In contrast to embryonic NBs, larval NBs grow back to their original size after each division and can divide hundreds of times. NB cell size is reduced over time upon inhibition of Notch signaling. Conversely, over-activation of the pathway results in the formation of ectopic NBs that after some delay re-grow to the size of primary NBs. Smaller and enlarged nucleoli have been observed, respectively, and the phenotypes have been linked to the growth regulator dMyc, which gets directly activated by Notch signaling, and the eukaryotic translation initiation factor 4E (eIF4E), a positive downstream target of dMyc. Ectopic NBs seem to be more sensitive to eIF4E levels, because mutant (*brat*, *lgl*, *aPKC*^{CAAX} [a membrane tethered form of aPKC]) and *Notch* over-activation phenotypes can be repressed by knockdown of *eIF4E*, while wild-type NBs are not affected. A possible explanation could be that the faster growing ectopic NBs cannot be sustained in the absence of *eIF4E* (or *dmyc*) and thus de-differentiation is inhibited or slowed down. This made eIF4E a target for treatment of CSC derived tumors.

How Notch and its downstream targets promote stemness by regulating cell growth, and how it affects and defines differential cell fates within the stem cell hierarchy is still not clear and needs further investigation.

3.4.2 Notch signaling and known NB self-renewal factors

When this project was initiated, apart from Notch signaling, no network of factors acting specifically in the NB to maintain stem cell identity had been described. It is also unclear how Brat, Pros and Numb act on this potential network to turn off NB self-renewal and turn on differentiation factors in GMCs. During the course of this project, two publications identified the basic helix-loop-helix Orange (bHLH-O) TFs Dpn (San-Juan and Baonza, 2011) and the Enhancer-of-Split complex member mγ (E(spl)mγ) to be crucial for NB self-renewal (Zacharioudaki *et al.*, 2012).

It has long been known that bHLH-O proteins of the E(spl)-complex are downstream targets of the Notch signaling pathway (Jennings *et al.*, 1994). Dpn is also a bHLH-O protein, and is expressed in NBs throughout embryonic and larval development (Bier *et al.*, 1992). Over-expressing *dpn* (San-Juan and Baonza, 2011) and some genes of the *E(spl)-complex* (mγ [strongest phenotype], m3, mδ) (Zacharioudaki *et al.*, 2012) causes over-proliferation of mostly type II NBs, a

phenotype similar to elevated Notch signaling where *dpn* and *E(spl)* genes are also up-regulated. Single mutations result in weak phenotypes, and only double mutants display a dramatic loss of NBs. Even though *dpn* has a putative binding site for the Notch pathway component Suppressor of Hairless (Su(H)), only *E(spl)* can rescue the Notch over-expression phenotype when mutated in this background (Zacharioudaki *et al.*, 2012). In addition, *E(spl)* genes are misregulated upon Notch pathway disruption, whereas *dpn* expression is not affected. Therefore, only *E(spl)-complex* genes seem to be direct Notch targets and Dpn might act in a different signaling pathway. However, both Dpn and E(spl)mγ act redundantly as NB self-renewal factors and true to their oncogenic character, need to be down-regulated in INPs and to some extend GMCs, to allow differentiation.

3.4.3 Large scale approaches to identify NB self-renewal factors

Identifying factors in *Drosophila* that act in stem cell maintenance and cause over-proliferation of stem cells when over-expressed, and solving the mechanisms by which they carry out their function, might aid in solving the mechanisms leading to stem cell derived mammalian tumors.

Multiple genetic screens for NB lineage defects have identified a huge number of potential regulators (Neumuller *et al.*, 2011; Sousa-Nunes *et al.*, 2009), but identifying NB maintenance factors from these loss-of-function screens proved to be difficult. As opposed to pro-differentiation factors (*e.g.* Pros) or factors involved in correct segregation of cell fate determinants (*e.g.* Mira, AurA), which result in rather specific NB over-proliferation phenotypes, mutating NB self-renewal factors is expected to result in the opposite phenotype – loss of NBs due to premature differentiation. However, factors causing loss of NB phenotypes are numerous and not only involved in NB identity maintenance, but also in cell division, growth, or survival (Neumuller *et al.*, 2011). Therefore, a regulatory network that controls self-renewal in NBs cannot be identified solely from loss-of-function screens.

An important step in the identification of this network would be to know all genes that are expressed in the different cell types of the *Drosophila* larval brain. However, it is not currently not possible to isolate pure populations of *Drosophila* neural cells in large numbers, and therefore, their transcriptomes are not known. Several attempts were made to obtain information about the gene expression pattern of NBs. One such technique is TU-tagging (Miller *et al.*, 2009). For this method the enzyme uracil phosphoribosyltransferase (UPRT) is expressed in a cell type-specific manner using the UAS/Gal4 system. UPRT under natural conditions couples ribose-5-phosphate to uracil to generate uridine monophosphate, which is incorporated into RNA. When the uracil analogon 4-thiouracil (hence, TU-tagging) is provided as a substrate, newly synthesized RNA is thus labeled and can be tagged, purified and analyzed. However, any technique using the UAS/Gal4 system in NBs will be limited by the fact that Gal4 as well as the expressed target genes will be inherited by both NB daughter cells. This results in labeling of newly synthesized RNA also in the differentiating population. An alternative method makes use of larval brain tumors, which are enriched for NB-like cells. mRNA is isolated from these mutant brains and compared to wild type brains, which are mostly made up of neurons (Carney *et al.*, 2012). Even though this approach has identified a significant number of NB specific genes, it is not very specific since it cannot be used to characterize wild type cell subpopulations, or to compare wild type to tumor mutant NBs.

The fact that mutations in genes involved in asymmetric cell division, or over-activation of self-renewal genes causes stem cell derived tumor formation, make larval NBs an ideal model system to study the relationship between stem cell self-renewal, asymmetric cell division and tumorigenesis.

3.5 AIM AND STRUCTURE OF THIS STUDY

The aim of this study was to identify a network of factors responsible for maintaining the stem cell capacity of the NB, and to determine how the cell fate determinants modify this potential self-renewal network during differentiation. This study is presented in three chapters as introduced below.

Chapter I

This chapter describes methodology to purify larval NBs and their differentiated neuronal progeny in order to identify NB self-renewal factors by characterizing and comparing the transcriptomes of both cell types. This information was utilized to propose a hypothetical gene network for self-renewal in NBs. The functional relevance of the identified factors was then tested with over-expression and knock down studies.

Chapter II

Of the TFs tested for their relevance in NB self-renewal, the gene *klumpfuss* (*klu*) had not previously been shown to play a role in larval NB identity maintenance. The second chapter focuses on the characterization of this gene.

Chapter III

The last chapter addresses how the transcriptional network for NB self-renewal is modified in the GMC upon differentiation. Methodology to separate NBs and their immediate GMC progeny is described and preliminary expression data is discussed.

4 CHAPTER I – TRANSCRIPTOME ANALYSIS OF *DROSOPHILA* NEURAL STEM CELLS

4.1 RESULTS AND DISCUSSION

The goal of the first part of my PhD was to identify equivalents to the asymmetrically segregated cell fate determinants in NBs – the proteins involved in maintenance of stem cell identity. To find such NB fate determinants, approaches we took included a phenotype-based candidate screen and transcriptome analysis of stem cells and their differentiated daughter cells. Genes that result in NB-specific knock down phenotypes, or are expressed specifically in stem cells are potential candidates for stem cell factors.

A genome-wide RNAi screen to analyze NB self-renewal was previously performed in our lab (Neumuller *et al.*, 2011). For this screen, RNAi lines from the Vienna *Drosophila* RNAi center (VDRC, stockcenter.vdrc.at) were crossed to a driver line, which drives expression of the RNAi construct and GFP in a NB-specific manner. Important factors for NB self-renewal and differentiation ensure proper development and survival, as was shown for knock down of, for example, *brat* or *pros*. Therefore, adult lethality of a cross was the first criterion during analysis. Larval brain phenotypes from lethal crosses were investigated by immunofluorescence in L3 stages. Several phenotypic categories based on number, shape and size of the various cell types in NB lineages were assigned and scored from zero to ten, with ten indicating the strongest phenotype. Most genes were then grouped in one of two major categories – under- or over-proliferation, corresponding to fewer or too many NBs, respectively. The under-proliferation category should contain genes involved in NB maintenance and identity, but also genes involved in cell division, growth, or survival. To differentiate between these different possibilities, and enrich for specific NB self-renewal genes, we decided to re-analyze 538 genes that resulted in strong under-proliferation phenotypes (cut-off of two for under-proliferation category, (Neumuller *et al.*, 2011)) by immunostainings for NB identity, differentiation and cell division markers. First, assuming that lower NB numbers upon knock down of a factor involved in stem cell maintenance would be due to premature terminal differentiation, we determined NB numbers by counting Dpn positive cells. Second, to identify defects in asymmetric cell division, we assessed

cortical and asymmetrically localization of Mira during mitosis. Third, we investigated localization of Pros, because its nuclear localization already in NBs hints to premature differentiation defects. Lastly, by staining for phosphorylated Histone H3 (pH3), a marker for dividing cells, we could determine whether NBs have ceased to divide. However, even with seemingly specific markers it was difficult to separate cell fate from general cell maintenance defects. In addition, NB identity factors might act redundantly, and their knock down might not result in lethality or NB loss. Therefore, we terminated this approach, and turned to expression profiling of NBs and neurons.

A second approach to find stem cell identity factors was to determine which genes are expressed in NBs and to compare this expression pattern to differentiated cells where stem cell factors should be expressed at lower levels. Different approaches to obtain transcriptome data of NBs and neurons are described below.

4.1.1 Single cell amplification

For transcriptional profiling of larval NBs and their differentiated progeny we first set out to amplify cDNA from single cells that were collected manually from dissociated larval brains, because a protocol to obtain large amounts of pure NBs and neurons was not yet developed at that time. We made use of the UAS/Gal4 system (Brand and Perrimon, 1993) to mark NBs and their progeny with nuclear GFP (UAS-stinger*GFP*, stinger = stable insulated nuclear eGPF vector) (Barolo *et al.*, 2000) with the NB-specific driver line *ase*-Gal4 (Figure 4A). NBs can be unambiguously identified by their large size and strong GFP signal (Figure 4B). For collection of neurons, we utilized a line that expresses GFP under the control of Embryonic Lethal Abnormal Vision (ELAV), a gene specifically expressed in neurons (Figure 4C). Both cell types were collected from dissociated larval brain cultures using a glass capillary (see 4.2.2) (Figure 4D).

We tested two protocols for whole transcriptome amplification – global amplification of single-cell cDNA (Kurimoto *et al.*, 2007) (Figure 4E), and the commercial kit "Whole Transcriptome-ovation system" (WT-ovation system) from NuGen Technologies Inc (Figure 4F).

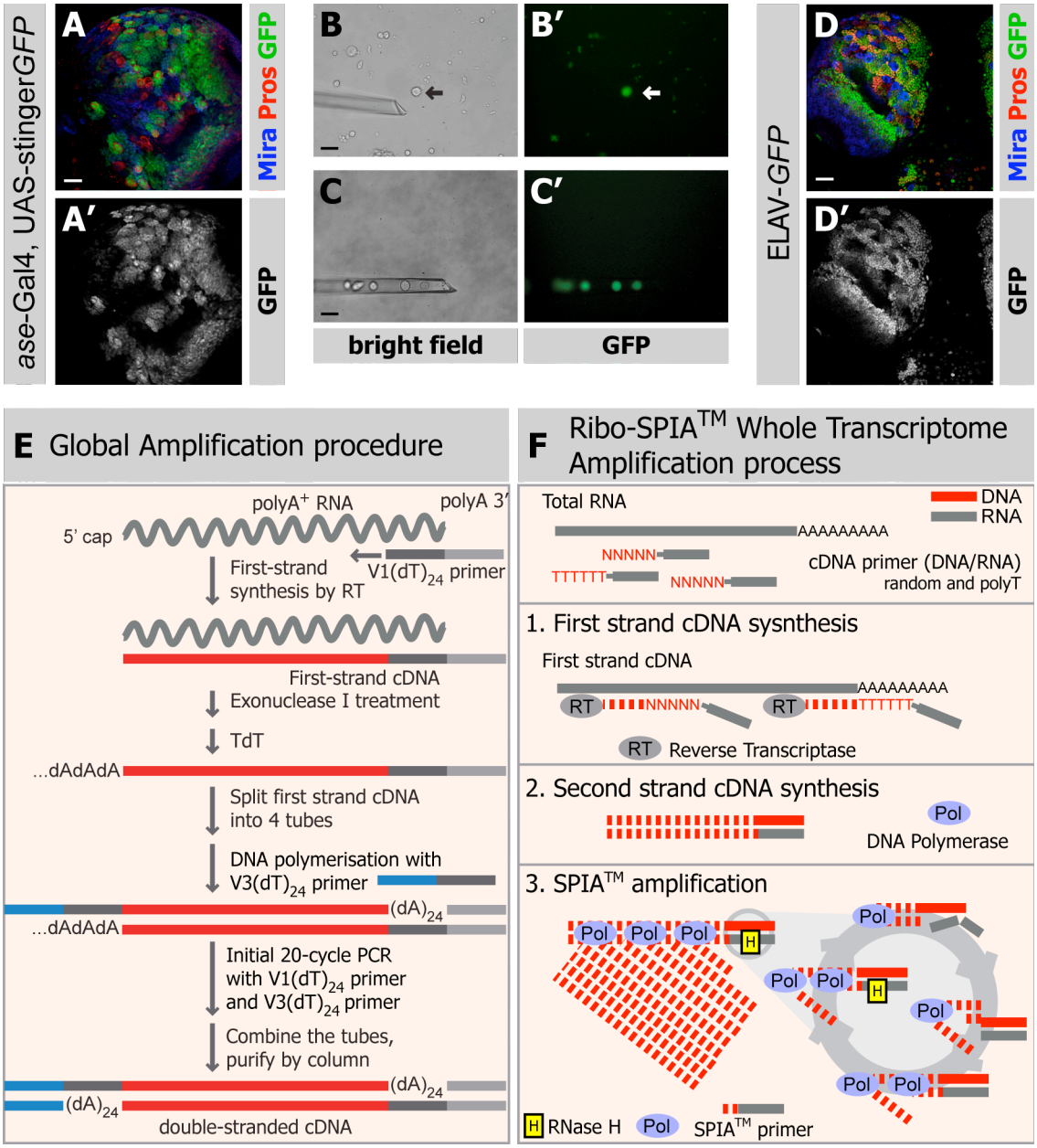

Figure 4. Whole transcriptome amplification protocols
(A-D') Single cell collection for transcriptional profiling of NBs and neurons. **(A, A')** NBs were marked with a nuclear GFP (stinger*GFP*), and can be unambiguously identified in a dissociated culture based on their size and GFP intensity **(B, B', arrow)**. **(C, C')** NBs in a glass capillary after collection. **(D, D')** Neurons were marked with the neuron specific Elav-*GFP*. **(E)** Global single-cell cDNA amplification. First strand cDNA is generated with a modified oligo(dT) primer, and a poly(A) tail is added. After second strand cDNA synthesis, double stranded cDNA is amplified by PCR. **(F)** Ribo-SPIA™ Whole Transcriptome Amplification. First and second strand cDNA is generated with a mixture of random and oligo(dT) DNA/RNA primers. During continuous rounds of DNA/RNA hybrid primer degradation by RNase H and generation of double strand cDNA by DNA polymerase, cDNA is amplified. Scale bars are 20 µm.

To establish the protocol for global amplification of single-cell cDNA, for convenience we made use of cultured *Drosophila* Schneider cell (S2 cells) instead of manually collected NBs and neurons. Briefly, first strand cDNA is generated using a modified oligo(dT) primer, followed by adding a poly(A)-tail to the first strand cDNA. Second strand cDNA is then generated using a second modified oligo(dT) primer. Double stranded cDNA is amplified by PCR using both modified oligo(dT) primers, leading to fragments analyzable with microarrays (Figure 4E, Extended Protocol in (Kurimoto *et al.*, 2007)). Therefore, linear amplification with a 3' bias and a selection against ribosomal RNAs (rRNAs) is expected from this method. In seven biological replicates with 20 Schneider cells each, we found the housekeeping gene RpS8 amplified to roughly the same levels over all replicates (Figure 5A, left). However, when we normalized the expression values of six genes, which were selected based on their described expression in S2 cells (Roy *et al.*, 2010) to RpS8, we found large differences, up to ten magnitudes for example for eIF-4a, in their expression levels across replicates (Figure 5A, right).

We then turned to a commercially available system to amplify cDNA from NBs and neurons (Figure 4F). In the "WT-ovation system" protocol (NuGen Technologies) first strand cDNA is generated using random and polyd(T) DNA/RNA hybrid primers. After second strand cDNA synthesis, so called SPIA™ amplification is performed. In a continuous reaction involving DNA/RNA hybrid primer degradation by RNase H and generation of double strand cDNA by DNA polymerase, large amounts of DNA are generated that can be analyzed by quantitative PCR (qPCR) or microarrays. With this protocol the whole transcriptome is amplified in a non-linear way, and no selection against rRNAs is performed. We collected a fixed number of type I NBs and neurons, which we pooled in lysis buffer and then split to control for technical reproducibility. We repeated this process to assess biological variations between samples. Since controlled and equal numbers of cells were used in each experiment we expected similar cycle threshold (C_t) values for genes when checked by qPCR. However, when we investigated expression levels of known genes expressed in NBs we detected strong differences in C_t-values in biological as well as technical replicates (Figure 5B, Latin and Roman numbers correspond to biological replicates). For example, C_t-values for the housekeeping gene *RpS8* vary between 21 and 26 for neuron and between 18 and 20 for NB samples; *mira* is amplified to C_t-values between 22 and 29 in NBs and 28 up to 38 in neurons. This variation between samples was high, considering that one

cycle roughly corresponds to a three-fold difference in expression. Oftentimes even, cDNA was amplified in some replicates, while it could not be detected in others, for example *cyclin A* (*cycA*) or *dpn* in neuron samples, or *embryonic lethal abnormal vision* (*ELAV*) in NB samples.

Taken together, both methods were unsuitable to analyze expression levels of NBs and neurons, because large errors were introduced during amplification of cDNA. For the "WT-ovation system" non-linear amplification was not the problem, if one always compares two samples amplified by the same method, but rather very low reproducibility between biological, as well as technical replicates. In retrospect, global amplification of cDNA might have been a suitable method to identify large differences in expression levels between NBs and neurons. Due to the high variability between replicates however, smaller differences would not have been detectable.

Since these approaches were not successful, but we had optimized our larval brain dissociation protocol and culturing conditions for NBs during this process, we decided to establish Fluorescence-activated cell sorting (FACS) to isolate large numbers of NBs and neurons for transcriptional profiling.

A Global Amplification

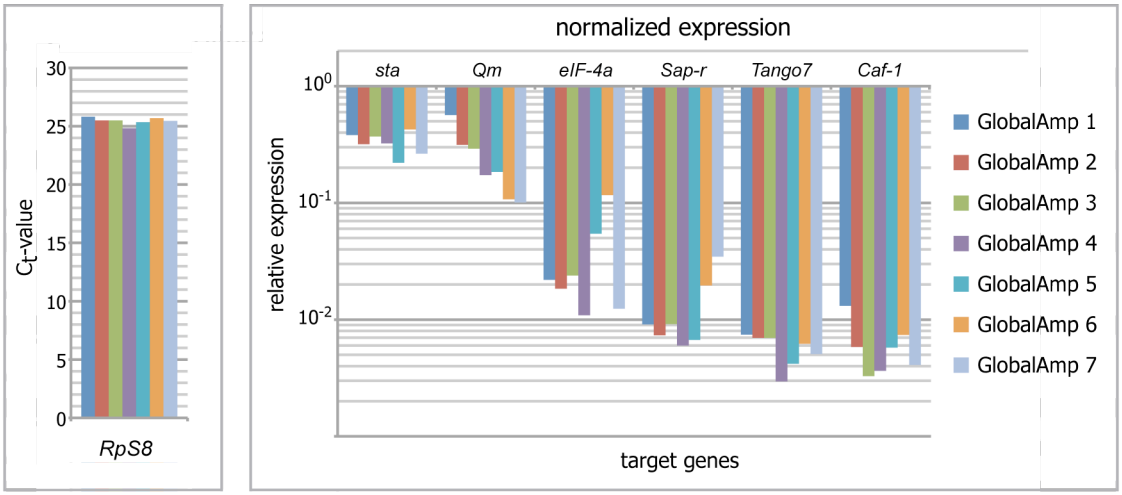

B Ribo-SPIA™ Whole Transcriptome Amplification process

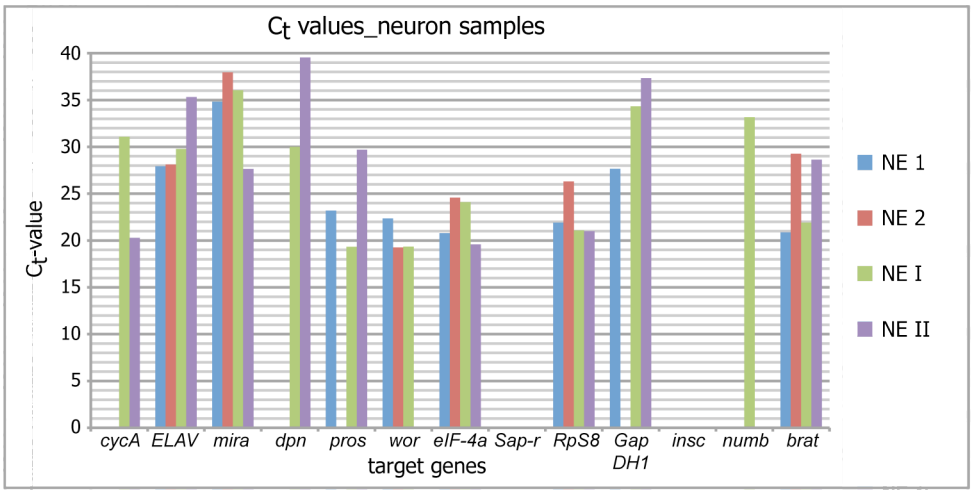

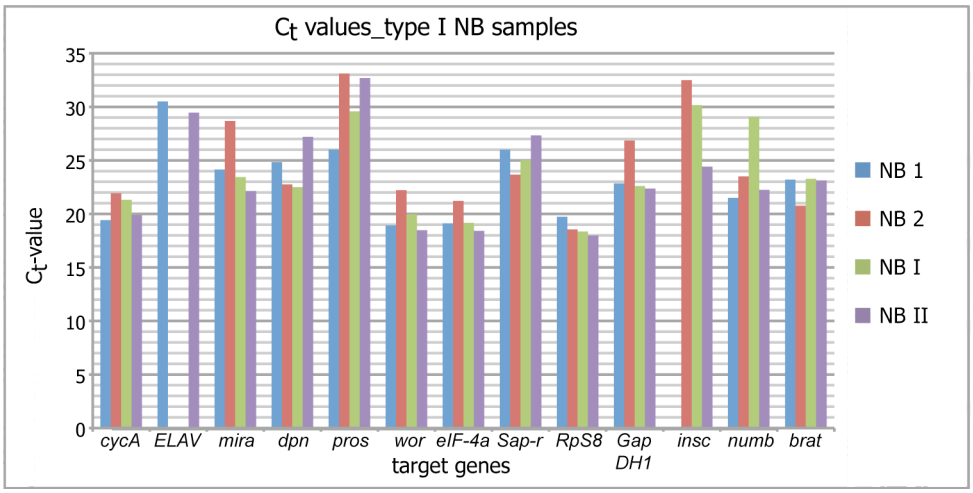

Figure 5. qPCR results from Global and Ribo-SPIA™ Whole Transcriptome Amplification of cDNA show high variability between replicates

(A) Global Amplification. The housekeeping gene RpS8 is amplified to the same level in all replicates (left), but relative fold changes of control targets show high variability between replicates (right), for example eIF-4a with ten magnitudes difference between samples six and seven. **(B)** Ribo-SPIA™ Whole Transcriptome Amplification. Same amount of starting material was used for all replicates and cycle threshold values (C_t-values) are plotted. For the housekeeping gene RpS8 C_t-values vary greatly between 21 and 26 for neuron samples and between 18 and 20 for NB samples. Most strikingly, for some targets cDNA was amplified for some replicates, but absent in others. Examples for neuron samples are *cycA*, *dpn* and even another housekeeping gene, *GapDH1*. This phenomenon is less pronounced in NB samples, but occurred in the case of, for example, *ELAV* or *insc*. In addition, in cases were cDNA from all replicates was amplified, very high variability between replicates could be observed.

4.1.2 FACS purification of larval NBs

The principle of flow cytometry, of which FACS is a specialized type of, is as follows: Laser light of a single wavelength is directed onto a stream of liquid, which contains the particles to be analyzed. Several detectors are aimed at the stream where it passes trough the light beam. One is in line with the light beam (Forward Scatter, FSC) and the information gathered at that point correlates with cell volume, *i.e.* cell size. Other detectors are aligned perpendicular to the light beam (Side Scatter, SSC), which provides information about the inner structures of the cell. Dead cells are more granulous and differently shaped compared to living cells and can therefore be recognized based on their stronger SSC signal. Lastly, one or more fluorescence detectors are aimed at the light beam. Fluorescent proteins or dyes in the specimen are excited by the laser and emit light at a longer wavelength, and therefore the presence or absence, and the strength of the fluorescent signal is yet another way to derive information about each particle in a sample. To then sort single cells of a heterogeneous mixture into several containers based on their light scattering and fluorescent characteristics, the liquid stream that contains the cells is broken up into droplets by a vibrating mechanism. The flow of particles is adjusted so that the probability of only one particle per droplet is very high. Just prior to the stream breaking into droplets, the fluorescence signal of interest is measured for each individual particle. Based on that signal a charge is placed on an electrical charging ring that is localized just at the point where the stream breaks into droplets, which causes the opposite charge on the droplet as it breaks from the stream. An electrostatic deflection system then sorts the droplets into different containers based on their charge. Sometimes the charge is placed directly onto the stream and the droplet, which is breaking off retains the same charge. Afterwards the stream is turned to neutral until the next droplet enters.

In *Drosophila*, several cell types have been successfully sorted by FACS. These include embryonic cell populations (Cumberledge and Krasnow, 1994; Shigenobu *et al.*, 2006), adult ovarian stem cells (Kai *et al.*, 2005) and follicle cells (Calvi and Lilly, 2004), hemocytes (Tirouvanziam *et al.*, 2004), and posterior wing imaginal disc cells (Neufeld *et al.*, 1998). Usually, cells are labeled with GFP in a cell type specific manner utilizing the UAS/Gal4 system and cells are sorted based on their fluorescence signal. Like for TU-tagging (see 3.4.3), labeling only NBs with this method is not possible,

because Gal4 and therefore GFP expression is inherited by both daughter cells. In addition, no Gal4 line exists that is specific and sufficiently strong for type I NBs but does not express in the optic lobes.

As mentioned before (see 4.1.1), cell size and GFP expression levels differ greatly between NBs, GMCs and neurons. Therefore, we combined forward scattering and GFP fluorescence intensity to separate different cell populations by FACS. We marked NB lineages with the type I lineage-specific *ase*-Gal4 line, which drives expression of UAS-stinger*GFP* (Barolo *et al.*, 2000). For our protocol we dissected L3 larval brains, and enzymatically and manually disrupted the tissue (protocol summarized in Figure 6A). Dissociated larval brains were then subjected to FACS where our gating strategy was as follows: we first gated for living cells based on FSC and SSC, which was followed by a selection against auto-fluorescent cells. In a third gate we plotted FSC against GFP fluorescence and found a separate population of large and strongly GFP positive cells, which we have identified as NBs. We determined a less well-defined population of smaller cells with a weaker GFP signal to be differentiated neurons. Lastly we gated against cell clusters by measuring the width (FSC-W) of the FSC signal over its area (FSC-A), whereby wider signals indicate several cells clustered together. In addition, we used a low-pressure FACS protocol to ensure cell survival. Finally, to account for the low frequency and large size of NBs, high numbers of sorting events had to be recorded on a logarithmic scale.

To assess the identity and purity of the sorted cell population we conducted several quality control experiments. We stained unsorted cultures and sorted cells for specific NB and neuronal markers (Figure 6B-D). In unsorted cell suspensions, large aPKC positive cells, with a strong GFP signal (yellow arrowheads, NBs), as well as smaller ELAV positive cells (differentiated cells) can be detected (Figure 6B). Upon sorting of these cultures, we could retrieve an essentially pure population of Dpn (see Figure 8C), Mira (see Figure 7E) and aPKC positive, and ELAV negative NBs (98.9 % NBs, 1.1 % neurons [n=3], p-value<0.01 [Student's t-test]) (Figure 6C). The size of these cells corresponds well to the described size of NBs *in vivo* (10-14 µm diameter), and is clearly larger than that of INPs (5-6 µm diameter). Neurons can be distinguished from GMCs and INPs by their smaller size and the absence of aPKC expression. When we sorted and investigated different cell populations in the bulk of smaller cells with weaker GFP expression (light blue in Figure 6A, "gate3"), we found that only the

indicated population (P4) contained small ELAV positive cells (Figure 6D). This cell population was devoid of Mira positive cells, and never contained any aPKC positive NBs. However, since no specific GMC markers exist we cannot exclude that very few GMCs or INPs might be present in this neuronal population. To exclude the presence of glia cells in all sorted populations, we stained unsorted cell cultures and FACS sorted cells with the glial marker Reversed polarity (Figure 6E-F'). We can detect few Repo positive glia cells in dissociated brains, but never in FACS sorted populations. Based on these experiments, we conclude that we have sorted very pure populations of larval NBs and their more differentiated daughter cells.

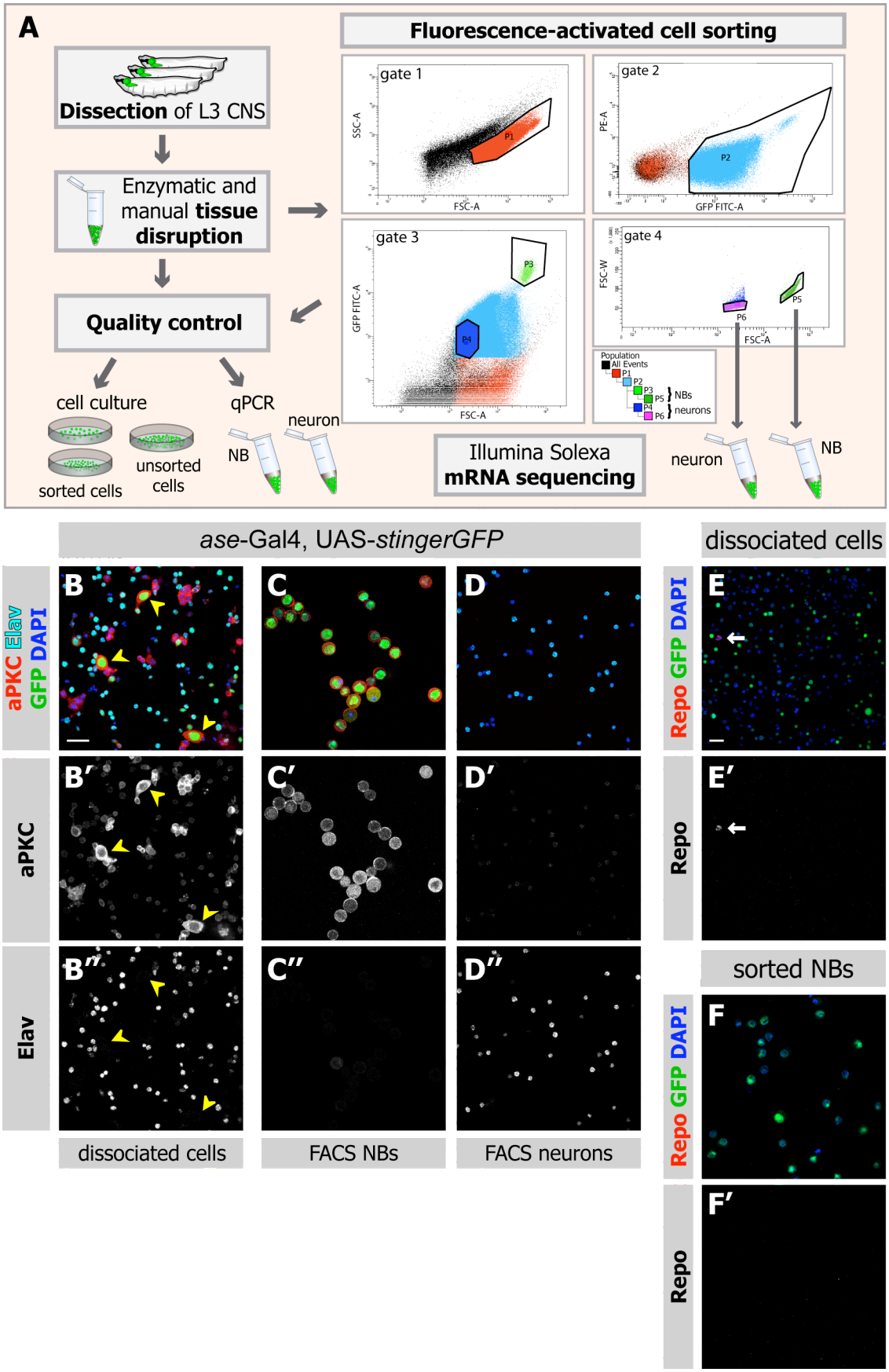
A
Fluorescence-activated cell sorting
Dissection of L3 CNS
Enzymatic and manual tissue disruption
Quality control
cell culture
qPCR
sorted cells
unsorted cells
NB
neuron
gate 1
gate 2
gate 3
gate 4
SSC-A
FSC-A
PE-A
GFP FITC-A
FSC-W
P1
P2
P3
P4
P5
P6
Population
All Events
NBs
neurons
Illumina Solexa
mRNA sequencing
neuron
NB
ase-Gal4, UAS-stingerGFP
dissociated cells
aPKC Elav
GFP DAPI
aPKC
Elav
Repo GFP DAPI
Repo
sorted NBs
B
B′
B″
C
C′
C″
D
D′
D″
E
E′
F
F′
dissociated cells
FACS NBs
FACS neurons

Figure 6. Pure populations of larval NBs and neurons can be obtained by Fluorescence-activated cell sorting (FACS)

(A) Scheme of FACS protocol. After dissection of the larval central nervous system (CNS), the tissue was enzymatically and manually disrupted and the cell suspension either subjected to quality control experiments (cell culture) or FACS. To sort NBs and neurons, a hierarchical sorting strategy was employed. Plotting forward scatter (FCS-A) versus side scatter (SSC-A) allows gating for living cells (gate 1), and was followed by gating against autofluorescent cells (gate 2). By plotting GFP intensity (GFP FITC-A) to cell size (FSC-A) a small population of large cells with high GFP signal (NBs), and a population of smaller cells with a lower GFP signal (differentiated cells) can be identified (gate 3). Finally, to remove cell clumps the area of the FCS signal (FSC-A) was plotted against its width (FSC-W), whereby wider signals indicate clustered cells (gate 4). Sorted cells were either subjected to quality control (cell culture or quantitative real time (qRT)-PCR analysis) or to paired-end Illumina Solexa mRNA sequencing. **(B-D'')** Immunofluorescence staining for the NB marker aPKC, the differentiation marker ELAV and DAPI of an unsorted cell suspension **(B-B'')**, sorted NBs **(C-C'')** and neurons **(D-D'')**. NBs are large aPKC positive cells with strong nuclear GFP signal (yellow arrowheads). Their differentiated sibling cells are small, with a weaker GFP signal and stain positive for ELAV. The sorted NBs and neurons stain only for aPKC and ELAV, respectively (see single channels). **(E** and **E')** Repo positive glia cells (arrow) can be found in unsorted cultures, but **(F** and **F')** never in sorted populations. Scale bars are 20 µm.

4.1.3 FACS sorted larval NBs are alive

We then tested the viability of sorted NBs and whether they still divide asymmetrically and give rise to GMCs and neurons. We analyzed the ability of NBs to asymmetrically localize cell fate determinants before and after FACS. We found that NBs in primary cell culture show basal localization of Mira, Numb and Pros (for Pros see Figure 8C), and apical localization of aPKC and Pins during telophase and metaphase (Figure 7A-C). This is consistent with a previous publication by Ceron *et al.* (2006). After FACS, the ability of sorted NBs to localize proteins asymmetrically was unchanged, as can be seen by the apical localization of aPKC (Figure 7D) as well as by the basal localization of Mira to the cortex of the future GMC (Figure 7E). When sorted NBs were arrested in mitosis using colchicine, a drug that inhibits microtubule polymerization by binding to tubulin, 79% of those cells showed the typical localization of aPKC and Mira to opposite cortexes (Figure 7F). Taken together, viability and mitotic activity of larval NBs are not affected by FACS.

In addition to immunofluorescence stainings, and to verify the lineage of NBs after FACS, we performed live imaging on cultured NBs in a dissociated cell culture before and after sorting (Figure 8A and B). In both cases, the NB (yellow arrow) divided multiple times and gave rise to smaller GMCs (yellow arrowheads), which always budded off at the same position. After some delay, the GMCs divided terminally and gave rise to two differentiating neurons (white arrowheads). When we quantified the lengths of each cell cycle we found that the first two NB divisions as well as the division of the GMC were not, or only very slightly affected by the FACS procedure (Figure 8C). In later divisions however, sorted NBs displayed a significant delay in their cell cycle length. Antibody staining of NBs that were cultured for five hours, showed that NBs had divided one to two times, giving rise to GMCs, but not yet neurons (Figure 8D). NBs, but not GMCs continued to express the NB marker Dpn. Pros localizes asymmetrically to the basal cortex in metaphase NBs (white arrows), and is nuclear in GMCs. To summarize, our results indicate that the FACS procedure introduces only very slight modifications in the cell cycle lengths of dividing NBs, while it does not affect the ability of NBs to divide asymmetrically. NBs after FACS still give rise to a self-renewing NB, which continues to express NB markers, and a differentiating daughter cell that expresses differentiation markers.

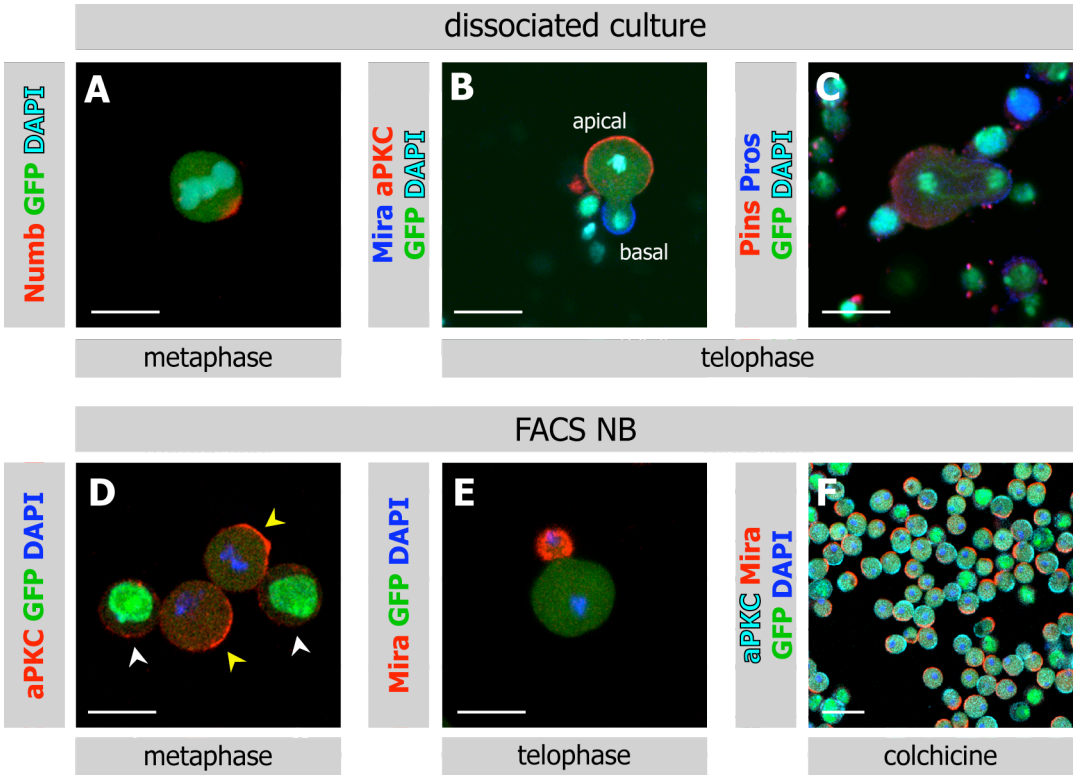

Figure 7. NBs in a dissociated culture and FACS sorted NBs express correct markers

(A) Numb localizes asymmetrically in NB in a dissociated cell culture during metaphase. **(B)** During telophase localization of aPKC to the apical and Miranda (Mira) to the basal cortex, as well as **(C)** apical localization of Partner of Insc (Pins) and basal localization of Pros can be seen. **(D)** Sorted NBs in metaphase (yellow arrowheads) asymmetrically localize aPKC, while no aPKC asymmetry can be seen in interphase NBs (white arrowheads). **(E)** Mira localizes to the future GMC in sorted telophase NBs. **(F)** FACS sorted NBs arrested in mitosis with colchicine display correct localization of aPKC and Mira (n=2). DNA is marked with DAPI, scale bars are 12 µm and 20 µm in (H).

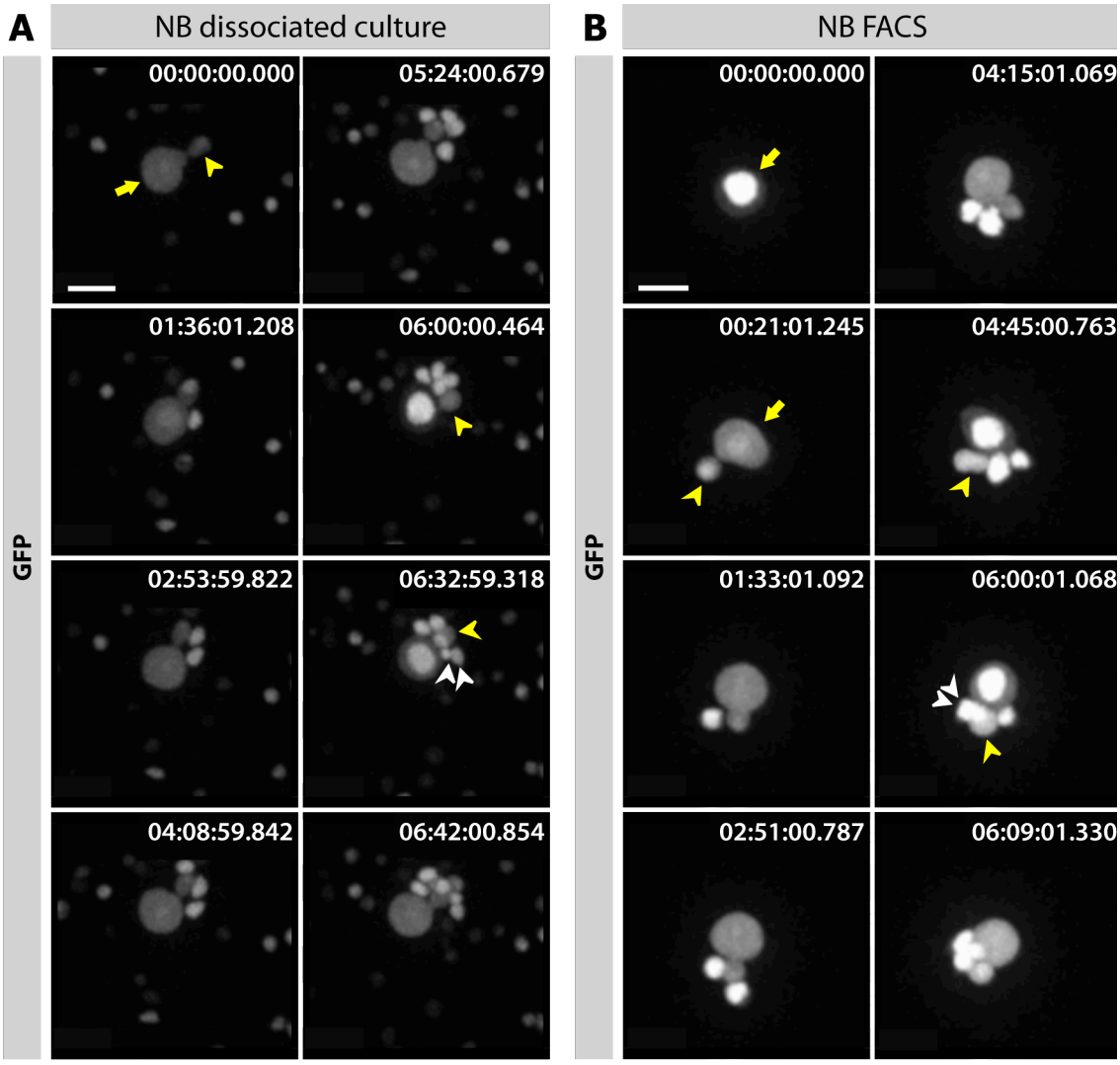
A
NB dissociated culture
GFP
00:00:00.000
05:24:00.679
01:36:01.208
06:00:00.464
02:53:59.822
06:32:59.318
04:08:59.842
06:42:00.854
B
NB FACS
GFP
00:00:00.000
04:15:01.069
00:21:01.245
04:45:00.763
01:33:01.092
06:00:01.068
02:51:00.787
06:09:01.330

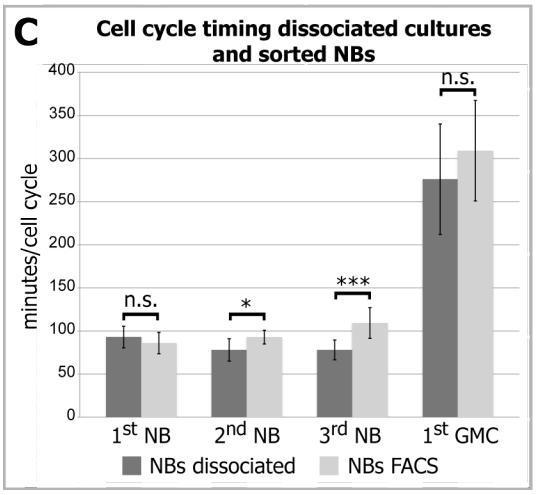
C
Cell cycle timing dissociated cultures and sorted NBs
minutes/cell cycle
400
350
300
250
200
150
100
50
0
n.s.
*
***
n.s.
1st NB
2nd NB
3rd NB
1st GMC
NBs dissociated
NBs FACS

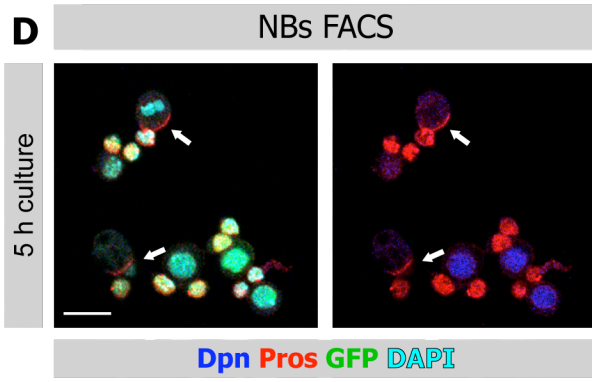
D
NBs FACS
5 h culture
Dpn Pros GFP DAPI

Figure 8. FACS sorted NBs divide asymmetrically

(A) Stills from a movie of a NB (yellow arrow) in an unsorted dissociated culture showing multiple rounds of asymmetric division. GMCs (yellow arrowhead) also divide and give rise to two neurons (white arrowheads). **(B)** Stills from a movie of a sorted NB showing multiple rounds of asymmetric divisions. The two first-born GMCs (yellow arrowhead) divide terminally to give rise to two neurons (white arrowheads). **(C)** Quantification of cell cycle lengths from ten NBs show that the first and second division of sorted NBs, as well as the division of the first GMC, are only slightly affected, while later divisions are delayed compared to unsorted NBs. Three subsequent divisions of ten NBs, and the time point of the first GMC division from three independent experiments each were measured. P-values (Student's t-test): 1st NB $p>0.05$, 2nd NB $p>0.01$, 3rd NB $p<0.001$, GMC $p>0.05$, n.s.=not significant. **(D)** Sorted Dpn positive NBs cultured for five hours show cortical localization of Pros (arrows), and multiple smaller Pros positive and Dpn negative GMCs. Scale bars are 12 µm.

4.1.4 Larval NB and neuron transcriptomes

After determining that FACS does not affect NB behavior, and that neurons still express differentiation markers, we collected enough material for deep sequencing of mRNAs from NBs and their differentiated progeny (scheme in Figure 6A). For our protocol, we first isolated total RNA, enriched for polyA$^+$-mRNA and hydrolyzed mRNA into 200-500 base pair (bp) long fragments. From double stranded cDNA that was synthesized from the RNA, libraries were generated, and sequenced by 76 bp paired-end Illumina mRNA sequencing (mRNAseq) (see 4.2.8 for details). To address biological and technical variability, we generated three samples each from NBs and neurons, of which we pooled two before RNA isolation and separated them again afterwards for further processing. In addition, a third biological replicate for NBs was generated, and sequenced twice (see Figure 9A for IDs). We got an average of around four million reads for the samples sequenced first on the Genome Analyzer IIX (Illumina), while we have a higher coverage, up to 30 million reads, for the two NB samples that were sequenced using the Hiseq2000 system (Illumina). Almost all reads mapped to genes, while only very few had no feature or mapped to more than one gene (Figure 9B).

For processing of the data, all rRNA reads were removed by alignment against known rRNA sequences (RefSeq). The remaining paired-end reads were then aligned against the *Drosophila melanogaster* genome (FlyBase r5.44) allowing a maximum of six mismatches and an intron size of 20 bp - 150 kb. Pseudogenes, snRNA, rRNA, tRNA and snoRNA were masked for downstream analysis. Gene expression was estimated as the number of fragments per kilobase of combined exon length (according to gene models in FlyBase r5.44) per one million of total mapped reads (FPKM value). For a detailed description of the bioinformatics analysis see 4.2.9.

When we compared the correlation coefficients of gene expression values (FPKM values) between technical and biological replicates from NBs and neurons, we found that technical replicates correlate perfectly, while biological replicates have slightly lower correlation coefficients (0.92 – 0.95) (Figure 9C). The correlation between NB and neuron samples is lower (0.41 – 0.61), which shows that a high number of genes are differentially regulated. Indeed, we found a total of 3532 genes that are differentially expressed between NBs and neurons (assuming a false discovery rate of

0.01, p-value<0.01), which corresponds to roughly 25 % of annotated genes in the *Drosophila* genome (Figure 9D). 1702 (48%) genes were expressed higher in NBs, while 1830 (52%) of these genes were up-regulated in neurons (data have been deposited in the NCBI Gene Expression Omnibus (GEO) and are accessible through GEO series accession number GSE38764). Of interest, a previous comparison of human dopaminergic neurons with progenitor cells (Marei *et al.*, 2011) has revealed a similar ratio of up- and down-regulated genes (47.5% of differentially regulated genes up in progenitors, 52.5% of genes up in neurons). We conducted a gene ontology (GO) term analysis from our results (Table 1, most highly enriched GO terms), which revealed processes like metabolism, cell cycle, DNA replication and ribosome biogenesis to be primarily up-regulated in NBs. It is not surprising that these GO terms were also found to be overrepresented in *brat* mutant tumors (Carney *et al.*, 2012). For genes up-regulated in neurons we found GO-term categories like cell communication, signal transduction, neuron differentiation and axonogenesis to be overrepresented. This is consistent with what is known about functional regulation in differentiated neurons.

To obtain more information about the quality of our deep sequencing data, we wanted to confirm expression levels of some known NB markers that were obtained by RNA Seq with qRT-PCR (Figure 9E). We sorted and collected NBs and neurons, applied the same procedure as for deep sequencing to the samples, and checked expression levels by qPCR. We could show with both methods that *mira*, *dpn*, *wor*, *numb* and *ase* were up-regulated in NBs, and that the genes *ELAV*, *brat* or *pros*, which are known to be involved in differentiation, are down-regulated in NBs. In almost all cases higher fold changes in transcription levels were detected with qPCR, however the trend of the transcriptional regulation was the same between the two methodologies. Thus, with our method we have generated high quality data of the transcriptional differences between a *Drosophila* larval NB and its differentiated sister cells.

A

	replica	ID
1	NB-1	8874
2	NB-2	8875
3	NB-2	8876
4	NB-3	9010
5	NB-3	9010
6	neuron-1	8877
7	neuron-1	8878
8	neuron-2	8879

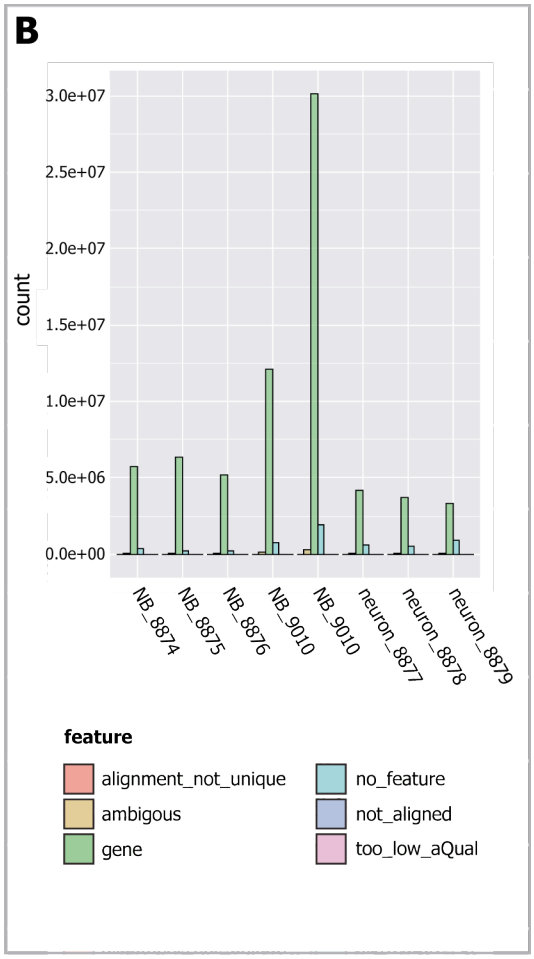

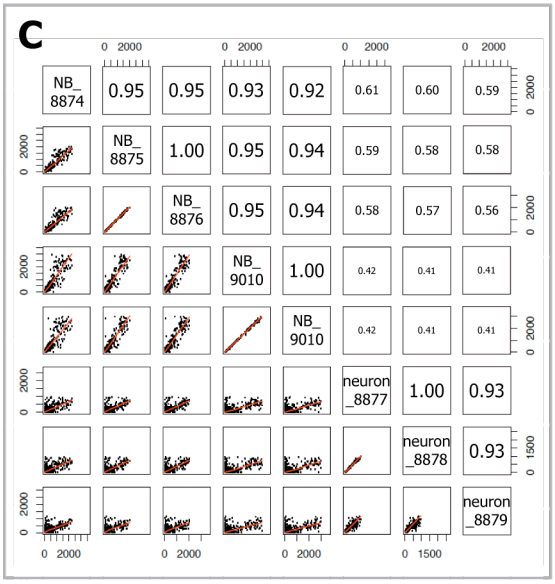

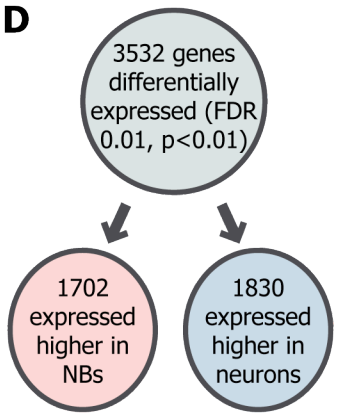

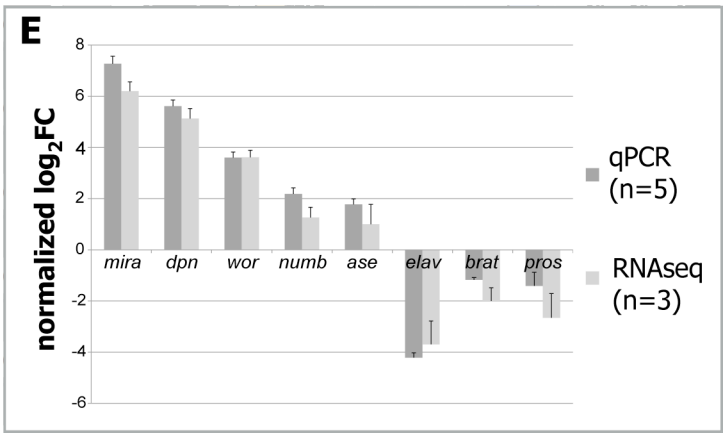

Figure 9. Bioinformatics analysis of RNAseq data from NBs and neurons
(A) Identification numbers of RNAseq samples. Three biological replicates from NBs, and two from neurons, as well as a technical replicate each, were sequenced. ID number 8875 and 8876 are technical replicates for a NB sample, and NB sample 9010 was sequenced twice. Samples 8877 and 8878 are technical replicates for a neuron sample. **(B)** Total of mapped reads to gene features. Between three to twelve million reads for the samples that were sequenced on the Genome Analyzer IIX were obtained, while 30 million reads were sequenced for the NB sample 9010 on the Hiseq200 machine. Most reads mapped to genes (green), and only few reads had no features (blue) or were ambiguous (yellow). **(C)** Correlation of gene expression values in fragments per kilobase of combined exon length per one million of total mapped reads (FPKM). Technical replicates correlate perfectly, while correlation for biological replicates is very high. Low correlation between NB and neuron samples indicates high numbers of differentially expressed genes. **(D)** 3532 genes are differentially expressed between NBs and neurons; 1702 are expressed higher in NBs, 1830 are expressed higher in neurons. **(E)** Expression levels of sorted NBs obtained by qRT-PCR and RNASeq data for known NB- and neuron-specific genes correlate (n denotes number of experiments, error bars represent standard deviation).

Table 1 Over-represented GO-terms in neuroblasts and neurons

Larval neuroblast		Larval neuron	
GO term (GO-ID)	Corr. p-value	GO term (GO-ID)	Corr. p-value
Metabolic process (8152)	9.63×10^{-41}	Cell communication (7154)	1.62×10^{-76}
Mitotic cell cycle (278)	1.18×10^{-40}	Signaling (23052)	4.32×10^{-76}
Mitotic spindle organization (7052)	6.06×10^{-34}	Response to stimulus (50896)	5.08×10^{-54}
Microtubule cytoskeleton organization (226)	9.70×10^{-33}	Signal transduction (7165)	1.46×10^{-53}
Cell cycle process (22402)	5.86×10^{-29}	Neuron projection morphogenesis (48812)	7.75×10^{-46}
DNA replication (6260)	1.25×10^{-28}	Neuron projection development (31175)	1.00×10^{-45}
Cellular biosynthetic process (44249)	3.48×10^{-28}	Axonogenesis (7409)	5.58×10^{-45}
M phase (279)	5.56×10^{-27}	Generation of neurons (48699)	5.58×10^{-45}
Microtubule-based process (7017)	1.26×10^{-25}	Neuron differentiation (30182)	1.12×10^{-44}
Ribonucleoprotein complex biogenesis (22613)	1.70×10^{-25}	Axon guidance (7411)	7.36×10^{-40}
Ribosome biogenesis (42254)	1.96×10^{-25}	Chemotaxis (6935)	2.09×10^{-39}
Macromolecule metabolic process (43170)	5.91×10^{-25}	Response to chemical stimulus (42221)	8.21×10^{-32}
Neurogenesis (22008)	8.01×10^{-25}	Regulation of signaling (23051)	1.97×10^{-30}
Gene expression (10467)	3.52×10^{-24}	Locomotion (40011)	2.21×10^{-30}
DNA metabolic process (6259)	5.53×10^{-23}	Nervous system development (7399)	2.22×10^{-28}

Gene ontology (GO term) analysis revealed processes expected for growing and dividing cells like metabolism, cell cycle, DNA replication and ribosome biogenesis to be enriched in NBs. Cell communication, signal transduction, neuron differentiation and axonogenesis are overrepresented in neurons. Corr. corrected.

4.1.5 Alternative splicing and 3'UTR extension

Our transcriptome data enabled us to investigate cell-type specific genes expression on a broad level, but it also allowed for the detection of splicing isoforms. This may be relevant for NB biology as RNA metabolism, transcription and splicing were among the processes that were transcriptionally up-regulated in NBs, and splicing was identified in a previous genome-wide RNAi screen as an important process in NBs (Neumuller *et al.*, 2011). In total, we found 69 genes that show an alternative primary transcript variant between NBs and neurons (see also Table 2 in appendix). Among those were genes known to be alternatively spliced, for example *longitudinals lacking* (*lola*) (Neumuller *et al.*, 2011), but also many genes for which tissue specific alternative splicing had not been described.

We found that the cell fate determinant *numb* has an alternative transcription start site and an alternatively spliced transcript in NBs and neurons. We have identified the isoform *numb*-RA to be primarily expressed in NBs, while differentiated neurons express an alternative isoform (*numb*-RB) (Figure 10A). A deletion analysis of *numb* has shown that *numb*-RA, but not *numb*-RB can segregate asymmetrically in NBs (Knoblich *et al.*, 1997). As Numb binds to α-Adaptin, which was shown to be required for pre-synaptic vesicle recycling (Gonzalez-Gaitan and Jackle, 1997), we speculate that Numb-PB could participate in this process in mature neurons.

Using our RNA sequencing data we could also address the recently identified phenomenon of 3'UTR elongation, which is thought to confer complex regulation on the posttranscriptional level (Hilgers *et al.*, 2011; Smibert *et al.*, 2012; Sandberg *et al.*, 2008). Shortening of 3'UTRs was discovered in murine T4 lympocytes and correlates with increased proliferation potential upon their activation (Sandberg *et al.*, 2008). The authors observed decreased protein expression upon forced expression of the full-length 3'UTR, which could be rescued in some cases by depleting predicted miRNA target sites in the long 3'UTRs. In addition, shortening of 3'UTRs was shown in cancer cells, which causes loss of miRNA binding sites and results in increased mRNA stability and protein expression of oncogenes (Mayr and Bartel, 2009). In fact, over-expression of oncogenes is more frequently detected than genetic modifications at these loci, and alternative cleavage and polyadenylation leading to 3'UTR shortening is a possible explanation for this phenomenon. Elongation of 3'UTRs has recently also been

described to be neural tissue specific during *Drosophila* development (Hilgers *et al.*, 2011; Smibert *et al.*, 2012). Both in *Drosophila* embryos as well as in the larval CNS, a large set of transcripts are extended beyond the predicted end of the 3'UTR. Interestingly, many of these are implicated in RNA binding or processing, and contain putative recognition motifs for the translational repressor Pumilio in their long 3'UTRs. Again, the authors proposed that this confers complex regulation by miRNAs or RNA binding proteins (Hilgers *et al.*, 2011). However, their findings do not link 3'UTR shortening with increased proliferation potential, but rather point to a correlation with cell type. Our data indicate that 3'UTR extension exists in both NBs and neurons in all those cases where transcripts could be detected in both samples despite the differential expression. This can be seen for *Hrb27c* and *brat*, two genes reported to display 3'UTR extension by Smibert *et al.* (2012) (Figure 10B). Intriguingly though, 357 of the 400 genes described in Smibert *et al.* (2012), are up-regulated in neurons, while only 40 genes are more highly expressed in NBs (see Table 3 in appendix). Therefore, even though 3'UTR elongation does not seem to be differentially regulated between NBs and neurons, the fact that the vast majority of genes displaying 3'UTR elongation are expressed higher in neurons, still points towards the idea that longer 3'UTRs are more prominent in non-proliferating cells and confer tight regulation of gene expression.

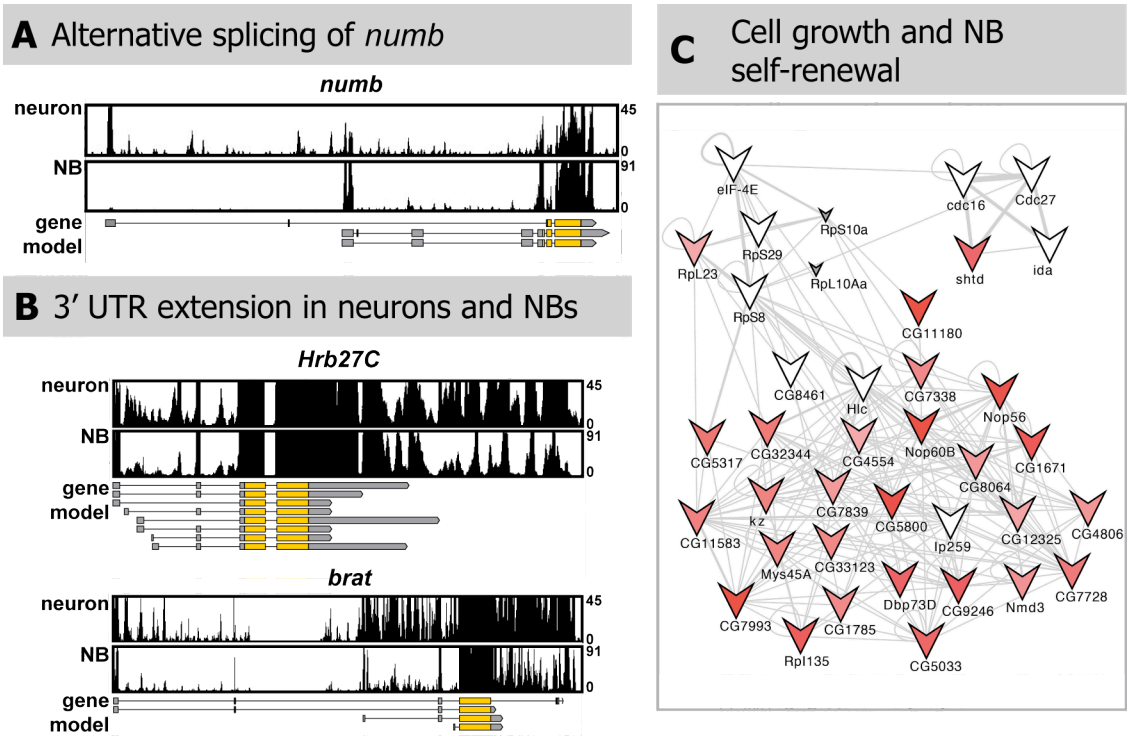

Figure 10. Bioinformatics analysis of transcriptome data
(A) Numb transcript is alternatively spliced. The gene model from flybase (r5.44) is indicated, numb-RB is specifically expressed in neurons (upper track), numb-RA in NBs (lower track). **(B)** *Hrb27c* and *brat* are shown as examples of genes with 3′UTR extensions. RNAseq tracks for neurons (upper track) and NBs (lower track) are shown. Note that for both genes the read coverage extends the 3′UTR annotated in flybase (r5.44). **(C)** A network of genes involved in cell growth and NB self-renewal, resulting in loss or under-proliferation of NBs upon knock down (Neumuller *et al.*, 2011). Correlation with gene expression data shows that 71% of genes are significantly up-regulated in NBs. Vee node shape denotes under-proliferation. Small grey nodes are genes not expressed in NBs or neurons. Red nodes are genes expressed significantly higher in NBs, the strength of color indicates fold change levels. White nodes are genes expressed at the same level in NBs and neurons.

4.1.6 Integrating transcriptional and phenotypic data

Recently developed transgenic RNAi technology has allowed for genome-wide RNAi screens in a tissue specific manner (Dietzl *et al.*, 2007). The genome-wide screen on NB self-renewal provided information on potential functions of genes based on their knock down phenotypes (Neumuller *et al.*, 2011). However, whether these genes are actually expressed in NBs and whether the resulting phenotypes could therefore be specific, and are not for example, due to off target effects, could not be determined. Our transcriptome data enabled us to correlate functional data from the genome-wide RNAi screen conducted in our lab (Neumuller *et al.*, 2011) with gene expression data, and an example is described. A set of 38 genes that cause NB loss or size reduction when knocked down in NBs was identified in the screen; besides a huge number of other genes. These genes were arranged in a potential network for growth and self-renewal (for original network see (Neumuller *et al.*, 2011)). When we plotted our expression data onto the existing network, as expected, we observed a tight correlation between the phenotypic data and our gene expression results (Figure 10C). All genes in the network are expressed in NBs, except for two (small grey nodes). Of these, 71 % are significantly up-regulated in NBs, as indicated by the red node color, and therefore might be responsible for the enhanced growth rate seen in NBs compared to GMCs and neurons.

Besides restricting functional data, our transcriptome data can also be used to expand functional regulatory networks from RNAi screens. An example is the functional network for asymmetric cell division, which was generated from a set of known regulators together with genome wide RNAi data (for original network see (Neumuller *et al.*, 2011)). We again found enrichment for genes resulting in an under-proliferation phenotype in the RNAi screen for NB self-renewal and differentiation (Neumuller *et al.*, 2011) to be expressed higher in NBs (vee node shape, red color). Genes that did not result in a phenotype upon knock down, but are differentially expressed between NBs and neurons can now expand this network. To limit the number of genes in the network, only genes with at least five previously reported protein interactions to members of the existing network were included (Figure 11) Such networks could form the basis for further studies to increase our understanding of neural stem cell biology.

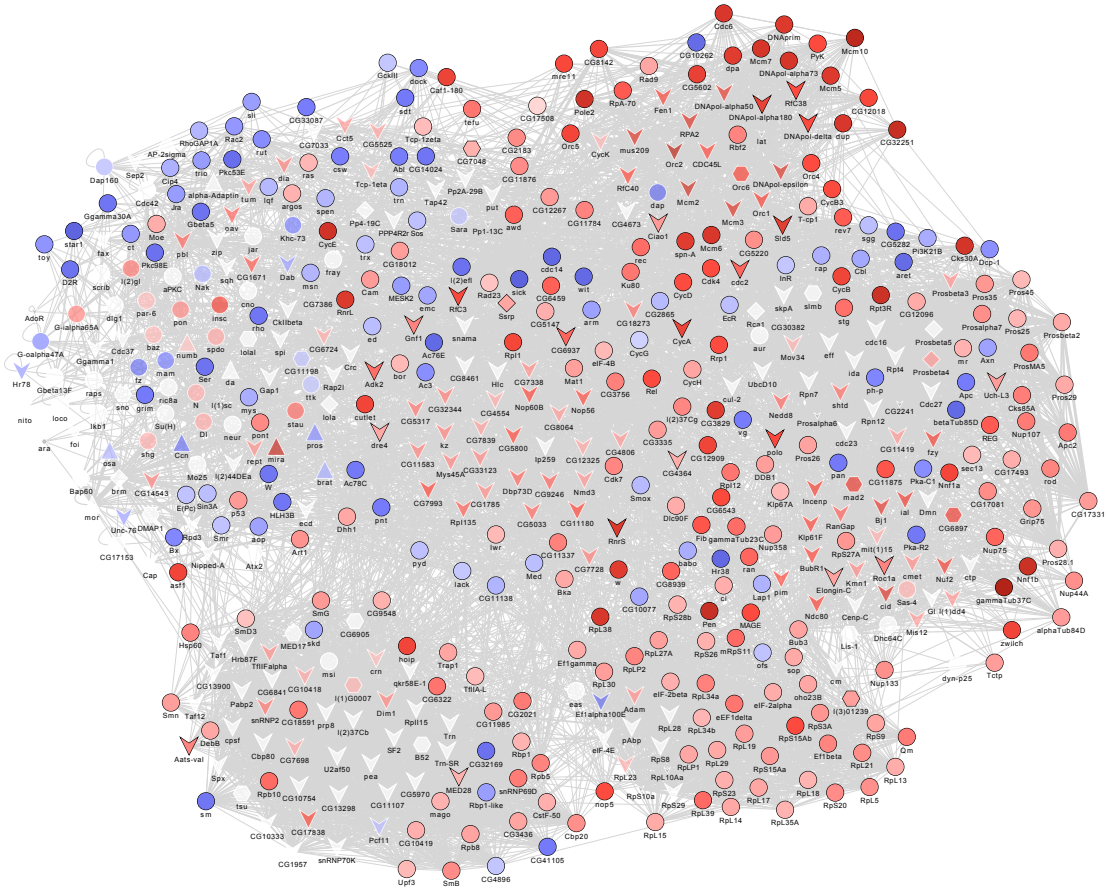

Figure 11. Expanded network of asymmetric cell division

An interaction network, starting from a set of 53 genes previously implicated in asymmetric cell division or spindle orientation, was generated based on databases (DroI , STRING and BioGRID) containing two-hybrid, biochemical, interlog, text-mining data and genetic interactions between *Drosophila* genes. Allowing only connections with genes that resulted in a phenotype in a genome-wide RNAi screen (Neumuller *et al.*, 2011) reduced the resulting network. Clustering algorithms (MCODE and MCL) were used to predict protein complexes. This network was expanded using the NB and neuron specific transcriptome data, and allowing only genes with a minimum of five direct interaction partners, based on the above databases.

Genes are shown as nodes, and the node of the color reflects the log fold change with grey denoting genes not found to be expressed, red denoting higher expression in NBs, and blue higher expression in neurons. Intensity of color reflects higher or lower log fold changes. The shape of the nodes denotes phenotypes from the RNAi screen – vee shape is under-proliferation, triangle is over-proliferation, diamond is over- and under-proliferation, hexagon is other (*e.g.* GFP aggregates), and ellipse is no phenotype.

4.1.7 A hypothetical transcriptional network for NB self-renewal

Re-growth of larval NBs to their original size after each cell division and maintenance of their identity over many divisions is a hallmark of these cells. This is in stark contrast to their differentiating sibling cells, which do not grow and divide terminally. NBs must therefore express a regulatory network of identity factors that is highly robust over time but can be rapidly and irreversibly modified by Numb, Pros and Brat in the GMC. Previous loss-of-function experiments have revealed a surprising level of redundancy among the known TFs acting in NBs (San-Juan and Baonza, 2011; Zacharioudaki *et al.*, 2012) (see introduction, 3.4.1) We therefore utilized our transcriptome data to identify a complete set of predicted TFs that are strongly and highly differentially expressed in NBs. In total, we found 28 TFs to match our criteria (FDR 0.01, logFC >3, FPKM value >15). We assumed that functionally related TFs are likely co-expressed and used stage and tissue specific microarray data (Chintapalli *et al.*, 2007) and the context likelihood of relatedness (CLR) algorithm (Faith *et al.*, 2007) to infer putative regulatory interactions (see 4.2.13 for more information).

The resulting hypothetical network for NB self-renewal contains six hubs (squares), which we have defined as hubs based on their connection to more than five genes in the network (Figure 12A). The first hub is *HLHmγ*, a direct nuclear target of the Notch signaling pathway (Almeida and Bray, 2005). *HLHmγ* connects to *dpn* and both were shown to act redundantly in controlling NB self-renewal (Zacharioudaki *et al.*, 2012). It also connects to *worniu* (*wor*), a member of the snail protein family. Wor is involved in localization of cell fate determinants and orientation of the mitotic spindle in the *Drosophila* embryo by regulating the expression of *inscuteable* and *string* (Cai *et al.*, 2001; Ashraf and Ip, 2001). However, its role in postembryonic NBs is still unknown. *HLHmγ* also has a connection to *klumpfuss* (*klu*), which is specifically expressed in many embryonic NBs. It is involved in the specification of the second born GMC in the embryonic NB4-2 lineage, possibly contributing to the contextual information in which Notch signaling influences differential cell fate choices (Yang *et al.*, 1997) (see also 5.1). Finally, *HLHmγ* connects to *grainy head* (*grh*), the most highly differentially expressed gene in our proposed network of NB self-renewal. Our data confirms the previously described existence of alternatively spliced NB-specific isoforms (N- and O-isoform) (Uv *et al.*, 1997). *Grh* is involved in regulating the proliferation of NBs and depending on the temporal and spatial context can act either pro- or anti-proliferative

(Cenci and Gould, 2005; Almeida and Bray, 2005; Maurange *et al.*, 2008). Surprisingly, Grh is actually a negative regulator of HLHmγ (Almeida and Bray, 2005), but it was proposed that such paradoxical elements are frequent components of transcriptional circuits and can maintain homeostatic concentrations or contribute to robust regulation (Hart *et al.*, 2012). Thus, *HLHmγ* is a major hub for transcriptional activation immediately downstream of Notch.

HLHmγ, *wor* and *ken* are connected to two other hubs that contain genes involved in ribosome biogenesis and growth control. Modulo (Mod) is the *Drosophila* homolog of Nucleolin, the major nucleolar protein of growing eukaryotic cells that is thought to play a role in rRNA transcription and ribosome assembly (Srivastava and Pollard, 1999). CG10565 is the fly ortholog of MPP11, a chaperone of the DNA-J family that is involved in ribosome assembly and was implicated in the regulation of cell growth (Otto *et al.*, 2005; Jaiswal *et al.*, 2011). *Bigmax* and *TFAM* are connected to *CG10565*, and are direct downstream targets of the major growth regulators Myc and Max and therefore might be involved in growth control (Orian *et al.*, 2003).

A fourth interesting hub is *Structure specific recognition particle* (*Ssrp*), a chromatin regulator that was found in the NB-specific RNAi screen to result in over-proliferation upon knock down (Neumuller *et al.*, 2011). Surprisingly, Ssrp RNAi causes gain rather than loss of NBs and might therefore maintain a chromatin state that allows differentiation.

Finally, Ken and Co-repressor of pangolin (Coop) have been implicated in Jak/STAT (Arbouzova *et al.*, 2006) and wingless signaling (Song *et al.*, 2010), respectively. Both of these pathways are linked to Notch signaling, although no such functional link is described in NBs.

Thus, our hypothetical transcriptional network provides potential explanations for several aspects of NB biology. For example, it could explain the direct effect of Notch signaling on cell growth that was described in *Drosophila* NBs (Song and Lu, 2011).

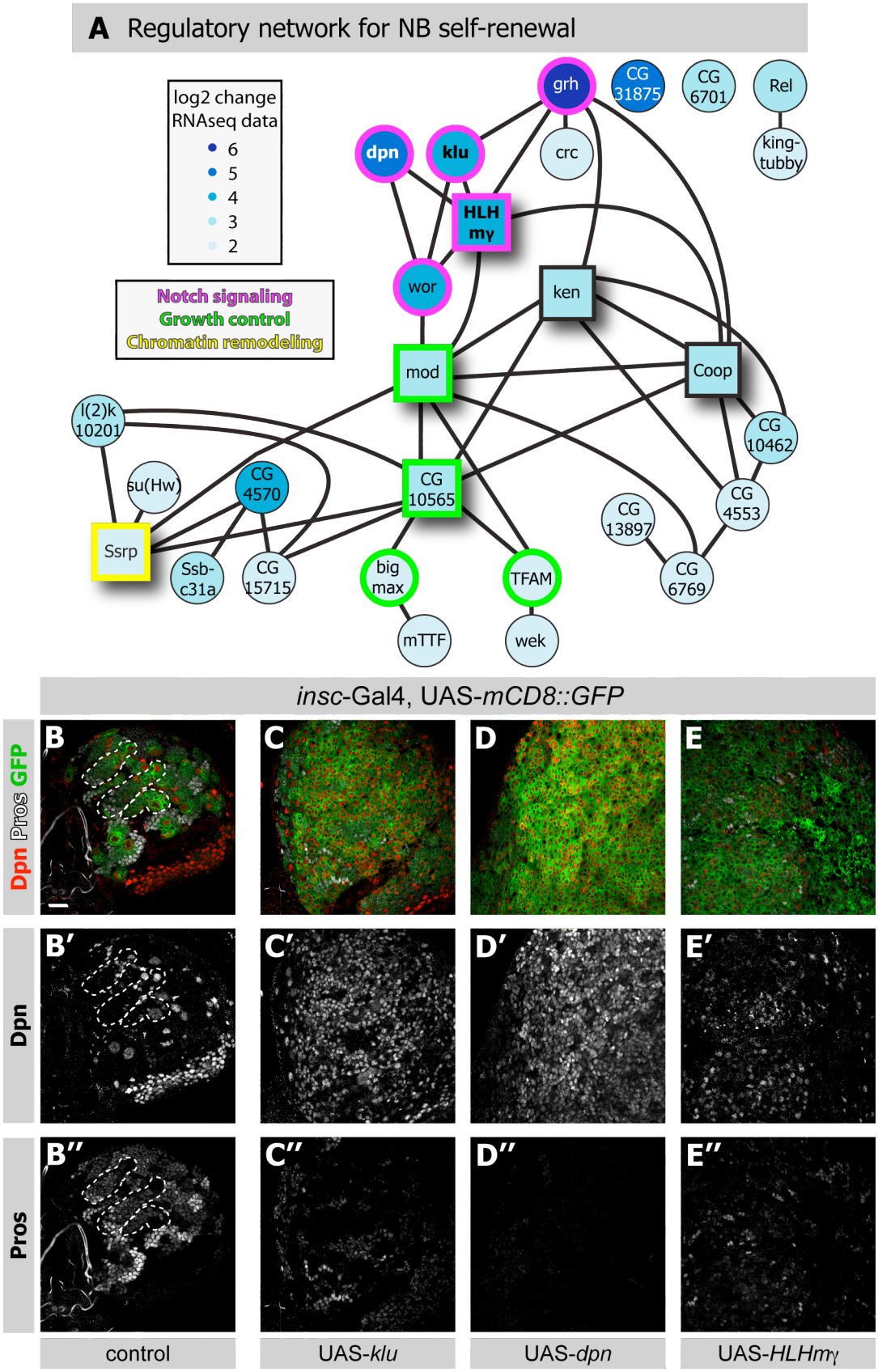
A Regulatory network for NB self-renewal
log2 change RNAseq data
6
5
4
3
2
Notch signaling
Growth control
Chromatin remodeling
grh
CG 31875
CG 6701
Rel
king-tubby
dpn
klu
crc
HLH mγ
wor
ken
mod
Coop
l(2)k 10201
CG 10462
su(Hw)
CG 4570
CG 10565
CG 4553
CG 13897
Ssrp
Ssb-c31a
CG 15715
big max
TFAM
CG 6769
mTTF
wek
insc-Gal4, UAS-mCD8::GFP
Dpn Pros GFP
B
C
D
E
Dpn
B′
C′
D′
E′
Pros
B″
C″
D″
E″
control
UAS-klu
UAS-dpn
UAS-HLHmγ

Figure 12. A hypothetical transcriptional network for NB self-renewal indicates a tight relationship between Notch signaling, growth and chromatin state.

(A) Hypothetical transcriptional network of 28 strong and differentially expressed TFs in NBs (FDR 0.01, log2FC >3, FPKM value >15) based on correlative *Drosophila* microarray expression data. Genes involved in growth control (*modulo*, *CG10565*, *bigmax*, *TFAM*), genes downstream of, or regulated by, Notch signaling (*HLHmγ*, *dpn*, *worniu*, *klumpfuss*, *grainy head*) and the chromatin remodeler *Structure specific recognition particle* are marked in green, magenta and yellow, respectively. Hubs are indicated with squares. **(B-E'')** Larval brains over-expressing *klu* (C-C''), *dpn* (D-D''), *HLHmγ* (E-E''), and control (B-B'') stained for Dpn and Pros. Ectopic expression of these genes leads to over-proliferation of Dpn positive cells at the expense of differentiating cells, as can be seen by the loss of Pros staining. Scale bars are 20 µm.

4.1.8 *HLHmγ*, *klu* and *dpn* over-expression causes ectopic NB formation

To test the functional relevance of the identified TFs, we performed knock down and over-expression studies. None of the factors we have identified from our transcriptome data and which are part of the hypothetical network for NB self-renewal were found to result in loss or under-proliferation of NBs in the RNAi screen by Neumuller *et al.* (2011). Some of the factors in our network cause lethality upon knock down in this screen (*crc*, *TFAM*, *ken* and *CG15715*). However, since NB number and size were not affected in L3 larval brains, which we confirmed, the observed lethal phenotype might be due to off-target effects or secondary phenotypes caused by expression of RNAi in other tissues. Most crosses of these NB specific TFs in the RNAi screen were actually viable and therefore were not analyzed further. Regardless of viability, we investigated knock down brain phenotypes of all factors in our potential network for NB self-renewal by immunofluorescence, utilizing both VDRC libraries (GD and KK), as well as Transgenic RNAi Project (TRiP) lines from Harvard Medical School (www.flyrnai.org). However, we could not detect any phenotypes affecting number, lineage or size of NBs.

We assumed high levels of redundancy to account for the lack of knock down phenotypes, which had in fact been shown for *dpn* and *HLHmγ* (Zacharioudaki *et al.*, 2012), and that key factors need to be down-regulated, rather than up, during differentiation. Thus, we generated over-expression constructs and used targeted insertion to generate fly stocks for all 28 NB-specific TFs. We expressed them in type I and type II NBs as well as GMCs and INPs using *insc*-Gal4. While most factors did not cause over-proliferation phenotypes, *HLHmγ*, *dpn* and *klu* over-expression resulted in a strong expansion of the NB pool, as can be seen by the excess of Dpn positive cells at the expense of Pros positive differentiating neurons (Figure 12B-D). As the *dpn* and *HLHmγ* over-expression phenotypes were already described for larval NBs (San-Juan and Baonza, 2011; Zacharioudaki *et al.*, 2012), we focused on the characterization of Klu, which is described in the next chapter.

4.2 EXPERIMENTAL PROCEDURES

4.2.1 Fly strains

Flies were raised on standard corn medium at 25 °C unless otherwise stated.

Stock	Type	Generated
;;*ase*-Gal4, UAS-*stingerGFP*	Gal4-line	(Zhu *et al.*, 2006), (Barolo *et al.*, 2000)
UAS-*Dicer2*; MZ1407(*insc*)-Gal4, UAS-*mCD8::GFP*	Gal4-line	(Neumuller *et al.*, 2011)
UASt.attB-*Rel*	UAS-line	This study
UASt.attB-*king-tubby*	UAS-line	This study
UASt –*grh*	UAS-line	(Almeida and Bray, 2005)
UASt.attB-*crc*	UAS-line	This study
UASt.attB-*HLHmγ*	UAS-line	This study
UASt.attB-*dpn*	UAS-line	This study
UASt.attB-*wor*	UAS-line	This study
UASt.attB-*ken*	UAS-line	This study
UASt.attB-*mod*	UAS-line	This study
UASt.attB-*bigmax*	UAS-line	This study
UASt.attB-*TFAM*	UAS-line	This study
UASt.attB-*wek*	UAS-line	This study
UASt.attB-*mTTF*	UAS-line	This study
UASt.attB-*Coop*	UAS-line	This study
UASt.attB-*Ssb-c31a*	UAS-line	This study
UASt.attB-*su(Hw)*	UAS-line	This study
UASt.attB-*l(2)k10201*	UAS-line	This study
UASt.attB-*6701*	UAS-line	This study
UASt.attB-*31875*	UAS-line	This study
UASt.attB-*10462*	UAS-line	This study
UASt.attB-*4553*	UAS-line	This study
UASt.attB-*6769*	UAS-line	This study
UASt.attB-*13897*	UAS-line	This study
UASt.attB-*15715*	UAS-line	This study
UASt.attB-*4570*	UAS-line	This study

UAS-*Rel* RNAi	UAS-RNAi	TID 49414 and 108469 (VDRC)
UAS-*king-tubby* RNAi	UAS-RNAi	TID 29110 and 29111 (VDRC)
UAS-*grh* RNAi	UAS-RNAi	TID 101428 and 106879 (VDRC)
UAS-*crc* RNAi	UAS-RNAi	TID 2934, 2935 and 109014 (VDRC)
UAS-*klu* RNAi	UAS-RNAi	TID 51276, 51277 (VDRC) and 28731 (BDSC)
UAS-*HLHmγ* RNAi	UAS-RNAi	TID 10950 (VDRC) and 25978 (BDSC)
UAS-*dpn* RNAi	UAS-RNAi	TID 106181 (VDRC) and 26320 (BDSC)
UAS-*wor* RNAi	UAS-RNAi	TID 6248 and 105362 (VDRC)
UAS-*ken* RNAi	UAS-RNAi	TID 48595 and 48596 (VDRC)
UAS-*mod* RNAi	UAS-RNAi	TID 52268 (VDRC) and 25978 (BDSC)
UAS-*bigmax* RNAi	UAS-RNAi	TID 11259 and 110630 (VDRC)
UAS-*wek* RNAi	UAS-RNAi	TID 12706 and 12707 (VDRC)
UAS-*mTTF* RNAi	UAS-RNAi	TID 25296 and 101656 (VDRC)
UAS-*Coop* RNAi	UAS-RNAi	TID 108055 (VDRC) and 29350 (BDSC)
UAS-*Ssb-c31a* RNAi	UAS-RNAi	TID 47383 and 103016 (VDRC)
UAS-*su(Hw)* RNAi	UAS-RNAi	TID 10724 and 100395 (VDRC)
UAS-*l(2)k10201* RNAi	UAS-RNAi	TID 4175 and 108881 (VDRC)
UAS-*6701* RNAi	UAS-RNAi	TID 36557 (VDRC) and 27560 (BDSC)
UAS-*31875* RNAi	UAS-RNAi	TID 45070 and 104638 (VDRC)
UAS-*10462* RNAi	UAS-RNAi	TID 31246 and 31247 (VDRC)
UAS-*4553* RNAi	UAS-RNAi	TID 14743 and 105569 (VDRC)
UAS-*6769* RNAi	UAS-RNAi	TID 103737 (VDRC)
UAS-*13897* RNAi	UAS-RNAi	TID 39733 and 108487 (VDRC)
UAS-*15715* RNAi	UAS-RNAi	TID 108387 (VDRC)
UAS-*4570* RNAi	UAS-RNAi	TID 21827 and 109328 (VDRC)

Over-expression and RNAi was driven by UAS-*dicer2*; MZ1407(*insc*)-Gal4, UAS-*mCD8::GFP* at 25 °C for 24 h and then shifted to 29 °C for five days.

4.2.2 Cell dissociation

Third instar larva were collected approximately six days after egg laying (AEL), washed once each in PBS and 70 % ethanol, and dissected in supplemented Schneider's medium (10 % FBS [Gibco], 2 % Penicillin/ Streptomycin [Life Technologies], 0.02 mg/mL insulin [Life Technologies], 20 mM L-glutamine [Life Technologies], 0.04 mg/mL L-glutathione [Sigma-Aldrich], Schneider's medium [Gibco]) at room temperature. Larval brains were collected and washed twice in Rinaldini solution (800 mg NaCl, 100 mg glucose, 100 mg $NaHCO_3$, 5 mg NaH_2PO_4, 20 mg KCl in 100 mL of water, (Ceron *et al.*, 2006)) on ice. They were then incubated in Rinaldini solution with the addition of a final concentration of 1 mg/mL collagenase I and 1 mg/mL papain (Sigma Aldrich) at 30 °C for one hour. Brains were carefully washed twice in Rinaldini solution and twice in supplemented Schneider's medium, and disrupted manually with a pipette tip in 200 µL supplemented Schneider's medium. The tissue pieces were forced through a cell strainer FACS tube (BD Falcon) and then either plated on cover slips blocked with heat-inactivated FBS (Gibco) for single cell collection, Poly-D-lysin-hydobromide (Sigma Aldrich) coated glass bottom dishes (MatTek Corporation) for immunostainings or live-imaging, or cells were subjected to FACS.

4.2.3 Single cell collection and whole transcriptome amplification

For collection of single cells, the cell suspension was plated on culture wells slides with silicon gaskets (Grace Bio-Labs, CDCS 2R-2.0), which were blocked with heat-inactivated fetal bovine serum (hi-FBS [Gibco]). The custom made capillary (Eppendorf) with a diameter of 12 µm was clamped into a capillary holder and micromanipulator (Eppendorf), in an angle so that the beveled edge of the capillary was visible from the side. Aspirating hi-FCS and releasing it again blocked the capillary. Then the capillary was filled with with Voltalef oil 10s (VWR Jencons). The collection of strongly GFP positive and large NBs was monitored under bright light and with fluorescence (Zeiss Axio Lab.A1).

Cells were lysed directly after collection in the respective lysis buffers for Global Amplification of single cell cDNA (Kurimoto *et al.*, 2007) or the WT-ovation system (Nugen Technologies, Inc). The flat lid of a PCR tube was removed and one µL of lysis buffer was put on a drop of Voltalef Oil 10s. The lid was placed under the microscope and the collected cells were released directly into the lysis buffer. The drop of oil and lysis buffer was then transferred into the PCR tube, which contained the remainder of the lysis buffer. Following brief centrifugation, generation and amplification of cDNA was carried out as described in (Kurimoto *et al.*, 2007), or following the manufacturer's instructions for the WT-ovation system (Nugen Technologies, Inc). For gene expression analysis see 4.2.10.

4.2.4 Immunohistochemistry and microscopy of cultured cells and larval brains

For immunostainings of sorted and unsorted cells, cells were plated on coated glass bottom dishes (MatTek Corporation). For coating of dishes, they were washed with 70 % Ethanol, dried, and coated with Poly-D-lysin-hydobromide (Sigma Aldrich) for 30 minutes. After washing with Mono Q water, dishes were dried under UV-light for one and half hours.

Cells were kept on glass bottom dishes for approximately three hours, depending on the experiment either on ice (no cell divisions), or at room temperature in supplemented Schneider's medium. Afterwards, cells were fixed for five minutes at room temperature with 5 % paraformaldehyde (PFA), 0.1 % Triton-X 100 in PBS, and washed twice for two minutes each with PBS. Cells were blocked in 5 % normal goat serum (NGS) in PBS at 4 °C overnight, and then incubated with primary antibody in blocking solution for one hour at room temperature. Following two 15 minutes wash steps in PBS, labeling with commercially available secondary antibodies (Invitrogen) in a one in 400 dilution was performed in blocking solution at room temperature for one hour. After repeating the two 15 minutes washes with PBS, Vecta shield with or without DAPI (Vector Laboratories, Inc.) was applied and dishes were stored at 4 °C until imaging.

For immunohistochemistry of larval brains, third instar larva were collected approximately six days AEL, and brains were dissected and kept in ice-cold PBS until they were fixed for 20 minutes in 5 % PFA, 0.1 % Triton-X 100 in PBS. All consecutive 15 minutes wash steps were done with 0.1 % Triton-X 100 in PBS. Brains were blocked in 5 % NGS for one hour, and incubated with primary antibodies over night at 4 °C. Labeling was carried out using commercially available secondary antibodies (Invitrogen) in a one in 400 dilution for two hours in blocking solution at room temperature.

Images were taken on a LSM510 or 780 (Carl Zeiss GmbH) and AIM and Zen software was used for image analysis (Carl Zeiss GmbH), and image processing was performed using Adobe Photoshop CS4 (version [v] 11.0.1).

4.2.5 Antibodies

Antibodies used: guinea pig anti-Dpn (1:1000, (Lee and Luo, 2001), courtesy of J. Skeath), mouse anti-Pros (1:100, MR1A, Developmental Studies Hybridoma Bank [DSHB]), mouse anti-Repo (1:100, 8D12, DSHB), rabbit anti-Mira (1:200, (Betschinger *et al.*, 2006)), rabbit anti-aPKC (1:500, Santa Cruz Biotechnology), mouse anti-PH3 (1:1000, Cell Signaling Technology), rat anti-ELAV (1:100, 7E8A10, DSHB), rabbit anti-Pins (1:200, (Schaefer *et al.*, 2000)) and rabbit anti-Numb (1:100, (Rhyu *et al.*, 1994)).

4.2.6 Fluorescence-activated cell sorting

Larval NBs and neurons were sorted with an FACSAriaIII machine (BD) with a 100 µm nozzle and at low pressure setting (20 psi) according to cell size and GFP intensity (see 4.1.2 for exact FACS strategy). Depending on the age of the larva, 100 – 150 NBs and 18 000 – 25 000 neurons per brain could be reproducibly sorted and purities of the sorted cell populations were reproducibly high.

For RNA isolation, NBs were sorted directly in 750 µL of TRIzol LS reagent (Invitrogen) and topped up to one mL with RNase-free water (Ambion). Neurons were sorted in 1.5 mL eppendorf tubes, centrifuged at 3000 rpm at 4 °C for 15 minutes, and after removal of the supernatant except for 50 µL, 750 µL of TRIzol LS was added. Up to five tubes were combined and filled up to one mL. For colchicine experiments, sorted cells were subjected to a 16 h treatment of 25 µM colchicine at room temperature and were then fixed and stained as described (4.2.4).

4.2.7 Live imaging

Live imaging of cells in culture was performed on a PerkinElmer UltraViewVox confocal spinning disc on a Zeiss Axio Observer microscope. Cells were kept in Schneider's medium in coated glass-bottom dishes and left to settle for two hours after dissociation. NBs were directly sorted onto the dishes, and left to settle for two hours before live-imaging as well. The interval for picture recording was set to three minutes and multiple positions were monitored. Cell cycle lengths were measured from nuclear break-down of NBs/GMCs until the next nuclear break-down.

4.2.8 RNA sequencing sample preparation

Per experiment, total RNA from 200 000 – 250 000 sorted NBs and 28 – 35 million neurons was isolated by TRIzol purification following the manufacturers instructions for low amounts of RNA (Invitrogen). Quality was assessed on a bioanalyzer (Agilent), and only non-degraded RNA was processed further. The obtained RNA was enriched for poly(A) plus mRNA with two rounds of Dynabeads mRNA purification (Invitrogen), and fragmented for two and a half minutes at 94 °C with fragmentation buffer (200 mM Tris pH 8.2, 500 mM KOAc, 150 mM MgOAc). Then first strand cDNA was synthesized using one µL of random hexamer primers (3µg/ µL) following standard cDNA protocols (SuperScript III, Invitrogen,). MiniQuick spin DNA columns (Roche) were used to eliminate dNTPs and enzymes. To generate second strand cNDA, 1x Second strand buffer (Invitrogen), 200 nM final concentration of ATP, CTP, GTP and UTP (5prime), 20 U of *E. coli* DNA ligase (Invitrogen), 40 Units of polymerase I (Invitrogen), and four Units of *E. coli* RNase H (Invitrogen) were added to the first strand cDNA and incubated for at 16 °C two hours. Double stranded cDNA was purified using the MinElute reaction clean-up kit (Qiagen), and quantified using the Quant-iT Picogreen dsDNA Assay (Invitrogen) in a NanoDrop Fluorospectrophotometer ND-3300.

Library preparation was carried out using a modified protocol from Illumina with NEBNext DNA sample Prep Reagent kits (NEB). Double stranded cDNA was end-repaired, poly(A) was added and adapters were ligated to DNA fragments. After size selection (200 – 600 bp), and UDGase-treatment (NEB) for strand-specificity, adapter-modified DNA fragments were enriched by PCR, and amount and quality was assessed by qPCR and bioanalyzer (Agilent), respectively. After each step, reactions were cleaned up using the QIAquick PCR purification kit (QIAGEN). 76 base paired-end sequencing was performed on a GAIIX or Hiseq2000 machine (Illumina).

4.2.9 Bioinformatics RNA sequencing

The strand specific paired-end reads were screened for ribosomal RNA by aligning with Burrows-Wheeler Alignment (BWA) (v0.6.1) (Li *et al.*, 2009a) against known rRNA sequences (RefSeq). The insert statistics were estimated by aligning the remaining reads uniquely to the transcriptome and by calculating the mean insert length and standard deviation. The rRNA subtracted paired-end reads were aligned with TopHat (v1.4.1) (Trapnell *et al.*, 2009) against the *Drosophila melanogaster* genome (FlyBase release 5.44) with a maximum of six mismatches. Based on FlyBase statistics, introns of a size between 20 – 150 000 bp were allowed. Maximum multi hits was set to one and InDels as well as Microexon-search was enabled. Additionally, a gene model was provided as Gene Transfer Format (GTF) (FlyBase r5.44). Pseudogenes, snRNA, rRNA, tRNA and snoRNA were masked for downstream analysis. Aligned reads in valid pairs were subjected to FPKM estimation with Cufflinks (v1.3.0) (Trapnell *et al.*, 2010; Roberts *et al.*, 2011). In this step bias detection and correction was performed, and only those fragments compatible with FlyBase annotation (r5.44) were allowed and counted towards the number of mapped hits used in the FPKM denominator. Furthermore, the aligned reads were counted with HTSeq and the polyA containing transcripts were subjected to differential expression analysis with DESeq (v1.8.3) (Anders and Huber, 2010). Parameters were chosen to match the DESeq publication. GO annotation is from flybase (r5.44), and analysis was done using BINGO, a plugin (Maere *et al.*, 2005) for cytoscape (http://www.cytoscape.org).

4.2.10 Quantitative PCR analysis of sorted NBs and neurons

qPCR data was generated using iQ™ SYBR Green supermix (Bio-Rad) following the manufacturers instructions and a two-step qPCR protocol on a BioRad CFX96 cycler. The following primer pairs at a final concentration of 250 nM were used.

Primers used in Figure 5.

Gene	Forward primer	Reverse primer
sta	CTACGTGAACATCCCCGTGATT	GCCACCACATCAGACCGATAG
Qm	CCACGTCATTCGCATCAACAAAATG	GACCAATACGAACTCGAGCAAC
eIF-4a	TCAACGTGAAGCAGGAGAACTG	AGATTACCGACTGGGTGATGGA
Sap-r	GTCTAGCAGCATCAAGGAGCC	GCTCGCTTAATGTCGTCCTGTT
Tango7	CACCAACCTGGAGCTGTCTTC	CAAGGCAGTCACAATGCACTTC
Caf-1	CAGAGTACGGAGGATGCTGAG	GTAAACATTCTCGGCCATCTGC
cycA	GCCATGCGGGAAAAGTACAAT	GCTGGTGCTCATCCTCTTTC
ELAV	CGCACCATTCGGAGCAATAAT	AGGCAATGATAGCCCTTGTGG
mira	CCCAATTGGAGCTGGACAACA	GGTGTTCCCAGCAGAGAGG
dpn	CGCTATGTAAGCCAAATGGATGG	CTATTGGCACACTGGTTAAGATGG
pros	GCTGTCACCGAAGGCATCAAG	GAAGAACTCCCGCAGAGTCG
wor	CAGTAATGGTGAAGAGGAGGAG	GATTAATAAATGGCCGGTGGTTG
RpS8	CTTGGTGAAGAACAGCATCGTG	GTCGTTCTCGTCCTCTTTCTGG
GapDH1	CGAAATCAAGGCTAAGGTCGAG	GAATGGGTGTCGCTGAAGAAGT
insc	GACATATCCCAGTTAGCGCGA	GACGATTTGGCCTTGGTTTTGC
numb	CGAGACCAAGGGCCTGATAG	ATCCCGGCATATGTAGCTGAAG
brat	GTGGTTAGTGGCGCTGGAG	GGATAGATAGTGGCCGAAAGC

Primers used in Figure 10B.

Gene	Forward primer	Reverse primer
mira	CCCAATTGGAGCTGGACAACA	GGTGTTCCCAGCAGAGAGG
dpn	CGCTATGTAAGCCAAATGGATGG	CTATTGGCACACTGGTTAAGATGG
wor	CAGTAATGGTGAAGAGGAGGAG	GATTAATAAATGGCCGGTGGTTG
numb	CGAGACCAAGGGCCTGATAG	ATCCCGGCATATGTAGCTGAAG
ase	CAGTGATCTCCTGCCTAGTTTG	GTGTTGGTTCCTGGTATTCTGATG
elav	CGCACCATTCGGAGCAATAAT	AGGCAATGATAGCCCTTGTGG
brat	GTGGTTAGTGGCGCTGGAG	GGATAGATAGTGGCCGAAAGC
pros	GCTGTCACCGAAGGCATCAAG	GAAGAACTCCCGCAGAGTCG

4.2.11 Bioinformatics analysis – alternative splicing

Aligned reads of the technical replicates were merged into one biological replicate (Li *et al.*, 2009b). The different biological replicates were analyzed with cuffdiff (v1.3.0) (Trapnell *et al.*, 2010). The reads were bias corrected and only reads compatible with the annotation (r5.44) were considered. Significant splice variant switches (FDR < 0.01) were retrieved with a custom R script.

4.2.12 Bioinformatics analysis – network generation

Starting from a set of 53 genes previously implicated in asymmetric cell division or spindle orientation, databases (DroID [www.droidb.org] [v5], STRING [v7.0 and v8.2] and BioGRID [v2.0.40]) were queried containing two-hybrid, biochemical, interlog, text-mining data and genetic interactions between *Drosophila* genes. The resulting network (drawn using cytoscape [http://www.cytoscape.org]), was reduced by allowing only connection with genes that resulted in a phenotype in a genome-wide RNAi screen (Neumuller *et al.*, 2011). Clustering algorithms (Molecular Complex Detection [MCODE], (Bader and Hogue, 2003)) and Molecular Complex Detection [MCL], (Enright *et al.*, 2002)) was used to predict protein complexes. This network was expanded using our transcriptome data and allowing only genes with a minimum of five direct interaction partners, based on the above databases.

4.2.13 Bioinformatics – microarray analysis and network inference

Microarray data were obtained from the FlyAtlas (Chintapalli *et al.*, 2007) project and supplemented with some of our own data ((Neumuller *et al.*, 2011) and unpublished data). All network inference and microarray analysis was performed in R using Bioconductor packages. Raw probe intensities were normalized using robust multi-array analysis (RMA) (Irizarry *et al.*, 2003). The CLR algorithm (Faith *et al.*, 2007) was used to infer putative regulatory interactions at a standardized difference scores (z-score) cut-off of six.

4.2.14 Generation of over-expression constructs

Total RNA was extracted from third instar larval brains and transcribed into first strand cDNA using oligo(dT) primers (Invitrogen) and SuperScriptIII (Invitrogen). Coding sequences, including stop codon, were amplified using Fusion Taq Polymerase (Finnzymes) with the following specific primer pairs:

Gene	Forward primer	Reverse primer
Bigmax	CACCATGAGCGATAATAACAACGCGTTG	TCAGCTGAAACCCTCGCTCG
Coop	CACCATGGAGATGGCCTACAATGCGT	TCAGCCAAACTCCAGTTCCTC
CG4553	CACCATGACTGCCCGCATGATCCAA	CTATTTATCACCACTGGCTCTG
CG4570	CACCATGGTTCTCGCTCCCGAAGTT	CTAGCAGAACTCGGTCTGATC
CG6701	CACCATGACAAAAAATAAAAAGAACATAATCAAC AAT	TTATGAAATGATACAGTTGAATTTTTTGT TC
CG6769	CACCATGTCGCACTTCACCTGCCT	TTAGATCAGAACCTGTGCACGATA
CG10565	CACCATGACGAGCGGTACGGTAGC	TCATTTGACCGCCGCCTGTG
CG13897	CACCATGGACATGCACAGGCTGATCT	TCAGTTCCAATTCGTGGAGCTTG
CG15715	CACCATGGCACGTGGACACCAGAA	TCAGACCTCCTTCAGCTCCT
CG31875	CACCATGTCGGCACGCAAGGAGAA	TCATCTATGGATGGCCTGTTGG
crc	CACCATGAGCACCTATATATTTATGCAAGC	CTAGCGCTTGCGTTCATGGTA
dpn	CACCATGGATTACAAAAACGATATTAATTCCG	CTACCACGGCCTCCAAGC
HLHmg	CACCATGTCGTCGCTACAAATGTCCG	CTACCAGGGACGCCAGAC
ken	CACCATGAAAGAGTTTCAAAGAATGTTGATGTT	CTATTCGCGCAGATTCTTTGTCA
king-tubby	CACCATGGAGGCCTACATCCGGC	TCACTCGCAGGCTATTTTGCCA
klu	CACCATGACGATGGCAGAAGGCAC	TTAGGCGCTCTCCGTCTTGA
l(2)k10201	CACCATGGATTCGGAAGCTGCGGG	CTAATCCAGGATGTCGTTAATGG
mod	CACCATGGCCCAAAAGAAAGCCGTCA	TAAAATCTTGCCCTTTTAACAAACGAT
mTTF	CACCATGATTAGAAGCCTTCTGCG	TCATCCTTCTGATACACTTTG
Rel	CACCATGAACATGAATCAGTACTACGACC	TCAAGTTGGGTTAACCAGTAGGG
Ssb-c31a	CACCATGCCCAAAACAAAGAAGAAGGATT	TTAATTCTCGATCGCGCGGGT
su(Hw)	CACCATGAGTGCCTCCAAGGAGGG	TCAAGCTTTCTCTTGTTCGCCTA
TFAM	CACCATGATCTACACCACAACACTGATG	CTATATATCTTTGGAGGCCAGCG
wek	CACCATGGGAGTTCCCACAAGCGA	CTAATCCTGTTTGGCCTTGGCC
wor	CACCATGGATAAACTCAAGTACAGCCG	TTAATAAATGGCCGGTGGTTGCA

After gel purification, entry clones were generated using the pENTR TOPO cloning kit (Invitrogen). Destination clones were generated with the Gateway System (Invitrogen), using a Gateway pUASt attB vector (kindly provided by Konrad Basler) and targeted insertion into fly embryos was performed as described (Groth *et al.*, 2004; Bischof *et al.*, 2007) using flystocks with a attP2 landing site on the third chromosome.

5 CHAPTER 2 – A ROLE FOR THE TRANSCRIPTION FACTOR KLUMPFUSS IN NEUROBLAST SELF-RENEWAL

5.1 INTRODUCTION

5.1.1 Klumpfuss is member of the EGR transcription factor family

Klein and Campos-Ortega first identified Klu in 1997 and showed that the gene is a zinc-finger TF involved in bristle and leg development. *Klu* mutants are semi-lethal and display loss of bristles and fusion of tarsal segments, hence the name Klumpfuss, meaning clubfoot. The authors found that Klu contains four C_2H_2 zinc-finger motifs in its C-terminus of which the last three are homologous to the zinc-fingers found in the early growth response (EGR) family of TFs. EGR genes contain three conserved zinc-finger motifs, can act as both positive and negative regulators of transcription, and are implicated in regulation of proliferation and cell growth (Thiel and Cibelli, 2002). The first zinc-finger of Klu resembles the divergent zinc-finger of another member of this family, the Wilm's Tumor-associated protein 1 (WT1). Wilm's tumor, or nephroblastoma, is a pediatric kidney cancer and WT1 was first identified to act as a tumor suppressor in this context (Haber *et al.*, 1990; Pelletier *et al.*, 1991; Madden *et al.*, 1991). Recent findings have associated WT1 with many, seemingly opposite roles. Context- and isoform-dependent, WT1 can act as a repressor or activator of transcription, and can be involved in regulation of proliferation, differentiation or apoptosis. Apart from its role as a tumor suppressor, it can potentially function as an oncogene as it is ectopically expressed in many cancers (Roberts, 2005; Hohenstein and Hastie, 2006). It is not clear whether WT1 is a true homolog of Klu since there is no sequence overlap between the two proteins outside of the zinc finger region. However, some described functions of Klu (see below) overlap with what is known about WT1, and understanding the mechanisms by which Klu acts in *Drosophila* might help to elucidate how WT1 executes its function in mammals.

The DNA binding sequences for the members of the EGR TF family are known (Madden *et al.*, 1991; Nakagama *et al.*, 1995), and the amino acids that contact the EGR target sequence are conserved in Klu as well as (Figure 13A). Therefore, it is possible that Klu also binds to a similar consensus sequence, however sequence specific DNA binding data is still missing, and therfore the down-stream targets of Klu are not known.

5.1.2 Klu acts as a transcriptional repressor during specification of SOPs

Klu was first found based on its β–galactosidase expression pattern in NBs during embryonic and larval stages, as well as in imaginal discs, which was confirmed by in-situ hybridization experiments and with a Klu-Gal4 line driving UAS-*GFP* (Klein and Campos-Ortega, 1997). Klu expression in wing imaginal discs starts in third instar larval stages in most proneural clusters, but it is not expressed in SOPs. Certain bristles and the corresponding SOPs are often missing in *klu* mutants (Klein and Campos-Ortega, 1997), indicating that it must either act during specification of SOP fate or is involved in SOP maintenance. Ectopic bristle and SOP formation, as well as premature formation of SOPs already in larval stages, was found in flies over-expressing *klu*, hinting that it can actually initiate SOP development (Kaspar *et al.*, 2008). It was shown that these phenotypes are due to Klu promoting the activity of proneural proteins on the level of transcription as well as on the posttranscriptional level. Since Klu, like WT1, acts as a transcriptional repressor it must execute this function via a double-negative feedback loop where it represses a yet to be identified antagonist of SOP formation (Kaspar *et al.*, 2008).

A Klu and related protein sequences

```
klu ZF 2-4   I A K A Y S C D V - - C R R S F A R S D M L T R H M R L H T G
hEGR1        H E R P Y A C P V D G C D R R F S R S D E L T R H I R I H T G
hEGR2        H E R P Y A C P V E S C D R R F S R S D E L T R H I R I H T G
hEGR3        H E R P Y P C P A E G C D R R F S R S D E L T R H I R I H T G
hEGR4        H E R P Y A C P A E G C D R R F S R S D E L T R H L R I H T G
stripe       - - K A Y A C P V E S C V R S F A R S D E L N R H L R I H T G
WT-1 ZF 2-4  G E R P Y Q C P F K D C E R R F S R S D Q L K R H Q R R H T G

klu ZF 2-4   V K P Y T C K V C G Q V F S R S D H L S T H Q R T H T G - - -
hEGR1        Q K P F Q C R I C M R S F S R S D H L T T H V R T H T G - - -
hEGR2        Q K P F Q C R I C M R N F S R S D H L T T H I R T H T G - - -
hEGR3        H K P F Q C R I C M R N F S R S D H L T T H I R T H T G - - -
hEGR4        H K P F Q C R I C M R S F S R S D H L T T H I R T H T G - - -
stripe       H K P F Q C R I C L R N F S R S D H L T T H V R T H T G - - -
WT-1 ZF 2-4  V K P F Q C K T C Q R K F S R S D H L K T H T R T H T G K T S

klu ZF 2-4   E K P Y K C - - P Q C P Y A A C R R D M I T R H M R T H T R Y
hEGR1        E K P F C C - - D Q C G R K F A R S D E K K R H A K V H L K Q
hEGR2        E K P F A C - - D I C G R K F A R S D E K K R H T K I H L R Q
hEGR3        E K P F A C - - D Y C G R K F A R S D E K K R H T K I H L R Q
hEGR4        E K P F A C - - E F C G R K F A R S D E K K R H A K I H L K Q
stripe       E K P F A C - - D V C G R R F A R S D E K K R H S K V H L K Q
WT-1 ZF 2-4  E K P F S C R W P Q C Q K K F A R S D E L V R H H V M H Q R N
```

B The NB4-2 lineage

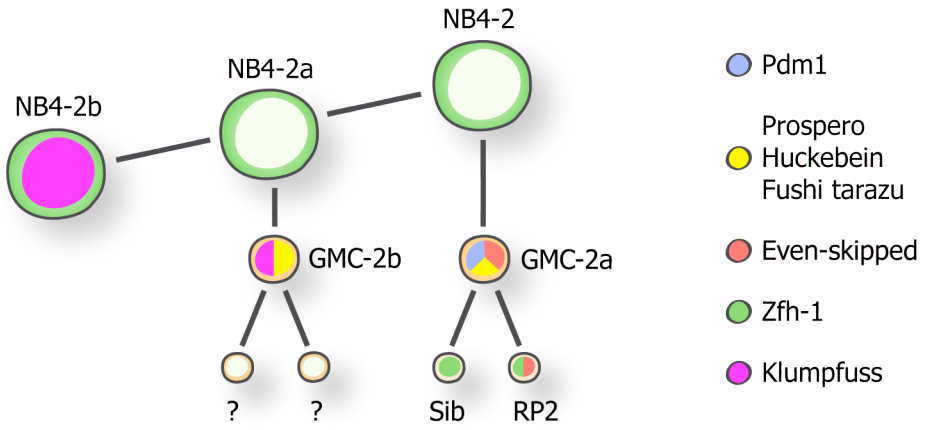

Figure 13. Klu is a zinc-finger transcription factor and involved in lineage specification in the embryonic NB4-2 lineage
(A) Comparison of the region containing zinc fingers 2-4 of Klu, and the corresponding region in human early growth response genes 1-4, Drosophila stripe, and zinc-finger 2-4 of Wilm's tumor 1. Red indicates the actual zinc fingers; green and magenta correspond to nucleotide and phosphate binding, respectively. **(B)** This scheme indicates the first two divisions of embryonic NB4-2. NB4-2 gives rise to NB4-2a and the Even-skipped (Eve) positive GMCs4-2a, which divides into the Eve and Zfh-1 positive RP2 motoneuron and its sibling cell. Following asymmetric division of NB4-2a, the second born GMC4-2b starts to express Klu, and gives rise to two unknown, Eve negative daughter cells. (Figure A adapted from (Klein and Campos-Ortega, 1997), Figure B from (Yang *et al.*, 1997))

5.1.3 Klu is involved in progeny specification in certain embryonic NB lineages

Klu was shown to be expressed in NBs during embryonic and larval stages (Klein and Campos-Ortega, 1997). In a screen for genes acting to differentiate between the cellular identities produced within one NB lineage, it was found to differentiate between the identities of the first two GMCs generated in the embryonic NB4-2 lineage (Figure 13B) (Yang *et al.*, 1997). Klu expression starts in the second born GMC, termed GMC-2b, and its loss leads to a duplication of the Even-skipped (Eve) positive RP2 motoneuron, one of the terminal daughter cells of the first-born GMC, the likewise Eve positive GMC-2a. It was shown that a small enhancer in *eve* mediates its expression. The genes Pros, Huckebein, Fushi tarazu, and Pdm1, which are all expressed in the GMC-2a, activate Eve expression, while Klu in the GMC-2b represses Eve (McDonald *et al.*, 2003). The duplication of RP2 neurons is therefore likely due to a GMC4-2b to GMC4-2a cell fate transformation, which causes duplicating of the GMC4-2a sublineage. Therefore, in the embryonic NB4-2 lineage Klu also acts as a transcriptional repressor and is involved in the differentiation of the second born GMC to make it distinct from its first-born sibling (Yang *et al.*, 1997).

Another function of Klu in the central nervous system during specification of NB progeny is its involvement in the generation of specific peptidergic neurons, the abdominal leucokinergic (ABLK) neurons (Benito-Sipos *et al.*, 2010). Also WT1 has been implicated in the development of neuronal tissue, for example in the formation of retinal ganglia (Wagner *et al.*, 2002). Loss of *klu* causes a strong reduction in APLK neuron numbers, indicating that it has a direct, yet still to be determined, role in APLK specification.

5.1.4 Klumpfuss positively regulates programmed cell death

WT1 has been positively implicated in programmed cell death (PCD) and was, for example, found to be up-regulated in adult neurons that undergo apoptosis (Lovell *et al.*, 2003). Also Klu was identified to regulate PCD in the *Drosophila* pupal retina (Rusconi *et al.*, 2004). The *Drosophila* retina is composed of about 750 single eye units called ommatidia. During normal eye development secondary and tertiary pigment cells (2°/3°s) form an 'interommatidial lattice' that lines the ommatidial core where the photoreceptor neurons are located. To generate the interommatidial lattice the 2°/3° cells must organize in a precise spatial pattern followed by selected removal of about one third of these cells by PCD. Klu was found to positively regulate cell death specifically in lattice cells since additional 2°/3° cells can be found in *klu* mutants, and increased cell death is observed upon over-expression. The expression pattern of Klu is dynamic in interommatidial cells during the period of PCD, with some cells expressing high and some low levels of Klu. It is thought that Klu acts in the cells that will undergo PCD, presumably by down-regulating the *Drosophila* epidermal growth factor receptor (dEGFR), however direct down-stream targets of Klu in this context have not been identified as of yet.

Also in the central nervous system might Klu positively regulate PCD. Its over-expression causes loss of APLK neurons, which could be rescued by inhibiting PCD (Benito-Sipos *et al.*, 2010). In contrast to Klu, WT1 can also act as a survival factor, as was shown in the developing kidney or heart (Hohenstein and Hastie, 2006; Kreidberg *et al.*, 1993).

In addition to the functions of Klu as a transcriptional repressor in SOP and progeny specification of certain embryonic NB lineages, and its role in PCD, we have found yet another overlap with a described role of WT1. Our study describes a role for Klu in proliferation and maintenance of larval NBs, and shows that Klu can act as an oncogene since its over-expression results in the formation of larval brain tumors.

5.2 Results

5.2.1 Phenotypical analysis of *klumpfuss* over-expression in larval brains

We tested the functional relevance of the factors in our hypothetical network for NB self-renewal by knock down and over-expression studies in both type I and type II NB central brain lineages. Except *dpn* and *HLHm*, we found *klu* to cause excess NB numbers when over-expressed. We showed that these ectopic NBs, which are only localized on the posterior side of the brain, express the NB markers Mira (Figure 14 A-D′) and Dpn, while the number of cells expressing the neuronal marker Pros is strongly decreased (Figure 12C-C″). This result suggests that down-regulation of Klu at a certain point during lineage progression is necessary to proceed with differentiation.

Based on the location of the supernumerary NBs on the posterior side of the brain we wanted to further investigate their identity, hypothesizing that the phenotype might originate from type II lineages. We used *insc*-Gal4 to over-express *klu* in both type I and type II lineages, and stained the brains with an antibody against the TF Ase. Ase is expressed in type I NBs, mature INPs in type II lineages, and GMCs in both lineages, but is absent in type II NBs. The stainings revealed that only very few Ase positive cells are still present in the brains over-expressing Klu (arrowheads), while almost all supernumerary NBs are indeed Ase negative and therefore are very likely type II NBs (Figure 14E-F′).

To finally prove that ectopic NBs originate only in type II lineages, we used two different driver lines to over-express *klu*. The PointedP1-Gal4 (PntP1-Gal4) driver line drives expression only in type II lineages (Zhu *et al.*, 2011), while *ase*-Gal4 is only active in type I lineages. The phenotype resulting from over-expression of *klu* using PntP1-Gal4 was indistinguishable from the phenotype induced by *insc*-Gal4 (Figure 15A-B′). Increasing Klu levels in type I lineages did not have any effect on NB numbers or size, and Pros positive neurons can be found in these brains (Figure 15C-E). However, upon closer examination of Ase positive GMCs, we found a slight but statistically significant increase from an average of five GMCs in wild type, up to seven GMCs in *klu* over-expression (n=4 brains, p-value<0.01 [Student's ttest]) (Figure 15F). This indicates that high levels of Klu affect either proliferation of NBs to produce more GMCs, or that differentiation and terminal division of GMCs is slowed down.

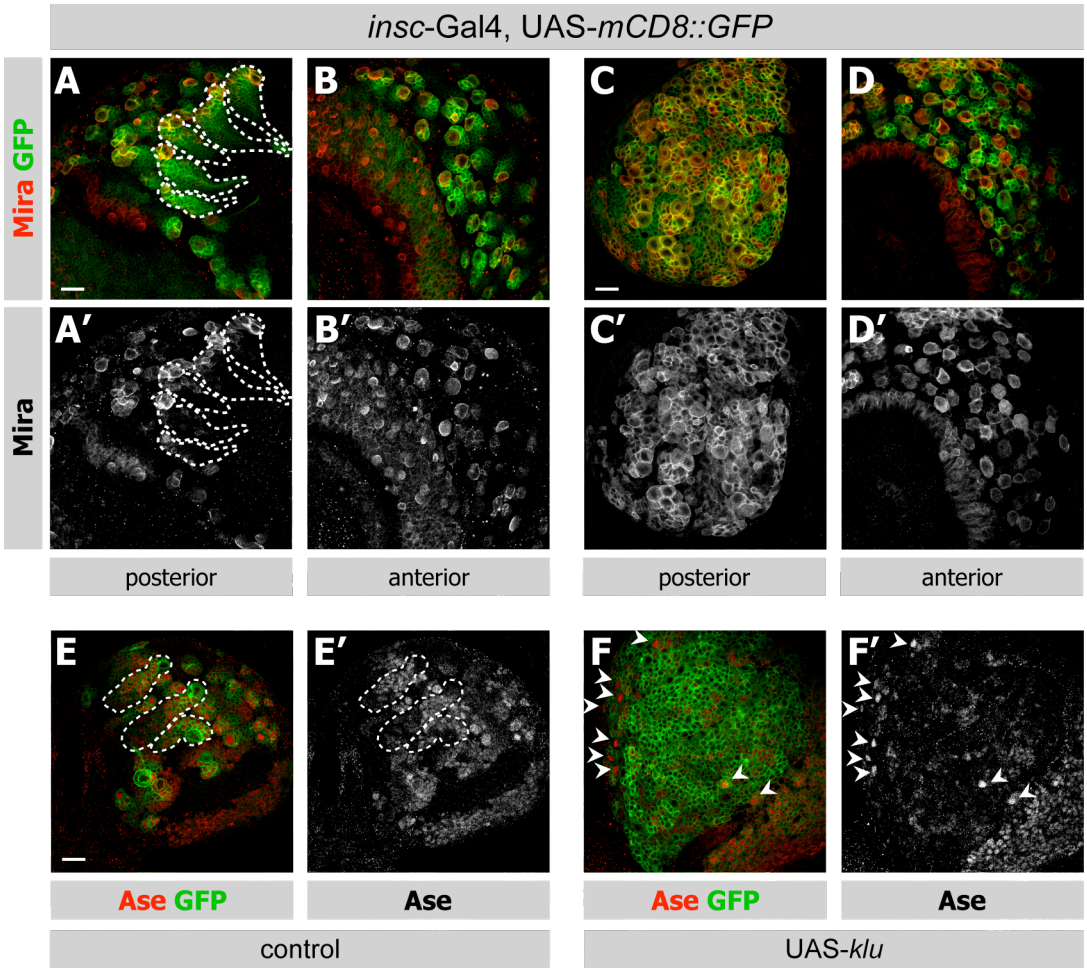

Figure 14. Ectopic NBs mis-expressing *klu* resemble type II NBs
(A-B′) Type II NBs (outlined in [A and A′]) are located on the posterior side of the larval brain, type I NBs can be found on the posterior and anterior side. All NBs express the NB marker Mira. **(C-D′)** In brains over-expressing *klu*, Mira positive ectopic NBs are seen on the posterior side (C and C′), while no increase in NBs numbers is detectable in anterior type I NBs (D and D′). **(E-F′)** The transcription factor Ase it is not expressed in primary type II NBs (outlined in [E and E′]), but turns on in INPs. Apart from some Ase positive type I NBs (arrowheads in [F and F′]), almost all ectopic NBs do not express Ase and based on their localization and expression pattern, are likely type II NBs. Scale bars are 20 µm.

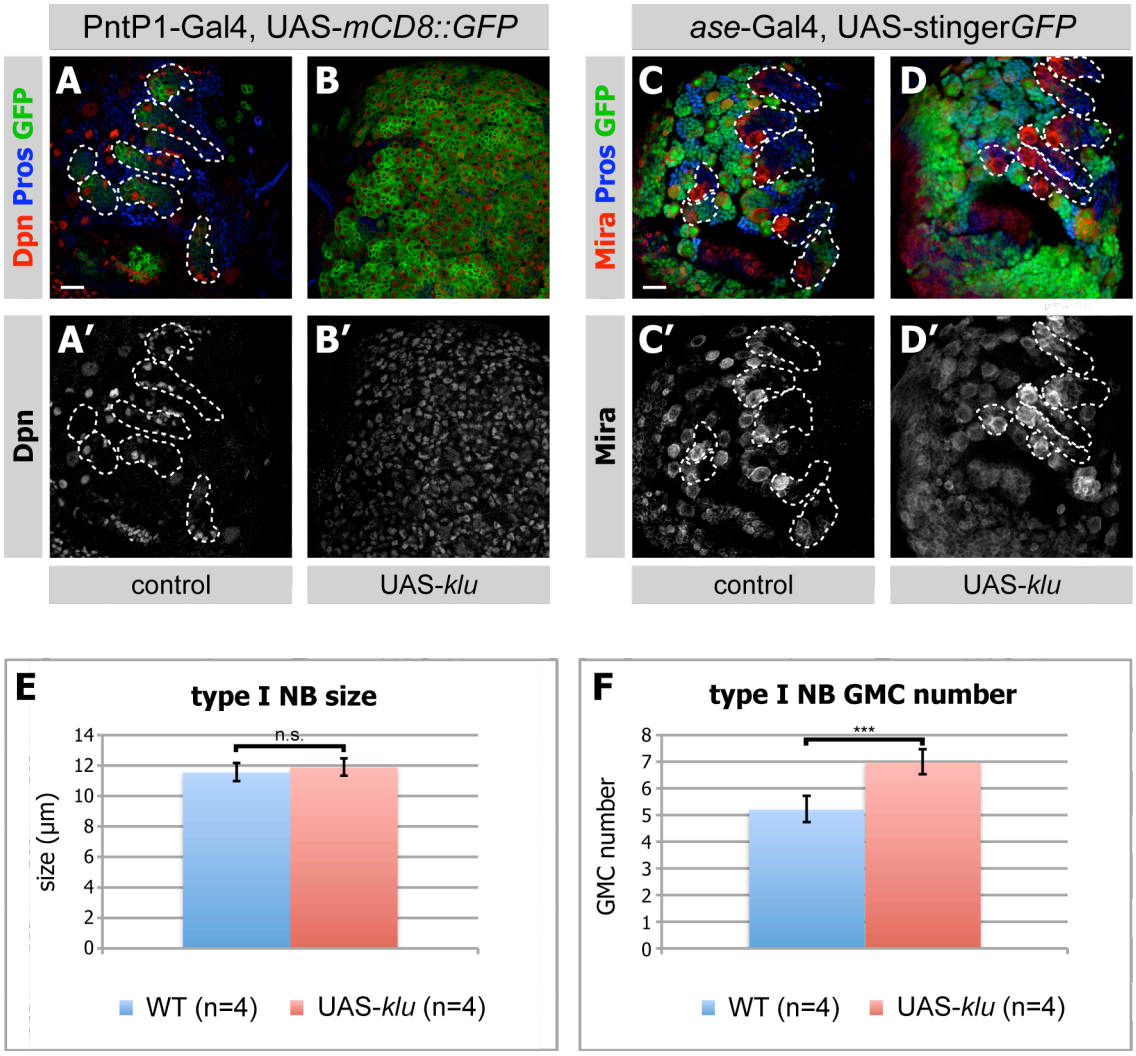

Figure 15. Over-expression of *klu* with PntP1-Gal4 results in tumor formation

(A-B') PointedP1-Gal4 (PntP1-Gal4) drives expression specifically in type II lineages, and expression of *klu* from PntP1-Gal4 resulted in tumors that showed an excess of ectopic Dpn positive NB-like cells at the expense of differentiating GMCs or neurons. **(C-D')** Ase-Gal4 expresses only in type I NB lineages and not in type II lineages (outlined in [C and C']), and over-expression of *klu* with ase-Gal4 does not lead to the formation of supernumerary NBs. **(E)** Type I NB size is not affected in when *klu* is mis-expressed, however, **(F)** a slight, but statistically significant increase in the number of GMCs could be observed. (n in E and F denotes number of brains counted, error bars represents standard deviation, n.s.=not significant, p-value in F<0.001 [Student's t-test]). Scale bars are 20 µm.

Taken together, these data demonstrate that the origin of the *klu* over-expression phenotype lays in type II NB lineages. More specifically, elevated Klu levels lead to an expansion of primary type II NBs numbers. In type I lineages, ectopic Klu expression in GMCs leads to a slight accumulation of these cells, however neurons can still be generated. Thus, Klu needs to be down-regulated in type II and to a lesser extend in type I lineages to allow differentiation.

5.2.2 Klu over-expression causes transplantable tumors

To test whether the over-expression of *klu* results in tumor formation, we transplanted fragments from control or *klu* over-expressing third instar larval brains into the abdomens of female host flies (Figure 16A). A tumor metastasizes in other tissues and even when taken out of its tissue of origin, continues to divide. Of 88 adult hosts transplanted with tissue from brains over-expressing Klu, 52 (59 %) developed tumors nine days after transplantation, while control transplants never resulted in tumors (Figure 16A and B). When we extracted tumor tissue and stained for NB and differentiation markers, we found that the tumors consisted mostly of Mira and Dpn positive NBs (Figure 16C and D). Few differentiating cells that stain positive for ELAV or Pros (Figure 16E and F) could be found. We could also detect micrometastasis in ovaries of host flies (arrows in Figure 16G).

Thus, our data shows that up-regulation of Klu causes formation of transplantable *Drosophila* brain tumors, which maintain their neural identity and can also invade other tissues.

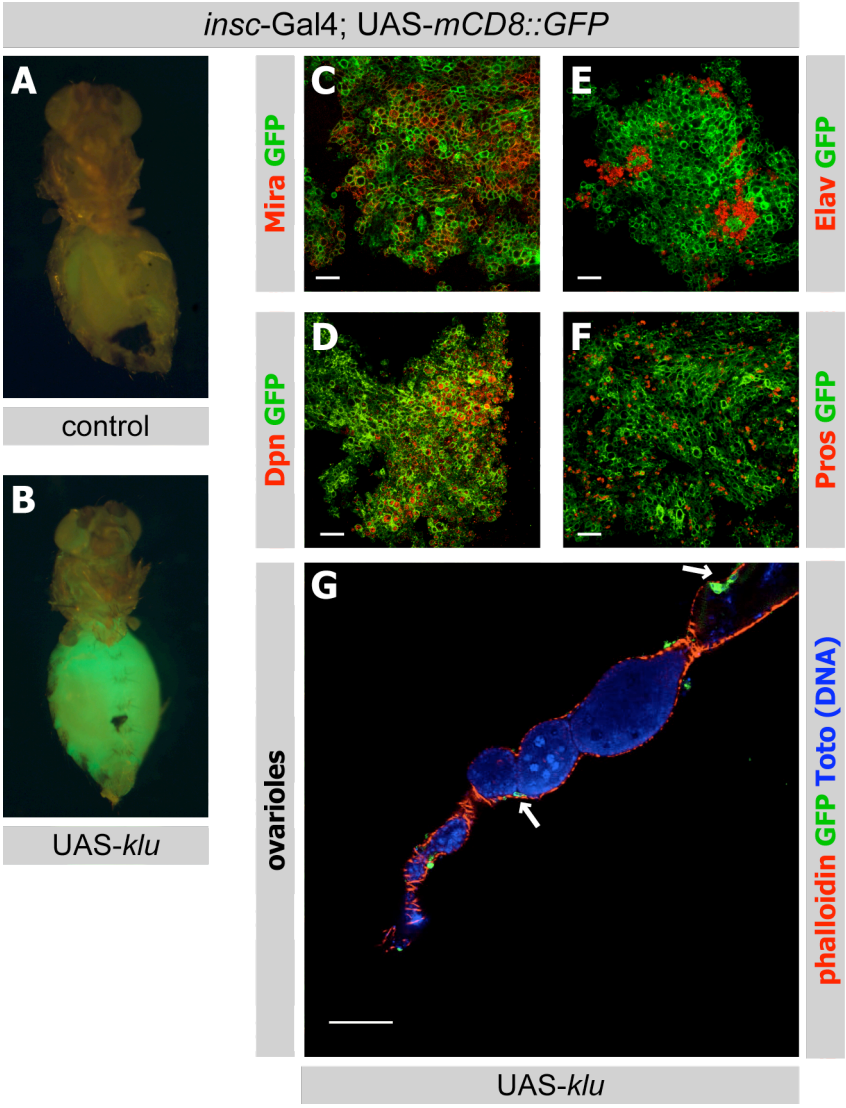

Figure 16. Over-expression of Klu causes transplantable tumors
(A, B) GFP-marked fragments from *klu* over-expression brain tumors transplanted into the abdomens of host flies resulted in tumors in the adult hosts (B, filled green abdomen) nine days after transplantation. **(C-F)** Extracted tissue stained with the NB markers Mira (C) and Dpn (D) and the differentiation markers ELAV (E) and Pros (F) showed that the tumor tissue mostly consists of NBs. **(G)** Micrometastasis (arrows) could be detected in ovaries of flies transplanted with brain pieces mis-expressing *klu*. Scale bars are 25 µm and 50 µm in (G).

5.2.3 Klu over-expression causes de-differentiation of immature INPs

We next wanted to investigate how the tumor arises. It is possible that asymmetric cell division is disrupted in brains over-expressing *klu*, which could lead to symmetric NB divisions and an expansion of the NB pool. Another possibility is that NBs still divide asymmetrically, but that already committed daughter cells de-differentiate into NB like cells. In the complex type II lineages these could be INPs during various maturation stages, or GMCs.

To test asymmetric cell division, we used the apical marker aPKC and the basal marker Mira. Like in wild type NBs (Figure 17A-B'), aPKC and Mira are localized to opposite sides of the cell cortex in dividing pH3-positive Klu over-expressing NBs (Figure 17C-D'). This indicates that asymmetric cell division is not affected.

To investigate whether the phenotype is indeed due to de-differentiation of daughter cells already committed to differentiation, we used *insc*-Gal4 together with *tub*-Gal80^{ts} to control *klu* expression in a spatial and temporal manner. *Tub*-Gal80^{ts} represses the transcriptional activity of GAL4 at permissive temperatures (18 °C), which is relieved when switched to 29 °C (McGuire *et al.*, 2004). With this system we could avoid the strong phenotype seen at later stages. In control type II lineages (Figure 17E-F" and scheme in G), the Dpn positive, Ase negative primary NB (marked with asterisk) divides asymmetrically and gives rise to Ase and Dpn negative immature INPs (white arrows). Two to three of these cells accumulate before the first born immature INP turns on Ase and is now called a mature INP (yellow arrowheads). After yet another delay and an accumulation of three to four Ase positive, Dpn negative mature INPs, Dpn turns on and completes their maturation (Bowman *et al.*, 2008).

After inducing Klu over-expression for 19 hours at 29 °C, the primary NB (asterisk) is still recognizable. When *klu* was induced for a longer period, it was not possible anymore to distinguish it from ectopic NBs that had already formed. The primary NB divides asymmetrically giving rise to one to three Ase and Dpn negative immature INPs (white arrows). However, Dpn is re-expressed pre-maturely in immature INPs and ectopic Dpn positive, Ase negative NBs (white arrowheads) can be seen close to the primary NB (Figure 17H-I" and scheme in J). Ase expression is never initiated indicating that maturation does not proceed. Therefore, immature INPs that continue

to express Klu never undergo maturation, and instead revert back into a NB-like cell, leading to tumor formation.

To test whether Klu over-expression can still induce de-differentiation in mature INPs, we utilized the Gal4 line R9D11-Gal4 that drives expression in mature Ase positive, Dpn negative INPs (Weng *et al.*, 2010) (Figure 18A-B"). Unlike PntP1-Gal4 or *insc*-Gal4, Klu over-expression using R9D11-Gal4 does not result in an over-proliferation phenotype. We conclude that Klu expression needs to be down-regulated during the transition from immature to mature INPs.

Taken together, we have shown that it is not impaired asymmetric cell division but rather de-differentiation of immature INPs that causes ectopic NB formation in the *klu* over-expressing brains. Increased Klu levels in mature INPs does not cause them to de-differentiate, which indicates that Klu needs to be down-regulated specifically during immature INP stages, before Ase turns on, to ensure proper maturation.

5.2.4 Characterization of Klu expression pattern

Having found that Klu expression needs to be turned off in immature INPs to ensure INP maturation we were curious to see whether it is indeed not expressed in these cells. We stained third instar larval brains with an antibody against Klu, which revealed high expression in type I and type II NBs (Figure 19A and C, marked with asterisks). Klu is not expressed in immature (arrow) and Ase positive mature INPs (open circles), but turns on again together with Dpn. This expression pattern is similar to Dpn, which is also only expressed in primary NBs and in mature INPs (Figure 19B and E). Ase on the other hand is also expressed in primary NBs, but turns on early during INP maturation and also continues to be expressed in GMCs in type I and type II lineages (Figure 19C and F, schematic in G). We also confirmed the specificity of this antibody by staining brains in which *klu* was knocked down (Figure 19H-I").

Thus the expression pattern of Klu matches our hypothesis from the over-expression experiments and confirms that Klu is expressed in NBs but is rapidly down-regulated during immature INP stages.

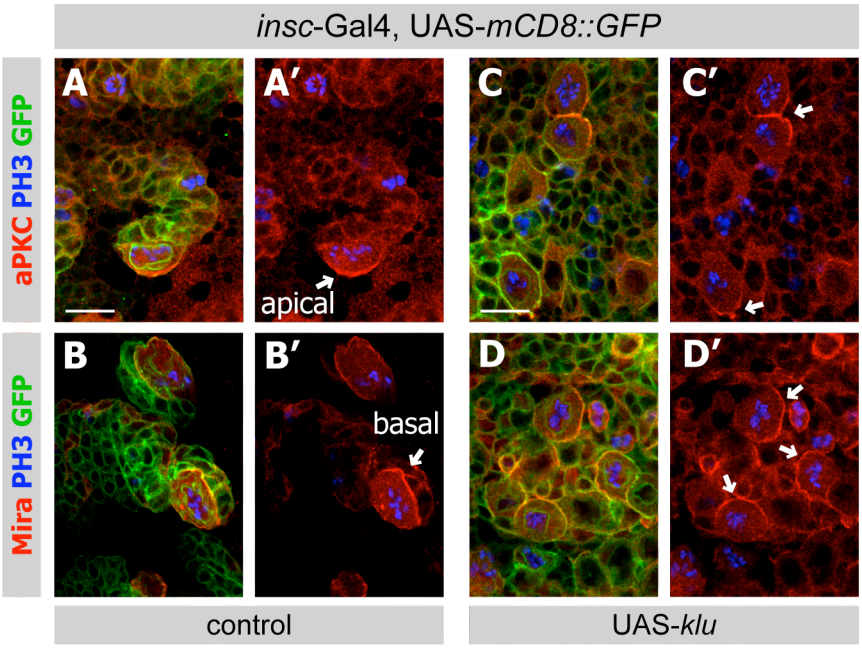
insc-Gal4, UAS-mCD8::GFP
aPKC PH3 GFP
Mira PH3 GFP
A
A′
apical
C
C′
B
B′
basal
D
D′
control
UAS-klu

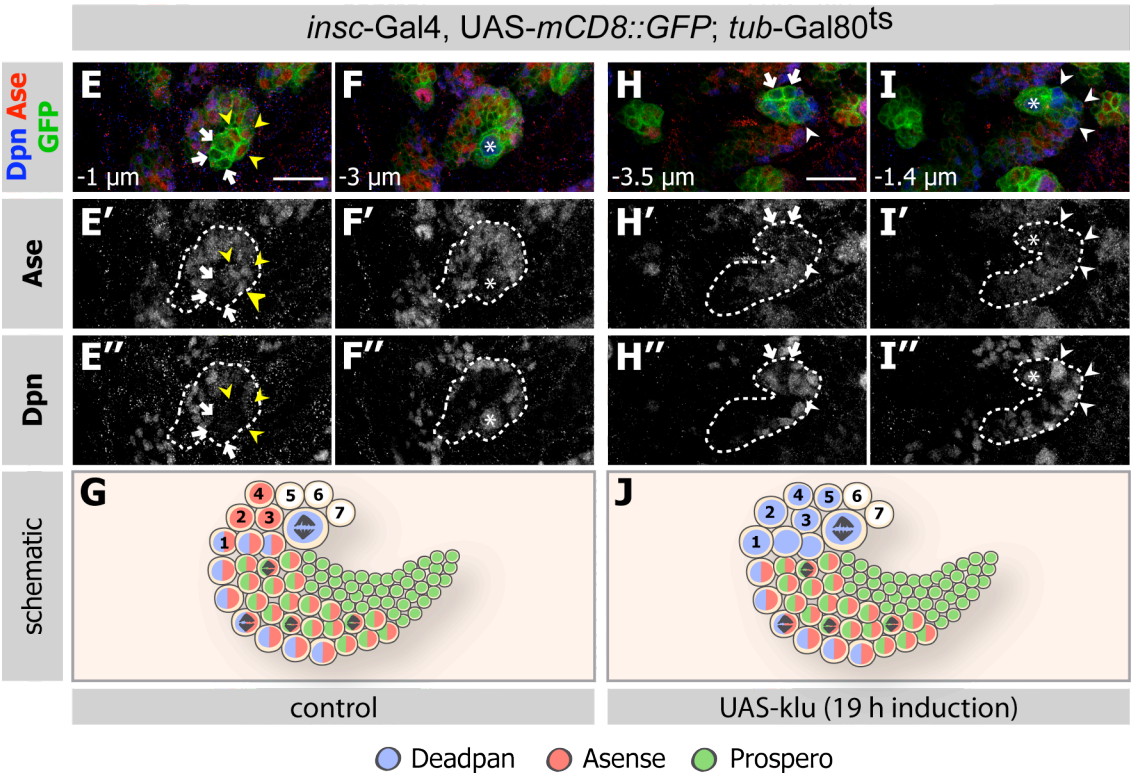
insc-Gal4, UAS-mCD8::GFP; tub-Gal80ts
Dpn Ase GFP
Ase
Dpn
schematic
E
-1 µm
F
-3 µm
H
-3.5 µm
I
-1.4 µm
E′
F′
H′
I′
E″
F″
H″
I″
G
J
control
UAS-klu (19 h induction)
Deadpan
Asense
Prospero

Figure 17. Immature INPs re-acquire NB identity upon ectopic expression of Klumpfuss

(A-B') Wild-type NBs in mitosis (phospho Histone H3 (pH3) positive) show asymmetric localization of aPKC (apical marker, [A and A']) or Mira (basal marker, [B and B']). **(C-D')** Over-expressing Klu does not result in mis-localization of aPKC (C an C') or Mira (D and D') in mitotic NBs (arrows). **(E-F'')** In control type II lineages (two subsequent focal planes of the same lineage are shown in E and F), two to three Ase and Dpn negative immature INPs (white arrows), and three to four Ase positive, Dpn negative mature INPs (yellow arrowheads) are located next to the Dpn positive, Ase negative primary NB (asterisk). **(G)** Schematic of a wild type type II lineage with the expression pattern of known NB, INP and GMC markers. Dividing cells are indicated by a mitotic spindle and the last born seven cells are labeled. **(H-I'')** Time-controlled induction of *klu* expression for 19 hours reveals blocked maturation of INPs and their de-differentiation into Dpn positive NB-like cells (two subsequent focal planes for *klu* over-expression are shown in H and I). Ase and Dpn negative immature INPs (white arrows) can be seen close to the primary Dpn positive NB (asterisk). Ectopic NB-like cells expressing Dpn, but not Ase are found close to the primary NB (white arrowheads in [H" and I"]). **(J)** Schematic drawing of phenotype. The youngest seven cells are indicated. Dpn expresses prematurely in immature INPs and causes their de-differentiation. (10 brains from two independent experiments were investigated). Scale bars are 10 µm in (A-D') and 20 µm in (E-F" and H-I").

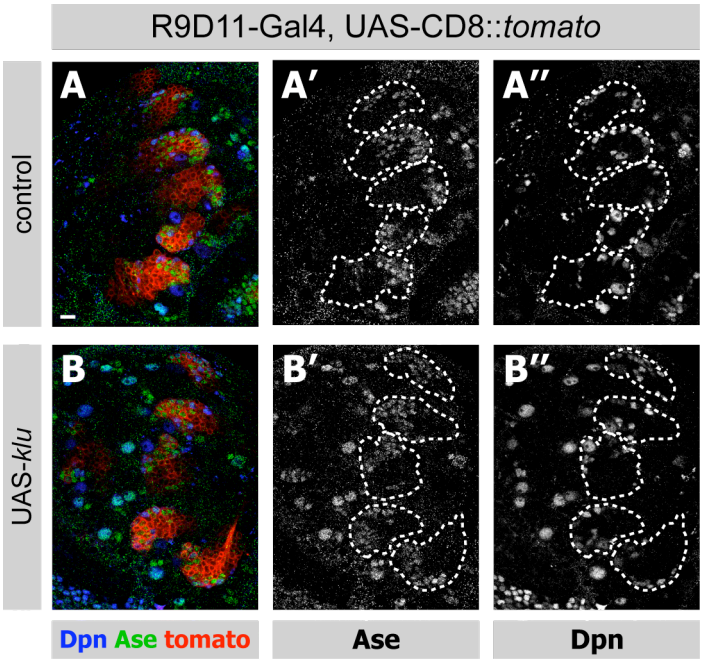

Figure 18. Over-expression of *klu* in mature INPs does not cause a tumor
(A) The Gal4 line R9D11-Gal4 starts expressing in mature Ase positive, Dpn negative INPs (Weng *et al.*, 2010). **(B)** Over-expression of *klu* in mature INPs or GMC using R9D11-Gal4 does not result in an over-proliferation phenotype. Scale bars are 10 µm.

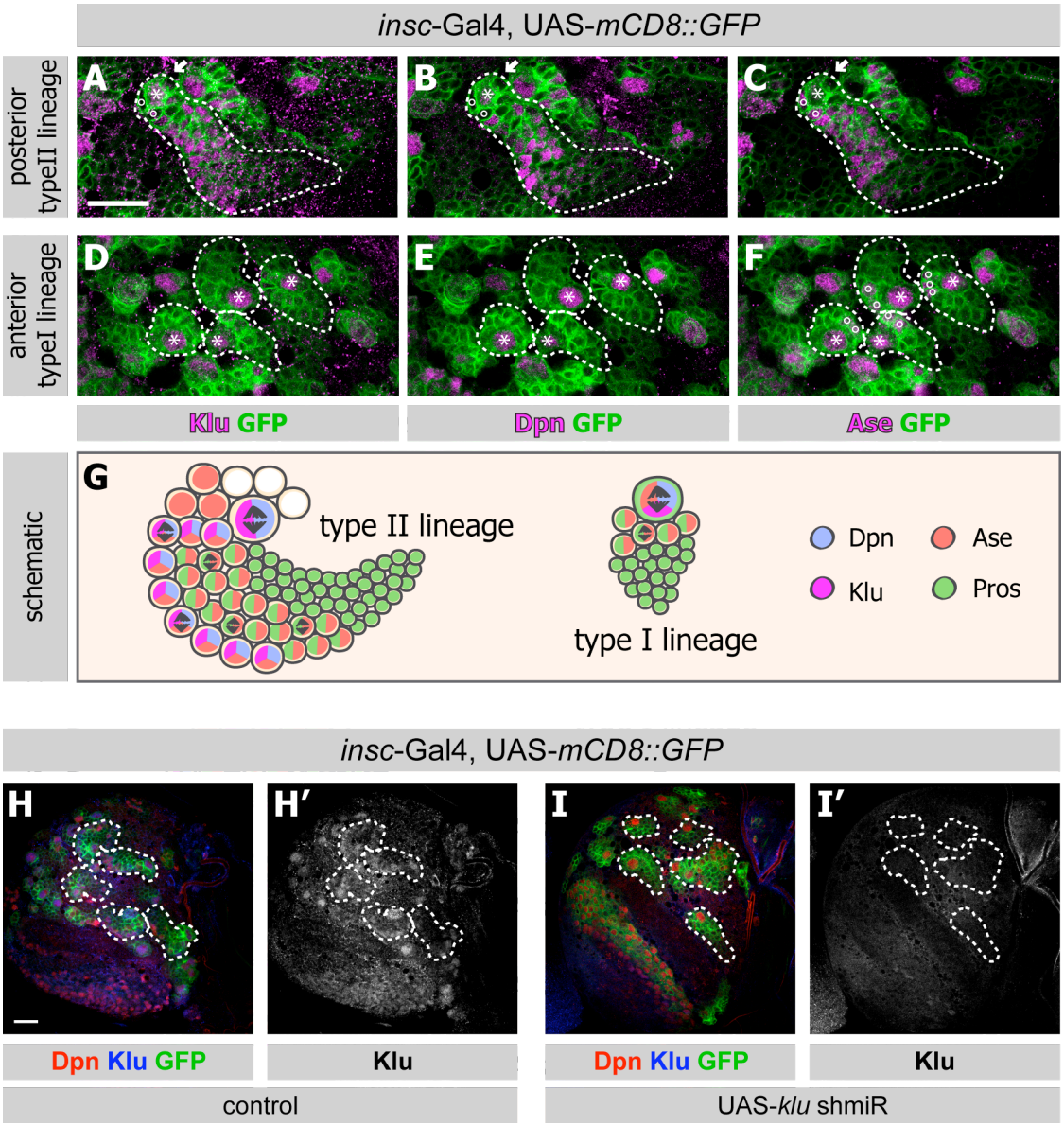

Figure 19. Klu is expressed in primary NBs in type I and II NB lineages
(A-C) In type II lineages, Klu (A) is expressed in primary NBs (asterisks). Like Dpn (B) and Ase (C) Klu is not expressed in immature INPs (white arrows), also not expressed in mature Ase positive INPs (open circles), and finally re-expressed together with Dpn in mature INPs. **(D-F)** In type I NBs, Klu is expressed in primary NBs and, like Dpn, not in Ase positive GMCs (open circles) and neurons. **(G)** Schematics of a type II and a type I lineage with indicated expression pattern for Dpn, Ase, Klu and Pros. **(H-I′)** Klu is expressed as described in control brains (H and H′) and absent when *klu* was knocked down using a specific shmiR line (I and I′). Scale bars are 20 µm.

5.2.5 Klu is required for NB growth and self-renewal

As mentioned before (see 4.1.8), previous RNAi screens have not identified any of the TFs in our network to cause loss of NBs. For Klu, the predicted quality of existing RNAi lines is low (see VDRC www.stockcenter.vdrc.at, 81 off-targets predicted) and we therefore generated a microRNA based RNAi (shmiR) line (Haley *et al.*, 2008). To test the knock down efficiency of this shmiR line we stained it with an antibody against Klu and observed complete absence or strong reduction of Klu antibody staining in NBs (Figure 19H-I").

In wild-type brains, eight type II lineages can be found per brain lobe. This number is highly reduced upon *klu* RNAi expression (Figure 20A and B). We investigated a total of 22 brains and found that on average, only one of these lineages remains (Figure 20C [p-value<0.001]). When we focused more closely on type I NB we also found a reduction in NB numbers, although in this case the average number is only reduced by 12 % (Figure 20D [n=5 for wild type and n=7 for *klu* shmiR, p-value<0.001]). In addition, knock down of *klu* results in a reduction of NB size (Figure 20E). Normally, the majority of NBs is between nine and twelve µm, while upon *klu* loss NB sizes ranges mostly from seven to nine µm. Thus, Klu is necessary to ensure self-renewal, maybe by promoting growth, of the majority of type II and to some extend, type I NBs.

5.2.6 Klu expression is required before second instar larval stages

Since we cannot exclude off target effects to be the cause for the NB loss and size reduction phenotypes, we attempted to recapitulate these phenotypes in klu^{R51} mutant Mosaic analysis with a repressible cell marker (MARCM) clones (Klein and Campos-Ortega, 1997). When clones were induced 50 – 68 hours AEL we could not find any previously observed NB number or size phenotypes. However, when we induced clones 30 – 48 hours AEL, NB size is reduced (Figure 20E). In 10.7 % of the 374 mutant clones investigated, we could not detect a primary NB (Figure 20F and G).

We further confirmed the loss of NB phenotypes by crossing two mutant alleles for Klu (klu^{G410}/klu^{R51}) transheterozygously, and again showed loss of type II lineages (Figure 21A and B) as well as a partial loss of type I NBs (Figure 21C [n=3 for wild type and n=4 for klu^{G410}/klu^{R51}, p>0.001]). We used our *klu* shmiR line in a time-shift assay and also found that Klu needs to be expressed before second instar larval stages (Figure 21D-F).

Since Klu was shown to positively regulate PCD in the *Drosophila* retina during pupal stages (Rusconi *et al.*, 2004), we investigated whether the loss of NBs might be due to apoptosis. We over-expressed *p35*, an inhibitor of apoptosis, together with GFP or our *klu* shmiR line, and found that this cannot rescue the loss of NBs (Figure 21G-I'). Thus, apoptosis cannot account for the phenotype we observed.

Taken together, we have identified a regulator of self-renewal that needs to be present in type II NBs and to a lesser extend in type I NBs to ensure NB identity maintenance. Klu might execute its function early on in larval development and seems to be dispensable during later stages.

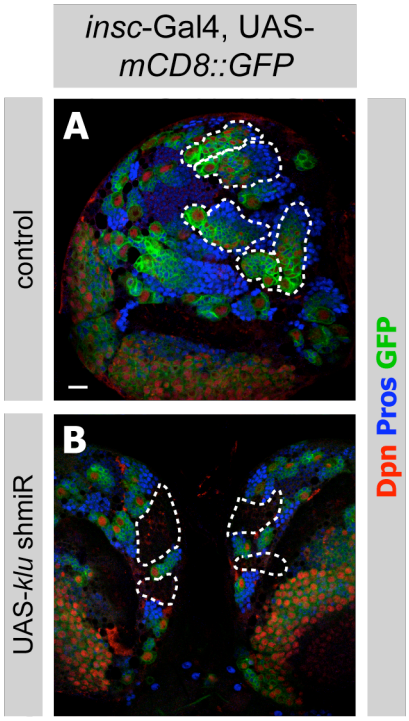
insc-Gal4, UAS-mCD8::GFP
control
UAS-klu shmiR
A
B
Dpn Pros GFP

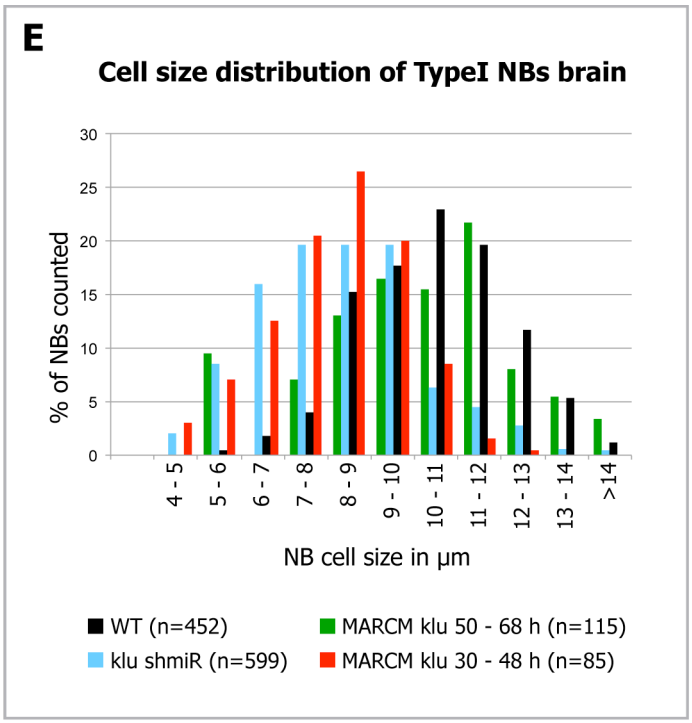
E
Cell size distribution of TypeI NBs brain
% of NBs counted
30
25
20
15
10
5
0
4 - 5
5 - 6
6 - 7
7 - 8
8 - 9
9 - 10
10 - 11
11 - 12
12 - 13
13 - 14
>14
NB cell size in µm
WT (n=452)
klu shmiR (n=599)
MARCM klu 50 - 68 h (n=115)
MARCM klu 30 - 48 h (n=85)

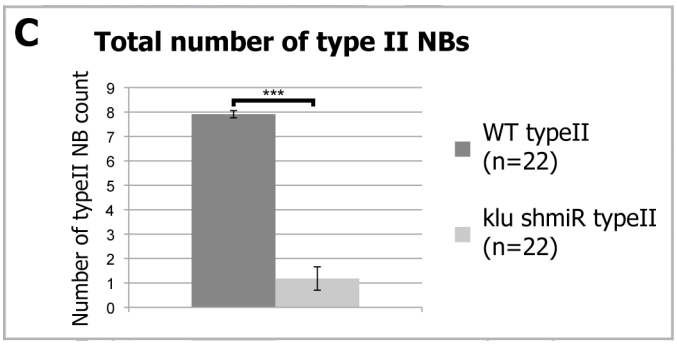
C
Total number of type II NBs
Number of typeII NB count
9
8
7
6
5
4
3
2
1
0
***
WT typeII (n=22)
klu shmiR typeII (n=22)

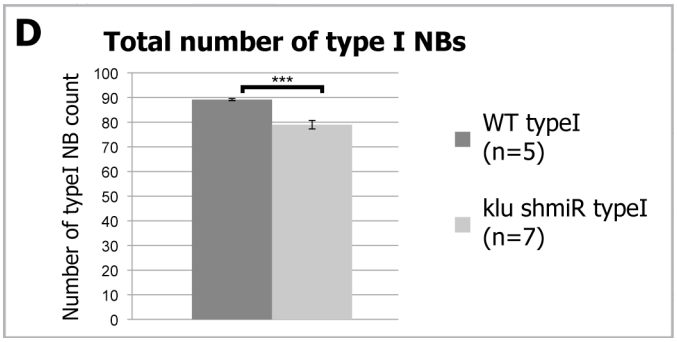
D
Total number of type I NBs
Number of typeI NB count
100
90
80
70
60
50
40
30
20
10
0
***
WT typeI (n=5)
klu shmiR typeI (n=7)

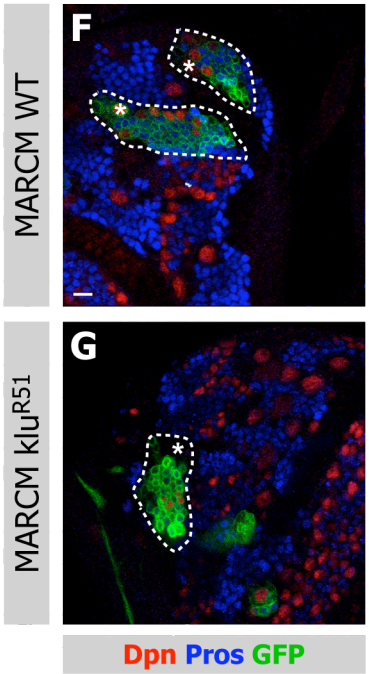
MARCM WT
MARCM kluR51
F
G
Dpn Pros GFP

Figure 20. Klumpfuss is required for NB self-renewal and growth
(A) Control larval brains are stained for Dpn and Pros and type II lineages are outlined. **(B)** *Klu* knock down by RNAi causes loss of type II lineages. Areas with loss of type II lineages are marked. **(C)** Quantification of type II NBs number upon knock down of *klu* by RNAi. On average, only one type II lineage can still be identified (n denotes number of brains counted, error bars represents standard deviation, p-value<0.001 [Student's t-test]). **(D)** Quantification of number of type I NBs upon *klu* knock down showed a reduction of total type I NBs per brain hemisphere (n denotes number of brains counted, error bars represents standard deviation, p-value<0.001 [Student's t-test]). **(E)** Quantification of type I NBs cell size in the larval central brain shows that loss of *klu* function leads to a reduction in NB size, but only when *klu* was removed before second instar larval stages (n denotes number of NBs measured). **(F)** Control type II MARCM clones induced 30-48 hours after egg laying (AEL) contain one Dpn positive primary NBs (asterisk), several Dpn positive mature INPs and Pros positive GMCs and neurons. **(G)** No primary NB (asterisk) can be found in 10.7 % of cases in MARCM clones of klu^{R51} induced at 30-48 hours AEL. A type II MARCM clone is shown. Scale bars are 15 µm.

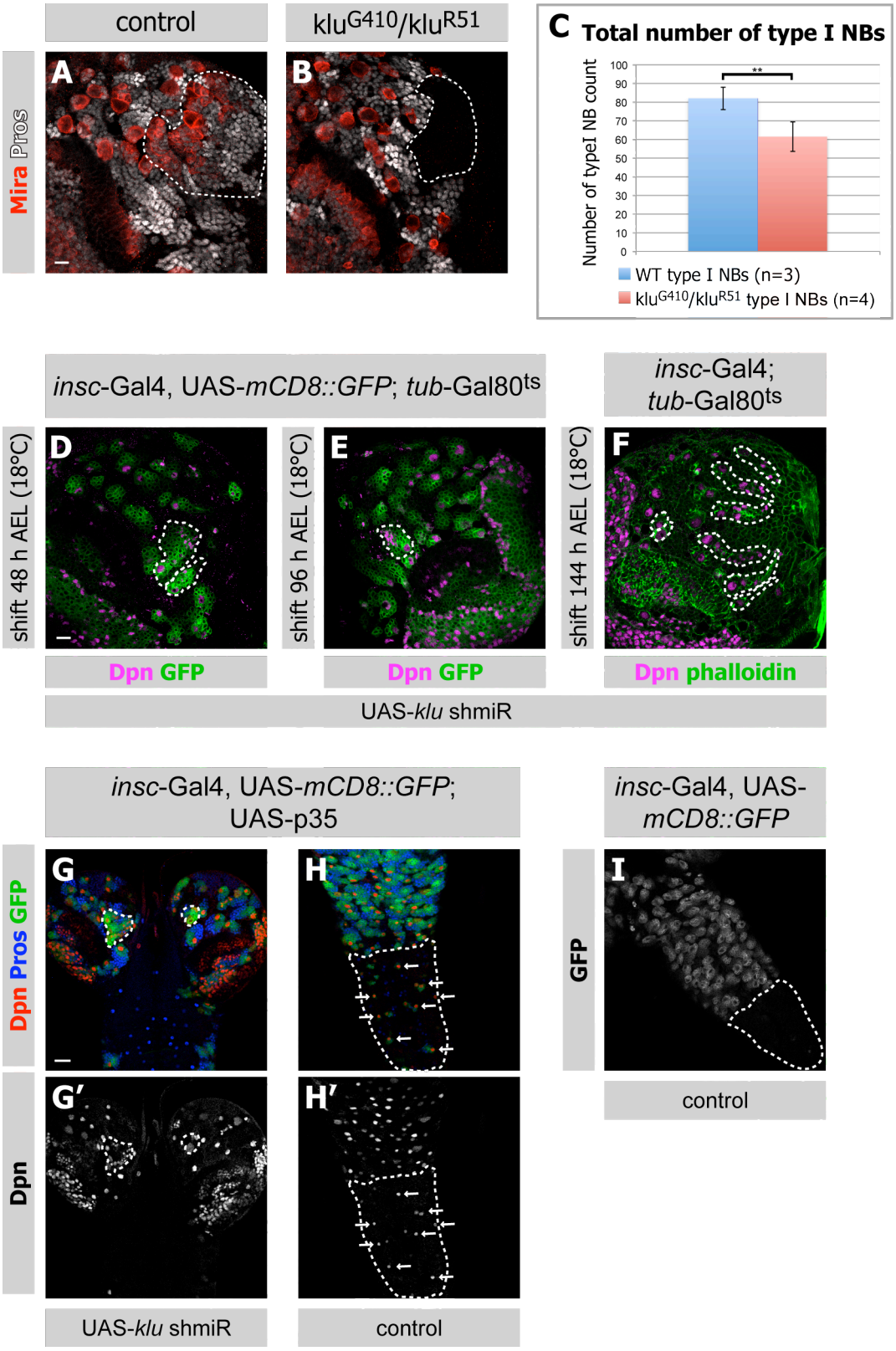
control
klu^{G410}/klu^{R51}
Mira Pros
A
B
C Total number of type I NBs
Number of typeI NB count
100
90
80
70
60
50
40
30
20
10
0
**
WT type I NBs (n=3)
klu^{G410}/klu^{R51} type I NBs (n=4)
insc-Gal4, UAS-mCD8::GFP; tub-Gal80^{ts}
insc-Gal4; tub-Gal80^{ts}
shift 48 h AEL (18°C)
shift 96 h AEL (18°C)
shift 144 h AEL (18°C)
D
E
F
Dpn GFP
Dpn GFP
Dpn phalloidin
UAS-klu shmiR
insc-Gal4, UAS-mCD8::GFP; UAS-p35
insc-Gal4, UAS-mCD8::GFP
Dpn Pros GFP
Dpn
GFP
G
H
I
G′
H′
UAS-klu shmiR
control
control

Figure 21. Transheterozygous combination of two Klu mutant alleles causes loss of type I and type II NBs that is not due to apoptosis

(A and **B)** Type II lineages (outlined in A) can be found in control brains, but not when the two mutant alleles klu^{G410} and klu^{R51} were crossed transheterozygously (loss of type II lineages outlined in B). **(C)** Loss of 15 % of type I NBs can also be observed in the transheterozygous combination of klu^{G410} and klu^{R51}. (n denotes number of brains counted, error bars represents standard deviation, p-value>0.001 [Student's t-test]). **(D-F)** Time-controlled knock down of *klu* using *tub*-Gal80^{ts} and shifting crosses from the restrictive (18° C) to the permissive temperature (29° C) after 48 hours (D), 96 hours (E) or 144 hours (F) AEL. The NB loss phenotype (outlined type II lineages) can only be observed when crosses were shifted before second instar larval stages. **(G-I)** Knock down of *klu* was induced in a background where apoptosis is disabled, and loss of type II NBs is still apparent (outlined in G and G'). An internal positive control is the presence of abdominal VNC NBs, which usually undergo apoptosis (arrows in outlined abdominal VNC, H and H'). In a control brain no NBs can be found in this region (abdominal VNC outlined in I). Scale bars are 15 µm and 20 µm in G-I.

5.3 DISCUSSION

5.3.1 NB self-renewal factors in type I and type II lineages

Asymmetric cell division provides a mechanism by which stem cells maintain their identity and sustain the stem cell pool, but at the same time give rise to daughter cell that will undergo differentiation. During the last decade the mechanism of asymmetric cell division in *Drosophila* NBs was studied in great detail (for reviews see for example (Neumüller and Knoblich, 2009; Knoblich, 2010; Reichert, 2011)), and the discovery of the cell fate determinants Brat, Pros and Numb has lead to some insight of how differentiation is initiated in GMCs and INPs. Their spatially restricted segregation into the differentiating daughter cell during cytokinesis ensures that this cell undergoes correct maturation and that terminal daughter cells acquire their neuronal or glial fate. Defects in asymmetric segregation of cell fate determinants leads to severe NB over-proliferation phenotypes due to de-differentiation of more committed daughter cells (Betschinger *et al.*, 2006; Lee *et al.*, 2006b; Bello *et al.*, 2006; Choksi *et al.*, 2006; Lee *et al.*, 2006a; Wang *et al.*, 2006). How the cell fate determinants execute their function has been understood to some extend, and a role for Numb as an inhibitor of Notch, which in turn regulates NB growth, as well as downstream targets of Pros have been described (Song and Lu, 2011; Choksi *et al.*, 2006). However, what had not been investigated is how the self-renewal potential of NBs is maintained during consecutive rounds of asymmetric cell divisions, and how the cell fate determinants might act on potential NB identity factors to inhibit their function in GMCs and INPs.

We established methodology to purify larval NBs and their neuronal progeny by FACS and sequenced the transcriptomes of both cell types. From this data we selected NB specific TFs and generated a network for NB self-renewal. We tested this network for genes potentially involved in NB identity maintenance and found the TFs *klu*, *HLHmγ* and *dpn* to play a role in this process. Continued expression of all three genes in immature INPs of the type II lineage lead to their de-differentiation into ectopic NBs. Therefore, *klu*, *HLHmγ* and *dpn* need to be down-regulated in immature INPs to ensure correct type II lineage progression. It can be assumed that the cell fate determinants *brat* and/or *numb* act to suppress factors like Klu in the immature INP to distinguish it from the stem cell, since their absence also causes de-differentiation of INPs. In addition, expression patterns of the stem cell and cell fate determinants are mutually exclusive. Indeed, simultaneous mutation of *klu* in a *brat* mutant background can

rescue the *brat* NB over-proliferation phenotype (Xiao *et al.*, 2012). Whether this is a direct effect where Brat, should it be involved in translational repression, might act directly on *klu* mRNA, or an indirect effect where Brat negatively acts for example on an unknown co-factor of Klu that is necessary for its function, or on an activator of *klu* expression, has yet to be determined.

In contrast to the phenotype in type II lineages, *klu* over-expression in GMCs did not lead to their de-differentiation into type I NBs. However, we found an increase in the number of GMCs. Potential explanations for this phenotype could be increased proliferation of type I NBs, or a delayed cell cycle of GMCs. Clonal data to assess the number of neurons produced in a single NB lineage would hint towards one or the other possibility, because one would expect more, or less neurons to be produced, respectively. The absence of the cell fate determinant Pros in INPs could explain why INPs, but not GMCs de-differentiate into ectopic NBs upon *klu* over-expression. It is possible that Pros is a negative regulator of *klu* expression, as it was shown in embryos to bind *klu* (Choksi *et al.*, 2006) (www.neuroblast.org). Pros might therefore assist to adjust *klu* levels in GMCs, but not in INPs, so that cell division and differentiation is still possible, albeit with some delay. Consistent with these results, *HLHmγ* and *dpn* are also bound, and possibly negatively regulated by Pros in GMCs (Choksi *et al.*, 2006).

5.3.2 Klu is a potential down-stream target of Notch signaling

HLHmγ was described to be the key downstream target of Notch in NBs (Jennings *et al.*, 1994; Zacharioudaki *et al.*, 2012), while Dpn on the other hand seems to function independently of Notch (Zacharioudaki *et al.*, 2012; Zhu *et al.*, 2012). In a recent publication also describing a role for Klu in NB self-renewal, it was shown that Klu, like HLHmγ, might also be a potential down-stream target of Notch signaling (Xiao *et al.*, 2012). As mentioned (see 3.4.1), up-regulation of Notch in type II lineages, causes immature INPs to de-differentiate leading to an increase in type II NB numbers. Aberrant Notch signaling also causes, albeit much milder, type I NB over-proliferation. Taken together this shows that Notch needs to be down-regulated in immature INPs and GMCs. This mechanism depends to some extend on Klu since its loss in the Notch over-activation background causes a partial rescue. Klu seems to act downstream of Notch, because its over-expression in a *Notch* mutant background leads to a complete rescue of the *Notch* NB loss phenotype. However, *klu* over-expression in this scenario does not result in ectopic NB formation, and neither does *klu* loss in an active *Notch*

background completely rescue the NB over-proliferation phenotype. This indicates that additional Notch down stream targets are required to transform immature INPs and GMCs back into NBs (Xiao *et al.*, 2012).

5.3.3 Klu is required for NB self-renewal

High levels of redundancy between NB self-renewal factors seem to prevent lethal or strong NB loss phenotypes upon knock down. We showed that mutating or knocking down *klu* leads to a loss of almost all type II lineages and a milder loss of type I lineages. Recently, a similar phenotype was also described for *dpn* (Zhu *et al.*, 2012). Consistently, upon investigation of *klu* mutant NBs numbers at different time-points after larval hatching (ALH), a gradual loss of NBs from about 80 at 72 hours ALH down to less than 60 at 96 ALH was observed (Xiao *et al.*, 2012). Since Klu was shown in the *Drosophila* retina to positively regulate PCD (Rusconi *et al.*, 2004), we blocked the apoptosis pathway. We still observed the same loss of NBs, indicating that Klu does not regulate PCD in this context. Symmetric NB divisions could also account for the observed loss of NBs, however we never found more than one Dpn positive cell in one lineage.

Klu was shown to be involved in the specification of SOPs via promotion of proneural genes activity on the level of transcription and translation. Since it acts as a transcriptional repressor, it was proposed to carry out this function via repression of an antagonist of SOP development (Kaspar *et al.*, 2008). Like for SOPs, wild-type NB numbers could never be observed in *klu* mutant larval brains (Xiao *et al.*, 2012). This indicates that NBs might have disappeared already in the embryo, or did not get specified during embryonic stages. The latter seems not very likely since Klu expression only starts when NBs have already delaminated (Yang *et al.*, 1997) and many larval type I NBs can be found in brains lacking *klu*. It would be worth investigating whether all embryonic NBs are present in *klu* mutants.

We also observed a decrease in *klu* NBs size, and it was shown recently that the absence of Notch signaling also leads to NB shrinkage and premature differentiation (Song and Lu, 2011). Since *klu* is a potential downstream target of Notch, it is possible that Notch executes its function in NB size and self-renewal maintenance at least in part via Klu. Expression of Ase in type II NBs or Pros in type I NBs would hint towards the possibility that NBs differentiate prematurely, however we could never observe this. More careful analysis, and also more information on how growth and maintenance of NB identity are actually related, are necessary in order to determine the exact origin of this phenotype.

Interestingly, the *klu* NB loss and size defects phenotype could only be observed when MARCM clones where generated before L2 larval stages. The same was true when we knocked down *klu* in a time-controlled manner. It is possible that older NBs are less dependent on the presence of Klu, because it might execute its function only in a certain temporal window. The time window during which loss of Klu leads to reduced NB size and loss of NB identity either overlaps with, or precedes bursts of two known temporal TFs, which were shown to be involved in specifying the Pros-dependent cell cycle exit of larval NBs (Maurange *et al.*, 2008). Additional indication that Klu might also act to determine a certain temporal competence comes from the fact that it is essential for specifying the temporal identity of the progeny of the second-born GMC in the embryonic NB4-2 lineage (Yang *et al.*, 1997). Loss of *klu* likely leads to a duplication of the first-born sublineage of NB4-2, because the transition towards the next temporal identity is inhibited. This shows the temporal specification potential of Klu and could explain the premature loss of NB phenotype in this particular temporal window. Another explanation for this time-dependent loss of NB phenotype is that the phenotype develops only some time after loss of klu. This could be due to protein perdurance, however we could not observe any residual Klu protein by immunofluorescence neither in MARCM clones, nor in the *klu* knock down.

An involvement of Klu in the specification of NB daughter cells was described in certain neuronal linages in the embryo (Benito-Sipos *et al.*, 2010; Yang *et al.*, 1997). A similar function during larval neurogenesis is possible, however during late third instar larval stages we have never observed Klu expression in GMCs. Therefore, Klu might not be involved in the generation of specific NB progeny in L3 larval brains.

We, and others have identified the three NB fate determinants Klu, HLHmγ and Dpn and have shown that their continued expression leads to conversion of daughter cells prone for differentiation back into NBs. However, how these factors interact and what co-factors might be involved, or how they influence each other's expression and what their down-stream target genes are, is still a mystery. Preliminary experiments showed us that Klu and Dpn appear to act non-redundantly in different pathways, since knock down of *klu* in a *dpn* over-expressing background does not rescue the UAS-*dpn* type II NB over-proliferation phenotype and vice versa. In addition, loss of *klu* or *dpn* leads to a partial loss of NBs, which is more pronounced when both genes have been knocked down. Further experiments are necessary to unravel how these factors act together to achieve and sustain NB identity.

5.3.4 Restricted developmental potential of mature INPs and type I GMCs

An interesting and recurring phenomenon is the higher sensitivity of immature INPs, compared to GMCs and mature INPs, to de-differentiate back into NBs. Like in *brat* mutants, and also in the case of over-expression of *klu*, *dpn* and *HLHmγ*, large numbers of ectopic NBs stemming almost exclusively from reverted immature INPs can be observed. We have shown that indeed only Ase negative immature INPs can de-differentiate back into NB-like cells, while Ase positive INPs and GMCs are less susceptible to mis-expression of Klu.

As already mentioned, elevated Notch signaling in type II NB lineages causes strong NB over-proliferation defects, while this phenotype in type I lineage is much weaker. Activation of *klu* further enhances ectopic NB formation in all type I lineages (Xiao *et al.*, 2012). Like for INPs, this Notch dependent reversion of GMCs into NBs also depends on Klu, because loss of *klu* in this background limits formation of supernumerary NBs. The reduced response of GMCs and mature INPs to increased Notch signaling could indicate a lower proliferation potential of these cells. This could be due to the presence of factors like Earmuff, (Weng *et al.*, 2010), Ase, or Pros that can repress self-renewal genes and activate downstream targets involved in differentiation (Choksi *et al.*, 2006; Southall and Brand, 2009). It is possible that only when activated Notch signaling in GMCs is supported by the presence of self-renewal factors, can the potential of GMCs and mature INPs to de-differentiate be increased.

Taken together, these data indicate that the genomes of INPs and GMCs are re-programmed during differentiation in a way that they become less responsive to self-renewal factors like Klu. However, how this re-programming is achieved is not known. The next chapter shows methodology for how this could be addressed and preliminary results are discussed.

5.4 EXPERIMENTAL PROCEDURES

5.4.1 Fly strains, RNAi and clonal analysis

Stock	Type	Generated
;;*ase*-Gal4, UAS-*stingerGFP*	Gal4-line	(Zhu *et al.*, 2006), (Barolo *et al.*, 2000)
UAS-*Dicer2*; MZ1407(*insc*)-Gal4, UAS-*mCD8::GFP*	Gal4-line	(Neumuller *et al.*, 2011)
;*insc*-Gal4, UAS-*mCD8::GFP*;; *tub*-Gal80^{ts}	Gal4-line	This study
UAS-*mCD8::GFP*;; PointedP1-Gal4	Gal4-line	(Zhu *et al.*, 2011)
R9D11-Gal4	Gal4-line	(Weng *et al.*, 2010)
C155-Gal4, UAS-*mCD8::GFP*, hsFlip122;; tub-Gal80 FRT2A	MARCM stock	Bloomington stock numbers 5146 and 5190
w;;UASt.attB-*klu*	UAS-line	This study
w;;UAS-*klu* RNAi	RNAi	TID 51276 and 51277 (VDRC)
w;;UAS-*klu* shmiR/CyO	RNAi	This study
klu^{G410}	P-element	(Klein and Campos-Ortega, 1997)
FRT2A *klu*^{212lR51C}	Amorphic mutant	(Klein and Campos-Ortega, 1997)
w;;FRT2A	FRT line	Bloomington stock number 1997

MARCM clones derived from FRT2A, *klu*^{212lR51C} were induced following Lee and Luo, 2001 (Lee and Luo, 2001).

To prevent embryonic lethality, embryonically derived phenotypes, and for time-course experiments, UAS-constructs were expressed with *tub*-Gal80^{ts}, reared at 18 °C and then shifted to 29 °C for the time indicated in the respective experiments. All other transgenes were expressed at 25 °C for 24 h and then shifted to 29 °C for five days.

5.4.2 Antibodies and Immunohistochemistry of larval brains

Antibodies used: guinea pig anti-Dpn (1:1000, (Lee and Luo, 2001), courtesy of J. Skeath), rat anti-Ase (1:50), mouse anti-Pros (1:100, MR1A, DSHB), rabbit anti-Mira (1:200, (Betschinger *et al.*, 2006)), rabbit anti-Klu (1:100, (Klein and Campos-Ortega, 1997)), rabbit anti-aPKC (1:500, Santa Cruz Biotechnology), mouse anti-PH3 (1:1000, Cell Signaling Technology), rat anti-ELAV (1:100, 7E8A10, DSHB), Alexa Fluor 488 and 567 phalloidin (Invitrogen) and Toto-3 iodide (1:1000, Invitrogen). For immunohistochemistry experiments of larval brains see 4.2.4.

5.4.3 Transplantation of larval brain pieces

Crosses of UAS-*Dicer2*; MZ1407-Gal4, UAS-*mCD8::GFP* with the control or ;;UAS-*klu* were set up at 29 °C and after five to six days transplantations of GFP-positive, larval brain pieces were performed as previously described (Caussinus and Gonzalez, 2005) (Ashburner, 1998), with minor modifications. Freshly eclosed host flies were collected and allowed to age at 25 °C such that they were three to four days old at the time of transplantation. These w^{1118} female adult hosts were anesthetized by CO_2 and immobilized on a metal plate kept on ice, with double-side sticky tape, ventral side up. Small pieces of GFP-positive larval brains were transplanted with a constructed glass capillary needle (needle puller- Narishige Japan model PN-30; needles made from Pasteur pipettes) tangentially into the mid-ventral abdomen of female host flies. Post recovery from anesthesia, the host flies were maintained at standard conditions at 29 °C. Surviving flies were transferred to fresh food bottles every third day. To assay tumor formation both the surviving and dead host flies were observed under a fluorescent microscope once or twice a week, or more frequently if required. Pictures of transplanted host flies (with or without) tumors were taken with a Sony Alpha NEX-5 compact camera.

5.4.4 Dissection and immunostainings on transplanted tumors

After tumor formation, the abdomens of host flies were dissected in ice-cold PBS and fixed in 2 % PFA (Sigma-Aldrich) for 30 minutes at room temperature, washed several times in PBS/ 0.5 % Triton X-100, and preincubated in PBS/ 0.5 % Triton X-100 containing 10 % NGS. Primary antibodies were incubated overnight at 4 °C and secondary antibodies were Dylight™ 549-labeled goat anti-mouse, -rabbit, or -rat IgG 1:400 (all from KPL). The nuclei were labeled with Toto-3 iodide diluted in PBST for three hours at room temperature. Then the samples were embedded and mounted in Vectashield mounting medium (Vector Laboratories, Inc.). Pictures of transplanted

tumors were taken using a TCS SP5 confocal microscope (Leica) and the images were processed using standard ImageJ 1.42a (NIH).

5.4.5 Dissection of ovarioles of transplanted flies and detection of micrometastases

After tumor formation, the abdomens of host flies were dissected, as previously described (Beaucher *et al.*, 2007) with minor modifications, in Grace's insect medium (GIBCO, Invitrogen) at room temperature (RT) and the dissected ovaries were immediately fixed in 4 % PFA, 0.2 % of Triton-X-100 dissolved in Grace's insect medium for 30 minutes without shaking. The fixative was then rinsed three times in PBS/ 0.5 % Triton-X-100 (PBST), then washed three times for 10 minutes each in PBST. Samples were then incubated for 1h at RT with Phalloidin-Alexa 568 (Molecular Probes, Invitrogen detection technologies) diluted 1:200 and Toto-3 Iodide (Molecular Probes, Invitrogen detection technologies) diluted 1:1000 in PBST for 1 h at RT. Samples were rinsed in PBST, and washed three times for 10 minutes each in PBST, rinsed two times in PBS, washed two times for 10 minutes each in PBS and then embedded in Vectashield overnight at 4°C. Then ovaries were dissected and the separated ovarioles were mounted onto a slide in Vectashield mounting medium (Vector Laboratories, Inc. Reactolab S.A., H-1000). The presence of metastases within ovarioles was detected using a Leica TCS SP5 confocal microscope and the images were processed using ImageJ 1.42a (NIH, USA).

5.4.6 Generation of klu shmiR line

We developed our own software to predict efficient shRNAs with minimal off-targets (available on request). The synthesized oligos were annealed and cloned into the WALIUM20 vector according to protocols by the The Transgenic RNAi Project (flyrnai.org). Primers used for klu:

AATTCGCTGATGCTGGCAAGTACATCAATATGCTTGAATATAACTATTGATGTACTTGCCAGC
ATCAACTG

CTAGCAGTTGATGCTGGCAAGTACATCAATAGTTATATTCAAGCATATTGATGTACTTGCCAG
CATCAGCG

6 CHAPTER 3 – A TIME-COURSE OF TRANCRIPTIONAL CHANGES DURING GMC MATURATION

6.1 INTRODUCTION

During the course of this project we have identified a hypothetical transcriptional network for NB self-renewal and have found three factors, Dpn, Klu and HLHmγ, to act as stem cell determinants. These stem cell determinants are turned off in GMCs and INPs by the cell fate determinants Brat, Pros and Numb, which determine a differentiation program for these cells. However, it is still unknown what this differentiation program actually comprises, and how different cell fates are established by the interplay between the self-renewal and differentiation determinants. Specific questions are numerous, for example, how is growth differentially regulated between NBs and GMCs? Why do GMCs and INPs stop proliferating while NBs continue to divide? How are self-renewal factors inhibited in GMCs and INPs on the level of protein modification and degradation, translation inhibition, or inhibition of transcription? And how exactly do the cell fate determinants play into this and what downstream targets do they repress and activate?

We have generated transcriptional data from self-renewing NBs and terminally differentiated neurons. This however does not allow us to address the posed questions, as we have no information of what is happening during maturation of GMCs. We do not know what the first events down-stream of the cell fate determinants are that distinguish a GMC from a NB, and how the differentiation program, which eventually leads to a terminal division of GMCs, is established over time (Figure 21A). A time-course of GMC maturation and determining which genes are down-regulated when, and by which mechanism, will help to further our understanding of how differentiation is initiated and established in NB daughter cells. However, so far, purification of NBs and GMCs has not been possible. We developed methodology to collect type I NBs and GMCs in a time-controlled manner by FACS and have used this method to investigate transcriptional changes of TFs from our NB network for self-renewal (see 4.1.7) in gradually aging GMCs.

6.2 RESULTS

6.2.1 GMCs can be obtained by FACS in a time-controlled manner

In order to obtain pure populations of GMCs at different time-points during differentiation we decided on a cell culture approach. We used the type I NB specific *ase*-Gal4 driver line and marked NBs and their progeny with stinger*GFP*. We sorted type I NBs according to the protocol already described (see 4.2.2 and 4.2.6) and took care to sort no longer than 40 minutes, because continued exposure of NBs to cold temperatures affects their survival. We first tested how many GMCs are produced in a certain amount of time and incubated sorted NBs in supplemented Schneider's medium at room temperature for three, five and seven hours (Figure 21B-D'). After three hours we found NBs with only one daughter cell (arrows in Figure 21B and B'), but also some which had not divided yet. After five hours we could see that almost all NBs had divided at least once, with many having produced already two GMCs (arrows in Figure 21C and C'). After an incubation of seven hours the majority of NBs had produced two to four daughter cells (arrows in Figure 21D and D') and few daughter cells had already divided terminally into neurons. Taken together, incubation of sorted NBs for three, five or seven hours generates an average of one, two or three GMC daughter cells, respectively. Therefore, the earliest time-point contains only GMCs that had just been born, while the latest time-point contains a mixture of mature GMCs just before terminal division, medium aged and young GMCs.

We then incubated sorted type I NBs for five hours and dissociated NBs and their daughter cells by manual disruption during incubation. FACS sorting of this culture revealed two populations of cells, which are of different sizes and GFP intensity (outlined in Figure 21E). We assumed the bigger and brighter cells to be the original NBs, since their size and GFP signal corresponds to NBs when they are sorted for the first time. The smaller cells with a weaker signal are very likely only GMCs since we (i) have sorted type I NBs, which only give rise to GMCs, (ii) GMCs have not yet divided terminally (see above and Figure 8C) and (iii) the size of these cells is clearly larger than that of neurons. Lastly (iv), we stained both cell populations for the NB marker Mira (Figure 21F-G') and found Mira positive cells only in the NB population, but not in our GMC population. It is noteworthy that in terms of GFP intensity, but not size, two populations of cells can be seen in both the GMC and the NB population. This results from the presence from either one or two copies of stinger*GFP* in the hetero- or

homozygous driver line, respectively. Due to incomplete dissociation, GMCs that are still attached to NBs can be found in the NB population. This causes impurity of the second sort NB sample and a lower yield of GMCs and NBs, because daughter cells in the NB sample are lost to the GMC population, and some NB/GMC duplets are recognized by their wider FSC signal (FSC-W vs FSC-A) and are being discarded. We conclude that we can sort the immediate daughter cells of NBs in a time-controlled manner in large enough quantities to allow for analysis with qRT-PCR.

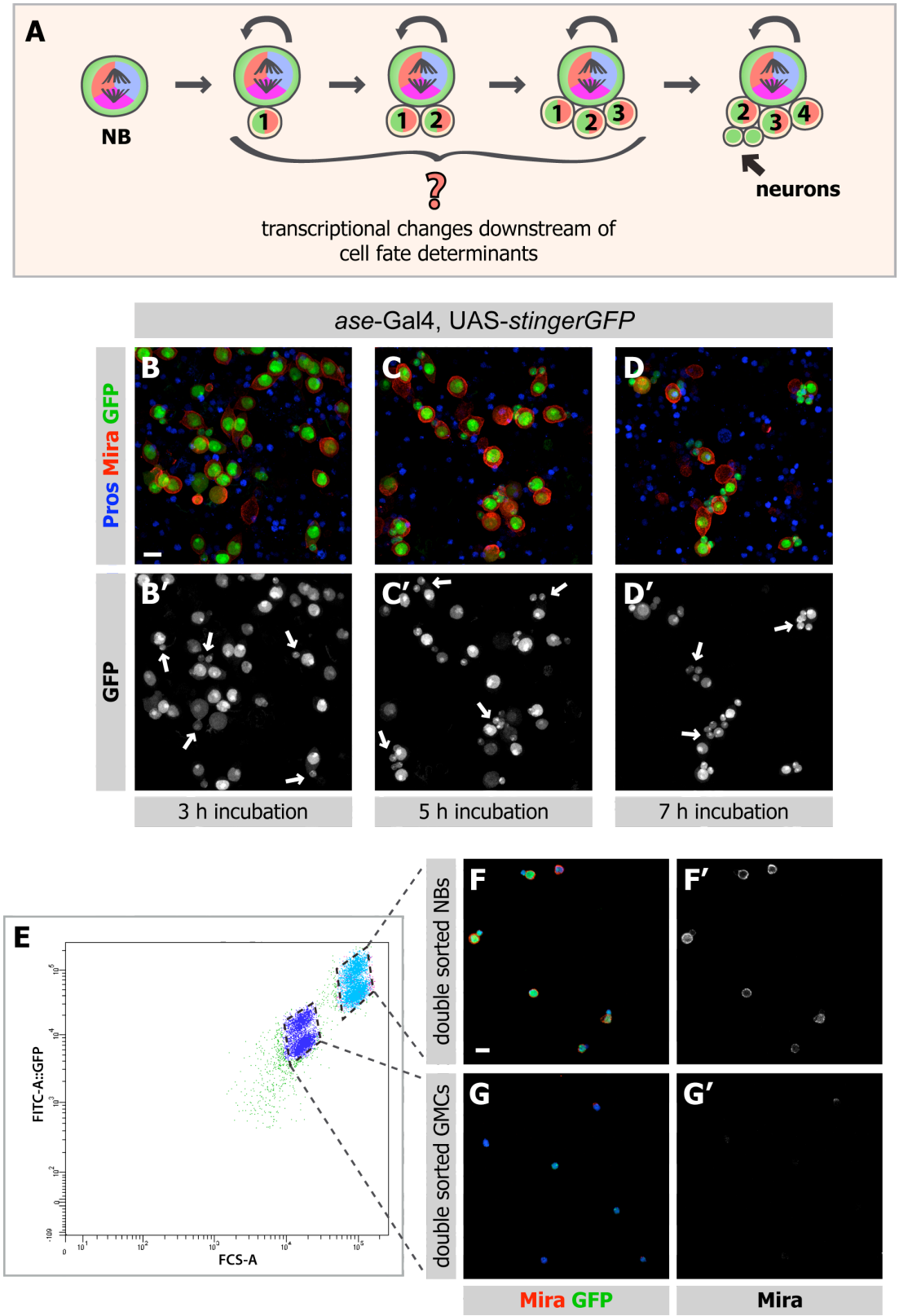
A
NB
1
1 2
1 2 3
2 3 4
neurons
?
transcriptional changes downstream of
cell fate determinants
ase-Gal4, UAS-stingerGFP
Pros Mira GFP
GFP
B
C
D
B′
C′
D′
3 h incubation
5 h incubation
7 h incubation
E
FITC-A::GFP
FCS-A
double sorted NBs
double sorted GMCs
F
F′
G
G′
Mira GFP
Mira

Figure 21. Type I NBs and their immediate daughter cells can be sorted separately

(A) Time-course of dividing NBs and GMCs. NBs divide and give rise to GMCs, which in turn after some delay divide terminally into neurons. Transcriptional changes induced by the cell fate determinants that lead to differentiation of GMCs are not known. **(B-D')** FACS sorted type I NBs incubated for three (B and B'), five (C and C') and seven hours (D and D') give rise to an average of one, two or three to four GMCs, respectively. Arrows in GFP channel point to NBs with the respective number of progeny. **(E-G')** Re-sorted type I NBs after five hours of incubation revealed two distinct populations of cells (E). Staining of these populations with the NB marker Mira showed Mira positive cells only in the population of larger cells with a higher GFP signal. GMCs are still attached to some of these NBs (F and F'). The smaller cells did not stain positive for the NB marker Mira (G and G') and are most likely GMCs.

6.2.2 *Grh*, *klu*, *dpn* and *HLHmγ* are early targets of cell fate determinants

To investigate when and which transcriptional differences between NBs and GMCs are established, we collected material from type I NBs and neurons, and from age-controlled GMCs that were obtained after three, five and seven hours from incubation of NBs. To obtain sufficient amounts of material we pooled several sorts for the GMC samples (six sorts for three and five hour time-points, three for seven hour time-point), and investigated the expression of all TFs from our proposed network for NB self-renewal with qPCR. The resulting time-course of TF expression from NBs, young, medium aged and old GMCs, as well as neurons, normalized to the housekeeping gene *actin 5C* (*Act5C*), and compared to the expression in NBs, is shown in Figure 22.

Surprisingly, three hours after sorting (red, GMC 3h), expression of many of the TFs we had found to be strongly and highly differentially expressed, actually increased in GMCs (*e.g. ken*, *king-tubby* or *CG10565*). Since we assumed that all of these TFs are involved in stem cell maintenance, we expected them to either be down-regulated in GMCs, or expressed at similar levels in NBs and GMCs. The only factors that showed a slight decrease in gene expression after three hours were *CG31875* and *CG15715*, but this change of expression was less than two-fold compared to NBs.

After five hours of incubation (green, GMC 5h), when the parental NB had already divided again in many cases, a strong decrease in expression for the genes known to be involved in stem cell maintenance – *HLHmγ*, *dpn* and to a lesser extend *klu*, as well as *grh*, can be seen. The expression levels of the two unknown genes *CG31875* and *CG15715* also decreased further. Genes that were up-regulated in GMCs show a decrease of expression compared to the three hour time-point, but in most cases their expression in GMCs is still higher compared to NBs.

Seven hours after sorting (purple, GMC 7h), and after up to four NBs divisions, the transcriptional down-regulation of the NB self-renewal factors in GMCs is more pronounced, while genes that were initially up-regulated in GMCs have decreased their expression to NB levels or are expressed lower compared to NBs. An exception is Ase, which is expressed in type I NBs, but is not part of the TF self-renewal network since its differential expression between NBs and neurons was not high enough. Ase expression is increased in GMCs, however a dual role was suggested for this TF – it is

thought to activate self-renewal and repress differentiation genes in NBs, but was also suggested to act as an activator of differentiation in GMCs (Southall and Brand, 2009). The expression of many genes from our hypothetical network for NB self-renewal is not strongly altered in GMCs compared to NBs, and their down-regulation is only apparent in neurons (*e.g. CG6701*, *mod*, *bigmax*, *Rel*). This suggests that they are not directly involved in the establishment of differential cell fates.

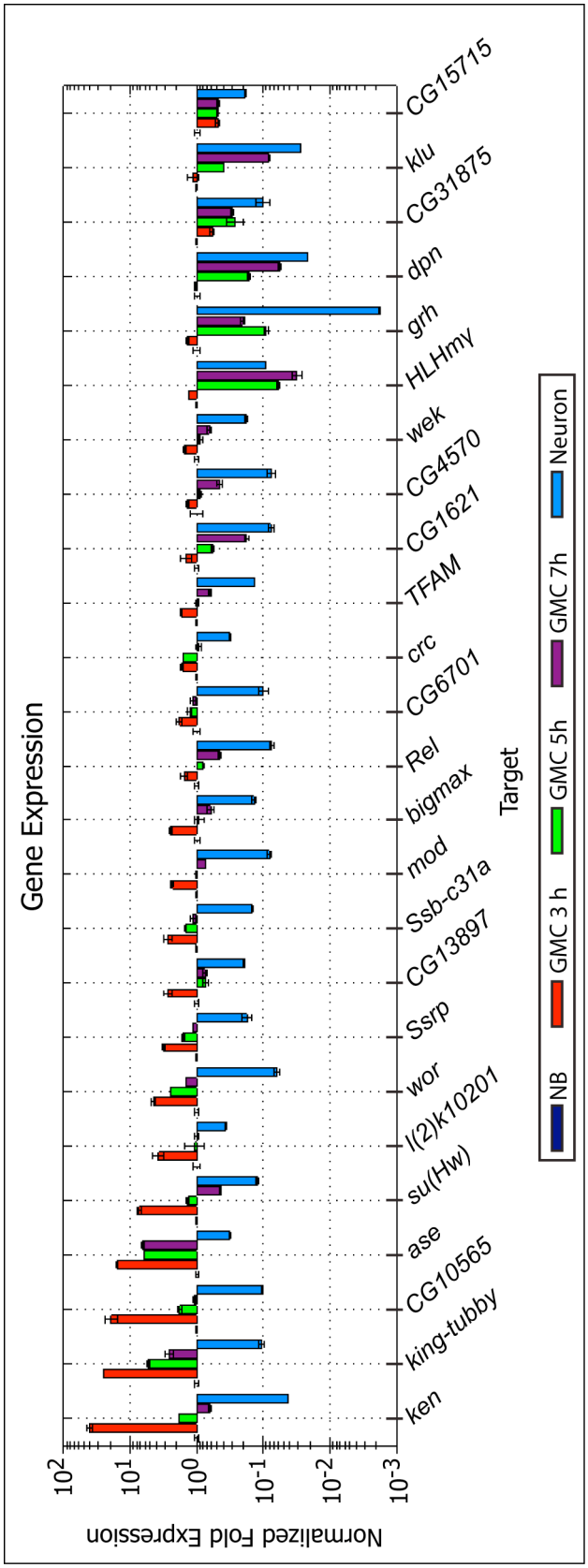
Gene Expression
Normalized Fold Expression
10^{2}
10^{1}
10^{0}
10^{-1}
10^{-2}
10^{-3}
ken
king-tubby
CG10565
ase
su(Hw)
l(2)k10201
wor
Ssrp
CG13897
Ssb-c31a
mod
bigmax
Rel
CG6701
crc
TFAM
CG1621
CG4570
wek
HLHmγ
grh
dpn
CG31875
klu
CG15715
Target
NB
GMC 3 h
GMC 5h
GMC 7h
Neuron

Figure 22. Time-course of gene expression in GMCs
Expression levels of NB specific TFs from the network for NB self-renewal in sorted NBs, GMCs re-sorted three, five and seven hours after the first sort, and neurons, normalized to the housekeeping gene *actin 5C* and to expression in NBs. Gene expression of TFs in GMCs sorted after three hours (red) does not decrease, but increases for many genes (*e.g. ken*, *king-tubby* or *CG10565*), except for *CG31875* and *CG15715*, which show a less then two-fold down-regulation compared to NBs. After five hours of incubation of NBs (green), expression levels of known NBs identity genes (*HLHmγ*, *grh*, *dpn*, *klu*) show a strong decrease in expression compared to NBs. This down-regulation is more pronounced when GMCs were obtained after seven hours of incubation (purple). Expression of many genes changes less than two-fold in GMCs during differentiation, but is only strongly decreased in neurons, indicating that these genes do not play a role during differentiation (*e.g. CG6701*, *mod*, *bigmax*, *Rel*).

6.3 DISCUSSION

We developed a method to investigate gene expression of NBs and their immediate daughter cells in a time-controlled manner. We found that three hours after sorting, during which the primary NB has divided on average only once, the investigated NB specific TFs from our transcriptional network for NB self-renewal showed no decrease in their expression. Rather the opposite is true and for many genes expression levels increased in GMCs compared to NBs. Only after five hours did expression of known NB determinants decrease. This was surprising, because the NBs had already divided at least once more at that point and we had expected that transcriptional differences between both cells would have been established already earlier. It is difficult to address whether down-regulation of *HLHmγ*, *klu*, *grh* and *dpn* occurred just before, or after the NB has grown back to its original size and has divided a second time. Additional time-points of GMC maturation would have to be investigated, but the best option would be to synchronize NB divisions so that all GMCs are of the same age.

Several scenarios can be imagined at this point. Firstly, down-regulation of NB self-renewal and up-regulation of differentiation genes occurs late, but prior to the second NB division. Secondly, the observed changes are actually misleading, because it is possible that the housekeeping gene *Act5C* is not suitable for normalization in this case. If *Act5C* is expressed comparatively higher in GMCs than in NBs, then changes in expression appear lower. RNAseq would be an alternative to circumvent this problem, since the data is normalized over the number of fragments per kilobase of combined exon length per one million of total mapped reads. Another drawback of the presented experiment is that we did not use double-sorted NBs for our NB sample, since thos sample was contaminated with GMCs. We therefore could not control for any cell culture derived changes in expression levels. The third and last scenario would be that down-regulation of NB identity genes indeed occurs only after the NBs has grown back to its original size and has divided again.

In the case that transcriptional changes are established before the NB divides a second time, or that *Act5C* is not a suitable housekeeping gene, open questions to address are how exactly the cell fate determinants affect the regulatory network for NB self-renewal, and what their downstream targets are in GMCs. As mentioned

previously, potential down-stream targets of the cell fate determinant Pros were identified by DamID in embryonic NBs. Indeed, *klu*, *grh*, *dpn* and *HLHmγ* are all direct Pros targets (Choksi *et al.*, 2006), indicating that their down-regulation in GMCs is caused by inhibition of transcription through Pros. We plan to determine Pros down-stream targets in larval NBs and GMCs by time-controlled loss of *pros* function and transcriptional profiling. In stark contrast to the NB, the GMC does not grow before it divides terminally, however it is not known how this difference is achieved. Pros does not seem to repress cell growth, since the ectopic NB-like cells that are present in *pros* mutants are very small (Bowman *et al.*, 2008). We therefore would like to investigate whether growth might be regulated by Brat and/or Numb and will also investigate their down-stream targets by knock down experiments and RNAseq. Investigation of genes that are up-regulated in GMCs, like *wor* or *ase*, might also provide information as to how they contribute to maturation of GMCs. Since both genes are also expressed in NBs it is possible that they bind to differentiation genes already in NBs and activate their expression shortly after GMCs are born, which then decreases the self-renewal potential of these cells. Also in these cases would transcriptome wide data provide a more global view on all transcriptional changes down-stream of the TFs.

In case it is true that transcriptional differences between GMCs and NBs are only apparent after the NBs has completed another round of cell division, then the question arises how initial differences are established between both cell types. Since the NB grows, while the GMC does not, it is possible that growth is not a direct effect of the action of the cell fate determinants, but that it is directly differentially regulated between NBs and GMCs. This could potentially be achieved by for example, differential segregation or stability of growth factors, e.g. ribosomal proteins, rRNA or even differences in Polymerase I expression or activity. Post-transcriptional differences and modifications between NBs and GMCs are also likely part of this process. Dpn and Klu proteins seem to disappear fast in GMCs, as they can never be seen by immunostainings with specific antibodies. It is not known whether this is an active process, maybe involving the cell fate determinants, or passive due to fast protein turnover. It is also not clear whether removal of stem cell factors on the protein level is sufficient for the GMCs to become initially different and whether these changes are manifested on the transcriptome level only later. A third option would be active processes in the NBs, which confer self-renewal capacity. A candidate protein would be the kinase aPKC, which is retained in the NBs after asymmetric cell division. It might

phophorylate and activate targets involved in growth control and/or self-renewal in NBs. Therefore, the NB could continue to divide while GMCs cannot, but instead GMCs are re-programmed to undergo differentiation.

To address all these questions, more experiments are necessary to expand on the preliminary results discussed in this section. As mentioned already, mRNA sequencing of wild type, as well as NB and cell fate determinant mutants should shed light on whether transcriptional differences between NBs and GMCs are indeed late events, but also what the down-stream targets of these determinants in NBs and GMCs are. Identifying differences on the protein level is difficult to address, because material is very limited in this system – should initial differences in lineage progression be dependent on protein modifications or stability. Protocols where less material is required or using mutants, which cause ectopic NB formation as an alternative model system, would have to be established. Unraveling how the transcriptional network for self-renewal is re-programmed into a network for differentiation would be the future goal of this project.

6.4 EXPERIMENTAL PROCEDURES

6.4.1 FACS of GMCs in a time-controlled manner

To isolate GMCs by FACS we opted for a two-step FACS protocol. We first dissected and dissociated larval brains and sorted type I NBs as described in 4.2.2 and 4.2.6. We incubated NBs in complete Schneider's medium (see 4.2.2), supplemented with 20-Hydroxyecdyson (Sigma-Aldrich) at a final concentration of 5 µg/µL for three, five or seven hours at room temperature. We disrupted NBs and GMCs manually by pipetting with 200 µL tips several times during incubation. We then subjected this cell culture to a second sort under standard conditions (see 4.2.6) and separated primary NBs and GMCs.

6.4.2 Quantitative PCR analysis of sorted NBs, neurons and GMCs

We isolated total RNA from all samples (NB, neuron and GMCs) using TRIzol (Invitrogen) following the manufacturer's instruction for low amounts of material. After genomic DNA digestion (TURBO DNA-free kit [Applied Biosystems]), we generated first strand cDNA using Superscript III (Invitrogen) and random hexamer primers (Invitrogen), and examined expression with qPCR. We used the iQ™ SYBR Green

supermix (Bio-Rad) following the manufacturers instructions and a two-step qPCR protocol on a BioRad CFX96 cycler, and the following primer pairs at a final concentration of 250 nM were used.

Gene	Forward primer	Reverse primer
Act5C	AGTGGTGGAAGTTTGGAGTG	GATAATGATGATGGTGTGCAGG
ase	CAGTGATCTCCTGCCTAGTTTG	GTGTTGGTTCCTGGTATTCTGATG
crc	CCACGCCCTTTAACTTTACC	GATATCATCGACCAGTTGGTTCTC
wor	CAGTAATGGTGAAGAGGAGGAG	GATTAATAAATGGCCGGTGGTTG
wek	GAGGGCATACTGTACCAAAC	CAGGCGACACCAGTATATCCAATC
HLHγ	CATTTCGCCAATCTCCAGCTAC	TCCTCCATCTTGGTCACATC
mod	GACGAACTTGACTTCAGATGCTAC	CCGCTATCGTTAAACACTTTCC
su(Hw)	CTGGAGAAGATCGAGAAGGATG	GTTAATGTGACCCAGATGGAAGG
dpn	CGCTATGTAAGCCAAATGGATGG	CTATTGGCACACTGGTTAAGATGG
Ssrp	GACGTTCGACTACAAGATTCCC	GATCCAAGGAGAGCACAAAGAAC
ken	CGTCTGCGAGAACAAAGTAAAG	AGGTTCCTTATCAACGGACTGG
klu	CAACAATAATGAGACCCACTCC	GATCTTCATCCTGTTCGGCATC
Rel	CTTTGAATGCGGACGGTGATAG	CCAGCAAAGGTCGTATGTAGTG
Ssb-c31a	TCCTTGAAGTGGCCGAAGAAG	CTACGACTTAGTTTGGCATGTGG
king-tubby	CAAGAAGATATTTCTGCTGGGAGG	CATTGCGAGACAAATCCGTG
l(2)k10201	AATTCCATGGAGGTGGACGAG	CGTTTGATGTCCAAAGCTGAAGG
CG6701	CTCTCACGTCTTCATGATCCTTC	CTGCTCCACATATTTCTCTCCC
CG13897	GAATGTGATAACAGCAACAACGGG	CTCTTAAAGGTCGACAACATGGG
CG15715	GATCCCAAGACGTATAAACAGCAC	GTGAAACGATCATCAGACCTCC
CG10565	TGGAGGAGATTAACCAGACAC	CATTGCTCCAGAGCTCATTC
CG4570	CCCATCGAGGATTCGATTTACC	CGAATCACTTCTGTACACCTC
TFAM	CTGTCTAAGAACTGGTCCGATG	GTAGATTTGTTGGTCCCGCTTG
bigmax	GAGGCCAAGTTTCAAGTGTTCC	GTGGTCAGCTGCTTAAAGTTCTC
CG31875	CTTCGCAAAGGTACGAAAGGAG	CATGAAGGAGAAGTACAGTCGAAG
grh	GTGTCTGTCCAGTAGGAGATAAG	CCTAAGGTCATAGCATAAGCAGGG

7 REFERENCES

Almeida, M. S., and Bray, S. J. (2005). Regulation of post-embryonic neuroblasts by Drosophila Grainyhead. Mech Dev *122*, 1282-1293.

Anders, S., and Huber, W. (2010). Differential expression analysis for sequence count data. Genome Biol *11*, R106.

Arama, E., Dickman, D., Kimchie, Z., Shearn, A., and Lev, Z. (2000). Mutations in the beta-propeller domain of the Drosophila brain tumor (brat) protein induce neoplasm in the larval brain. Oncogene *19*, 3706-3716.

Arbouzova, N. I., Bach, E. A., and Zeidler, M. P. (2006). Ken & barbie selectively regulates the expression of a subset of Jak/STAT pathway target genes. Curr Biol *16*, 80-88.

Ashraf, S. I., and Ip, Y. T. (2001). The Snail protein family regulates neuroblast expression of inscuteable and string, genes involved in asymmetry and cell division in Drosophila. Development *128*, 4757-4767.

Atwood, S. X., and Prehoda, K. E. (2009). aPKC phosphorylates Miranda to polarize fate determinants during neuroblast asymmetric cell division. Curr Biol *19*, 723-729.

Bader, G. D., and Hogue, C. W. (2003). An automated method for finding molecular complexes in large protein interaction networks. BMC Bioinformatics *4*, 2.

Barolo, S., Carver, L. A., and Posakony, J. W. (2000). GFP and beta-galactosidase transformation vectors for promoter/enhancer analysis in Drosophila. Biotechniques *29*, 726, 728, 730, 732.

Beaucher, M., Goodliffe, J., Hersperger, E., Trunova, S., Frydman, H., and Shearn, A. (2007). Drosophila brain tumor metastases express both neuronal and glial cell type markers. Dev Biol *301*, 287-297.

Bello, B., Reichert, H., and Hirth, F. (2006). The brain tumor gene negatively regulates neural progenitor cell proliferation in the larval central brain of Drosophila. Development *133*, 2639-2648.

Bello, B. C., Izergina, N., Caussinus, E., and Reichert, H. (2008). Amplification of neural stem cell proliferation by intermediate progenitor cells in Drosophila brain development. Neural Develop *3*, 5.

Benetka, W., Mehlmer, N., Maurer-Stroh, S., Sammer, M., Koranda, M., Neumuller, R., Betschinger, J., Knoblich, J. A., Teige, M., and Eisenhaber, F. (2008). Experimental testing of predicted myristoylation targets involved in asymmetric cell division and calcium-dependent signalling. Cell Cycle *7*, 3709-3719.

Benito-Sipos, J., Estacio-Gomez, A., Moris-Sanz, M., Baumgardt, M., Thor, S., and Diaz-Benjumea, F. J. (2010). A genetic cascade involving klumpfuss, nab and castor

specifies the abdominal leucokinergic neurons in the Drosophila CNS. Development *137*, 3327-3336.

Berdnik, D., Torok, T., Gonzalez-Gaitan, M., and Knoblich, J. A. (2002). The endocytic protein alpha-Adaptin is required for numb-mediated asymmetric cell division in Drosophila. Dev Cell *3*, 221-231.

Berger, C., Harzer, H., Burkard, T. R., Steinmann, J., van der Horst, S., Laurenson, A. S., Novatchkova, M., Reichert, H., and Knoblich, J. A. (2012). FACS purification and transcriptome analysis of drosophila neural stem cells reveals a role for Klumpfuss in self-renewal. Cell Rep *2*, 407-418.

Betschinger, J., Mechtler, K., and Knoblich, J. A. (2006). Asymmetric segregation of the tumor suppressor brat regulates self-renewal in Drosophila neural stem cells. Cell *124*, 1241-1253.

Bier, E., Vaessin, H., Younger-Shepherd, S., Jan, L. Y., and Jan, Y. N. (1992). deadpan, an essential pan-neural gene in Drosophila, encodes a helix-loop-helix protein similar to the hairy gene product. Genes Dev *6*, 2137-2151.

Bischof, J., Maeda, R. K., Hediger, M., Karch, F., and Basler, K. (2007). An optimized transgenesis system for Drosophila using germ-line-specific phiC31 integrases. Proc Natl Acad Sci U S A *104*, 3312-3317.

Boone, J. Q., and Doe, C. Q. (2008). Identification of Drosophila type II neuroblast lineages containing transit amplifying ganglion mother cells. Dev Neurobiol *68*, 1185-1195.

Bowman, S. K., Neumuller, R. A., Novatchkova, M., Du, Q., and Knoblich, J. A. (2006). The Drosophila NuMA Homolog Mud regulates spindle orientation in asymmetric cell division. Dev Cell *10*, 731-742.

Bowman, S. K., Rolland, V., Betschinger, J., Kinsey, K. A., Emery, G., and Knoblich, J. A. (2008). The tumor suppressors Brat and Numb regulate transit-amplifying neuroblast lineages in Drosophila. Dev Cell *14*, 535-546.

Brand, A. H., and Perrimon, N. (1993). Targeted gene expression as a means of altering cell fates and generating dominant phenotypes. Development *118*, 401-415.

Bray, S. J. (2006). Notch signalling: a simple pathway becomes complex. Nat Rev Mol Cell Biol *7*, 678-689.

Cabernard, C., and Doe, C. Q. (2009). Apical/basal spindle orientation is required for neuroblast homeostasis and neuronal differentiation in Drosophila. Dev Cell *17*, 134-141.

Cai, Y., Chia, W., and Yang, X. (2001). A family of snail-related zinc finger proteins regulates two distinct and parallel mechanisms that mediate Drosophila neuroblast asymmetric divisions. EMBO J *20*, 1704-1714.

Calvi, B. R., and Lilly, M. A. (2004). Fluorescent BrdU labeling and nuclear flow sorting of the Drosophila ovary. Methods Mol Biol *247*, 203-213.

Carney, T. D., Miller, M. R., Robinson, K. J., Bayraktar, O. A., Osterhout, J. A., and Doe, C. Q. (2012). Functional genomics identifies neural stem cell sub-type expression profiles and genes regulating neuroblast homeostasis. Dev Biol *361*, 137-146.

Caussinus, E., and Gonzalez, C. (2005). Induction of tumor growth by altered stem-cell asymmetric division in Drosophila melanogaster. Nat Genet *37*, 1125-1129.

Cenci, C., and Gould, A. P. (2005). Drosophila Grainyhead specifies late programmes of neural proliferation by regulating the mitotic activity and Hox-dependent apoptosis of neuroblasts. Development *132*, 3835-3845.

Ceron, J., Tejedor, F. J., and Moya, F. (2006). A primary cell culture of Drosophila postembryonic larval neuroblasts to study cell cycle and asymmetric division. Eur J Cell Biol *85*, 567-575.

Chell, J. M., and Brand, A. H. (2010). Nutrition-responsive glia control exit of neural stem cells from quiescence. Cell *143*, 1161-1173.

Chia, W., Somers, W. G., and Wang, H. (2008). Drosophila neuroblast asymmetric divisions: cell cycle regulators, asymmetric protein localization, and tumorigenesis. J Cell Biol *180*, 267-272.

Chintapalli, V. R., Wang, J., and Dow, J. A. (2007). Using FlyAtlas to identify better Drosophila melanogaster models of human disease. Nat Genet *39*, 715-720.

Choksi, S. P., Southall, T. D., Bossing, T., Edoff, K., de Wit, E., Fischer, B. E., van Steensel, B., Micklem, G., and Brand, A. H. (2006). Prospero Acts as a Binary Switch between Self-Renewal and Differentiation in Drosophila Neural Stem Cells. Dev Cell *11*, 775-789.

Chu-Lagraff, Q., Wright, D. M., McNeil, L. K., and Doe, C. Q. (1991). The prospero gene encodes a divergent homeodomain protein that controls neuronal identity in Drosophila. Development *Suppl 2*, 79-85.

Cumberledge, S., and Krasnow, M. A. (1994). Preparation and analysis of pure cell populations from Drosophila. Methods Cell Biol *44*, 143-159.

Dietzl, G., Chen, D., Schnorrer, F., Su, K. C., Barinova, Y., Fellner, M., Gasser, B., Kinsey, K., Oppel, S., Scheiblauer, S., Couto, A., Marra, V., Keleman, K., and Dickson, B. J. (2007). A genome-wide transgenic RNAi library for conditional gene inactivation in Drosophila. Nature *448*, 151-156.

Doe, C. Q. (2008). Neural stem cells: balancing self-renewal with differentiation. Development *135*, 1575-1587.

Doe, C. Q., Chu-LaGraff, Q., Wright, D. M., and Scott, M. P. (1991). The prospero gene specifies cell fates in the Drosophila central nervous system. Cell *65*, 451-464.

Enright, A. J., Van Dongen, S., and Ouzounis, C. A. (2002). An efficient algorithm for large-scale detection of protein families. Nucleic Acids Res *30*, 1575-1584.

Faith, J. J., Hayete, B., Thaden, J. T., Mogno, I., Wierzbowski, J., Cottarel, G., Kasif, S., Collins, J. J., and Gardner, T. S. (2007). Large-scale mapping and validation of Escherichia coli transcriptional regulation from a compendium of expression profiles. PLoS Biol *5*, e8.

Frank, D. J., Edgar, B. A., and Roth, M. B. (2002). The Drosophila melanogaster gene brain tumor negatively regulates cell growth and ribosomal RNA synthesis. Development *129*, 399-407.

Gonzalez-Gaitan, M., and Jackle, H. (1997). Role of Drosophila alpha-adaptin in presynaptic vesicle recycling. Cell *88*, 767-776.

Gonzalez, C. (2007). Spindle orientation, asymmetric division and tumour suppression in Drosophila stem cells. Nat Rev Genet *8*, 462-472.

Groth, A. C., Fish, M., Nusse, R., and Calos, M. P. (2004). Construction of transgenic Drosophila by using the site-specific integrase from phage phiC31. Genetics *166*, 1775-1782.

Guo, M., Jan, L. Y., and Jan, Y. N. (1996). Control of daughter cell fates during asymmetric division: interaction of Numb and Notch. Neuron *17*, 27-41.

Haber, D. A., Buckler, A. J., Glaser, T., Call, K. M., Pelletier, J., Sohn, R. L., Douglass, E. C., and Housman, D. E. (1990). An internal deletion within an 11p13 zinc finger gene contributes to the development of Wilms' tumor. Cell *61*, 1257-1269.

Haley, B., Hendrix, D., Trang, V., and Levine, M. (2008). A simplified miRNA-based gene silencing method for Drosophila melanogaster. Dev Biol *321*, 482-490.

Harrison, H., Farnie, G., Howell, S. J., Rock, R. E., Stylianou, S., Brennan, K. R., Bundred, N. J., and Clarke, R. B. (2010). Regulation of breast cancer stem cell activity by signaling through the Notch4 receptor. Cancer Res *70*, 709-718.

Hart, Y., Antebi, Y. E., Mayo, A. E., Friedman, N., and Alon, U. (2012). Design principles of cell circuits with paradoxical components. Proc Natl Acad Sci U S A *109*, 8346-8351.

Hilgers, V., Perry, M. W., Hendrix, D., Stark, A., Levine, M., and Haley, B. (2011). Neural-specific elongation of 3' UTRs during Drosophila development. Proc Natl Acad Sci U S A *108*, 15864-15869.

Hirata, J., Nakagoshi, H., Nabeshima, Y., and Matsuzaki, F. (1995). Asymmetric segregation of the homeodomain protein Prospero during Drosophila development. Nature *377*, 627-630.

Hohenstein, P., and Hastie, N. D. (2006). The many facets of the Wilms' tumour gene, WT1. Hum Mol Genet *15 Spec No 2*, R196-201.

Horvitz, H. R., and Herskowitz, I. (1992). Mechanisms of asymmetric cell division: Two Bs or not two Bs, that is the question. Cell *68*, 237-255.

Ikeshima-Kataoka, H., Skeath, J. B., Nabeshima, Y., Doe, C. Q., and Matsuzaki, F. (1997). Miranda directs Prospero to a daughter cell during Drosophila asymmetric divisions. Nature *390*, 625-629.

Irizarry, R. A., Bolstad, B. M., Collin, F., Cope, L. M., Hobbs, B., and Speed, T. P. (2003). Summaries of Affymetrix GeneChip probe level data. Nucleic Acids Res *31*, e15.

Isshiki, T., Pearson, B., Holbrook, S., and Doe, C. Q. (2001). Drosophila neuroblasts sequentially express transcription factors which specify the temporal identity of their neuronal progeny. Cell *106*, 511-521.

Ito, K., and Hotta, Y. (1992). Proliferation pattern of postembryonic neuroblasts in the brain of Drosophila melanogaster. Dev Biol *149*, 134-148.

Izergina, N., Balmer, J., Bello, B., and Reichert, H. (2009). Postembryonic development of transit amplifying neuroblast lineages in the Drosophila brain. Neural Dev *4*, 44.

Izumi, Y., Ohta, N., Hisata, K., Raabe, T., and Matsuzaki, F. (2006). Drosophila Pins-binding protein Mud regulates spindle-polarity coupling and centrosome organization. Nat Cell Biol *8*, 586-593.

Jaiswal, H., Conz, C., Otto, H., Wolfle, T., Fitzke, E., Mayer, M. P., and Rospert, S. (2011). The chaperone network connected to human ribosome-associated complex. Mol Cell Biol *31*, 1160-1173.

Jennings, B., Preiss, A., Delidakis, C., and Bray, S. (1994). The Notch signalling pathway is required for Enhancer of split bHLH protein expression during neurogenesis in the Drosophila embryo. Development *120*, 3537-3548.

Kai, T., Williams, D., and Spradling, A. C. (2005). The expression profile of purified Drosophila germline stem cells. Dev Biol *283*, 486-502.

Kaspar, M., Schneider, M., Chia, W., and Klein, T. (2008). Klumpfuss is involved in the determination of sensory organ precursors in Drosophila. Dev Biol *324*, 177-191.

Klein, T., and Campos-Ortega, J. A. (1997). klumpfuss, a Drosophila gene encoding a member of the EGR family of transcription factors, is involved in bristle and leg development. Development *124*, 3123-3134.

Knoblich, J. A. (2008). Mechanisms of asymmetric stem cell division. Cell *132*, 583-597.

Knoblich, J. A. (2010). Asymmetric cell division: recent developments and their implications for tumour biology. Nat Rev Mol Cell Biol *11*, 849-860.

Knoblich, J. A., Jan, L. Y., and Jan, Y. N. (1995). Asymmetric segregation of Numb and Prospero during cell division. Nature *377*, 624-627.

Knoblich, J. A., Jan, L. Y., and Jan, Y. N. (1997). The N terminus of the Drosophila Numb protein directs membrane association and actin-dependent asymmetric localization. Proc Natl Acad Sci U S A *94*, 13005-13010.

Kraut, R., and Campos-Ortega, J. A. (1996). inscuteable, a neural precursor gene of Drosophila, encodes a candidate for a cytoskeleton adaptor protein. Dev Biol *174*, 65-81.

Kraut, R., Chia, W., Jan, L. Y., Jan, Y. N., and Knoblich, J. A. (1996). Role of inscuteable in orienting asymmetric cell divisions in Drosophila. Nature *383*, 50-55.

Kreidberg, J. A., Sariola, H., Loring, J. M., Maeda, M., Pelletier, J., Housman, D., and Jaenisch, R. (1993). WT-1 is required for early kidney development. Cell *74*, 679-691.

Kurimoto, K., Yabuta, Y., Ohinata, Y., and Saitou, M. (2007). Global single-cell cDNA amplification to provide a template for representative high-density oligonucleotide microarray analysis. Nat Protoc *2*, 739-752.

Lee, C. Y., Andersen, R. O., Cabernard, C., Manning, L., Tran, K. D., Lanskey, M. J., Bashirullah, A., and Doe, C. Q. (2006a). Drosophila Aurora-A kinase inhibits neuroblast self-renewal by regulating aPKC/Numb cortical polarity and spindle orientation. Genes Dev *20*, 3464-3474.

Lee, C. Y., Wilkinson, B. D., Siegrist, S. E., Wharton, R. P., and Doe, C. Q. (2006b). Brat Is a Miranda Cargo Protein that Promotes Neuronal Differentiation and Inhibits Neuroblast Self-Renewal. Dev Cell *10*, 441-449.

Lee, T., and Luo, L. (2001). Mosaic analysis with a repressible cell marker (MARCM) for Drosophila neural development. Trends Neurosci *24*, 251-254.

Lefort, K., Mandinova, A., Ostano, P., Kolev, V., Calpini, V., Kolfschoten, I., Devgan, V., Lieb, J., Raffoul, W., Hohl, D., Neel, V., Garlick, J., Chiorino, G., and Dotto, G. P. (2007). Notch1 is a p53 target gene involved in human keratinocyte tumor suppression through negative regulation of ROCK1/2 and MRCKalpha kinases. Genes Dev *21*, 562-577.

Li, H., Handsaker, B., Wysoker, A., Fennell, T., Ruan, J., Homer, N., Marth, G., Abecasis, G., and Durbin, R. (2009a). The Sequence Alignment/Map format and SAMtools. Bioinformatics *25*, 2078-2079.

Li, R., Yu, C., Li, Y., Lam, T. W., Yiu, S. M., Kristiansen, K., and Wang, J. (2009b). SOAP2: an improved ultrafast tool for short read alignment. Bioinformatics *25*, 1966-1967.

Lin, S., Lai, S. L., Yu, H. H., Chihara, T., Luo, L., and Lee, T. (2010). Lineage-specific effects of Notch/Numb signaling in post-embryonic development of the Drosophila brain. Development *137*, 43-51.

Lovell, M. A., Xie, C., Xiong, S., and Markesbery, W. R. (2003). Wilms' tumor suppressor (WT1) is a mediator of neuronal degeneration associated with the pathogenesis of Alzheimer's disease. Brain Res *983*, 84-96.

Lu, B., Rothenberg, M., Jan, L. Y., and Jan, Y. N. (1998). Partner of Numb colocalizes with Numb during mitosis and directs Numb asymmetric localization in Drosophila neural and muscle progenitors. Cell *95*, 225-235.

Luo, D., Renault, V. M., and Rando, T. A. (2005). The regulation of Notch signaling in muscle stem cell activation and postnatal myogenesis. Semin Cell Dev Biol *16*, 612-622.

Madden, S. L., Cook, D. M., Morris, J. F., Gashler, A., Sukhatme, V. P., and Rauscher, F. J. r. (1991). Transcriptional repression mediated by the WT1 Wilms tumor gene product. Science *253*, 1550-1553.

Maere, S., Heymans, K., and Kuiper, M. (2005). BiNGO: a Cytoscape plugin to assess overrepresentation of gene ontology categories in biological networks. Bioinformatics *21*, 3448-3449.

Maurange, C., Cheng, L., and Gould, A. P. (2008). Temporal transcription factors and their targets schedule the end of neural proliferation in Drosophila. Cell *133*, 891-902.

Mayr, C., and Bartel, D. P. (2009). Widespread shortening of 3'UTRs by alternative cleavage and polyadenylation activates oncogenes in cancer cells. Cell *138*, 673-684.

McDonald, J. A., Fujioka, M., Odden, J. P., Jaynes, J. B., and Doe, C. Q. (2003). Specification of motoneuron fate inDrosophila: Integration of positive and negative transcription factor inputs by a minimaleve enhancer. J. Neurobiol. *57*, 193-203.

McGuire, S. E., Mao, Z., and Davis, R. L. (2004). Spatiotemporal gene expression targeting with the TARGET and gene-switch systems in Drosophila. Sci STKE *2004*, pl6.

Miller, M. R., Robinson, K. J., Cleary, M. D., and Doe, C. Q. (2009). TU-tagging: cell type-specific RNA isolation from intact complex tissues. Nat Methods *6*, 439-441.

Nakagama, H., Heinrich, G., Pelletier, J., and Housman, D. E. (1995). Sequence and structural requirements for high-affinity DNA binding by the WT1 gene product. Mol Cell Biol *15*, 1489-1498.

Neufeld, T. P., de la Cruz, A. F., Johnston, L. A., and Edgar, B. A. (1998). Coordination of growth and cell division in the Drosophila wing. Cell *93*, 1183-1193.

Neumuller, R. A., Betschinger, J., Fischer, A., Bushati, N., Poernbacher, I., Mechtler, K., Cohen, S. M., and Knoblich, J. A. (2008). Mei-P26 regulates microRNAs and cell growth in the Drosophila ovarian stem cell lineage. Nature *454*, 241-245.

Neumüller, R. A., and Knoblich, J. A. (2009). Dividing cellular asymmetry: asymmetric cell division and its implications for stem cells and cancer. Genes Dev *23*, 2675-2699.

Neumuller, R. A., Richter, C., Fischer, A., Novatchkova, M., Neumuller, K. G., and Knoblich, J. A. (2011). Genome-wide analysis of self-renewal in Drosophila neural stem cells by transgenic RNAi. Cell Stem Cell *8*, 580-593.

Ohlstein, B., and Spradling, A. (2007). Multipotent Drosophila intestinal stem cells specify daughter cell fates by differential notch signaling. Science *315*, 988-992.

Orian, A., van Steensel, B., Delrow, J., Bussemaker, H. J., Li, L., Sawado, T., Williams, E., Loo, L. W., Cowley, S. M., Yost, C., Pierce, S., Edgar, B. A., Parkhurst, S. M., and

Eisenman, R. N. (2003). Genomic binding by the Drosophila Myc, Max, Mad/Mnt transcription factor network. Genes Dev *17*, 1101-1114.

Otto, H., Conz, C., Maier, P., Wolfle, T., Suzuki, C. K., Jeno, P., Rucknagel, P., Stahl, J., and Rospert, S. (2005). The chaperones MPP11 and Hsp70L1 form the mammalian ribosome-associated complex. Proc Natl Acad Sci U S A *102*, 10064-10069.

Pellegrinet, L., Rodilla, V., Liu, Z., Chen, S., Koch, U., Espinosa, L., Kaestner, K. H., Kopan, R., Lewis, J., and Radtke, F. (2011). Dll1- and dll4-mediated notch signaling are required for homeostasis of intestinal stem cells. Gastroenterology *140*, 1230-1240.e1-7.

Pelletier, J., Schalling, M., Buckler, A. J., Rogers, A., Haber, D. A., and Housman, D. (1991). Expression of the Wilms' tumor gene WT1 in the murine urogenital system. Genes Dev *5*, 1345-1356.

Petronczki, M., and Knoblich, J. A. (2001). DmPAR-6 directs epithelial polarity and asymmetric cell division of neuroblasts in Drosophila. Nat Cell Biol *3*, 43-49.

Qin, H., Percival-Smith, A., Li, C., Jia, C. Y., Gloor, G., and Li, S. S. (2004). A novel transmembrane protein recruits numb to the plasma membrane during asymmetric cell division. J Biol Chem *279*, 11304-11312.

Rajan, A., and Perrimon, N. (2012). Drosophila cytokine unpaired 2 regulates physiological homeostasis by remotely controlling insulin secretion. Cell *151*, 123-137.

Rebollo, E., Roldan, M., and Gonzalez, C. (2009). Spindle alignment is achieved without rotation after the first cell cycle in Drosophila embryonic neuroblasts. Development *136*, 3393-3397.

Rebollo, E., Sampaio, P., Januschke, J., Llamazares, S., Varmark, H., and Gonzalez, C. (2007). Functionally unequal centrosomes drive spindle orientation in asymmetrically dividing Drosophila neural stem cells. Dev Cell *12*, 467-474.

Reichert, H. (2011). Drosophila neural stem cells: cell cycle control of self-renewal, differentiation, and termination in brain development. Results Probl Cell Differ *53*, 529-546.

Reya, T., Morrison, S. J., Clarke, M. F., and Weissman, I. L. (2001). Stem cells, cancer, and cancer stem cells. Nature *414*, 105-111.

Rhyu, M. S., Jan, L. Y., and Jan, Y. N. (1994). Asymmetric distribution of numb protein during division of the sensory organ precursor cell confers distinct fates to daughter cells. Cell *76*, 477-491.

Roberts, A., Trapnell, C., Donaghey, J., Rinn, J. L., and Pachter, L. (2011). Improving RNA-Seq expression estimates by correcting for fragment bias. Genome Biol *12*, R22.

Roberts, S. G. (2005). Transcriptional regulation by WT1 in development. Curr Opin Genet Dev *15*, 542-547.

Rolls, M. M., Albertson, R., Shih, H. P., Lee, C. Y., and Doe, C. Q. (2003). Drosophila aPKC regulates cell polarity and cell proliferation in neuroblasts and epithelia. J Cell Biol *163*, 1089-1098.

Roy, S., Ernst, J., Kharchenko, P. V., Kheradpour, P., Negre, N., Eaton, M. L., Landolin, J. M., Bristow, C. A., Ma, L., Lin, M. F., Washietl, S., Arshinoff, B. I., Ay, F., Meyer, P. E., Robine, N., Washington, N. L., Di Stefano, L., Berezikov, E., Brown, C. D., Candeias, R., Carlson, J. W., Carr, A., Jungreis, I., Marbach, D., Sealfon, R., Tolstorukov, M. Y., Will, S., Alekseyenko, A. A., Artieri, C., Booth, B. W., Brooks, A. N., Dai, Q., Davis, C. A., Duff, M. O., Feng, X., Gorchakov, A. A., Gu, T., Henikoff, J. G., Kapranov, P., Li, R., MacAlpine, H. K., Malone, J., Minoda, A., Nordman, J., Okamura, K., Perry, M., Powell, S. K., Riddle, N. C., Sakai, A., Samsonova, A., Sandler, J. E., Schwartz, Y. B., Sher, N., Spokony, R., Sturgill, D., van Baren, M., Wan, K. H., Yang, L., Yu, C., Feingold, E., Good, P., Guyer, M., Lowdon, R., Ahmad, K., Andrews, J., Berger, B., Brenner, S. E., Brent, M. R., Cherbas, L., Elgin, S. C., Gingeras, T. R., Grossman, R., Hoskins, R. A., Kaufman, T. C., Kent, W., Kuroda, M. I., Orr-Weaver, T., Perrimon, N., Pirrotta, V., Posakony, J. W., Ren, B., Russell, S., Cherbas, P., Graveley, B. R., Lewis, S., Micklem, G., Oliver, B., Park, P. J., Celniker, S. E., Henikoff, S., Karpen, G. H., Lai, E. C., MacAlpine, D. M., Stein, L. D., White, K. P., and Kellis, M. (2010). Identification of functional elements and regulatory circuits by Drosophila modENCODE. Science *330*, 1787-1797.

Rusan, N. M., and Peifer, M. (2007). A role for a novel centrosome cycle in asymmetric cell division. J Cell Biol *177*, 13-20.

Rusconi, J. C., Fink, J. L., and Cagan, R. (2004). klumpfuss regulates cell death in the Drosophila retina. Mech Dev *121*, 537-546.

San-Juan, B. P., and Baonza, A. (2011). The bHLH factor deadpan is a direct target of Notch signaling and regulates neuroblast self-renewal in Drosophila. Dev Biol *352*, 70-82.

Sandberg, R., Neilson, J. R., Sarma, A., Sharp, P. A., and Burge, C. B. (2008). Proliferating cells express mRNAs with shortened 3' untranslated regions and fewer microRNA target sites. Science *320*, 1643-1647.

Santolini, E., Puri, C., Salcini, A. E., Gagliani, M. C., Pelicci, P. G., Tacchetti, C., and Di Fiore, P. P. (2000). Numb is an endocytic protein. J Cell Biol *151*, 1345-1352.

Schaefer, M., Petronczki, M., Dorner, D., Forte, M., and Knoblich, J. A. (2001). Heterotrimeric G proteins direct two modes of asymmetric cell division in the Drosophila nervous system. Cell *107*, 183-194.

Schaefer, M., Shevchenko, A., Shevchenko, A., and Knoblich, J. A. (2000). A protein complex containing Inscuteable and the Galpha-binding protein Pins orients asymmetric cell divisions in Drosophila. Curr Biol *10*, 353-362.

Schober, M., Schaefer, M., and Knoblich, J. A. (1999). Bazooka recruits Inscuteable to orient asymmetric cell divisions in Drosophila neuroblasts. Nature *402*, 548-551.

Schwamborn, J. C., Berezikov, E., and Knoblich, J. A. (2009). The TRIM-NHL protein TRIM32 activates microRNAs and prevents self-renewal in mouse neural progenitors. Cell *136*, 913-925.

Shen, C. P., Jan, L. Y., and Jan, Y. N. (1997). Miranda is required for the asymmetric localization of Prospero during mitosis in Drosophila. Cell *90*, 449-458.

Shigenobu, S., Arita, K., Kitadate, Y., Noda, C., and Kobayashi, S. (2006). Isolation of germline cells from Drosophila embryos by flow cytometry. Dev Growth Differ *48*, 49-57.

Siller, K. H., Cabernard, C., and Doe, C. Q. (2006). The NuMA-related Mud protein binds Pins and regulates spindle orientation in Drosophila neuroblasts. Nat Cell Biol *8*, 594-600.

Siller, K. H., and Doe, C. Q. (2008). Lis1/dynactin regulates metaphase spindle orientation in Drosophila neuroblasts. Dev Biol *319*, 1-9.

Skeath, J. B., and Thor, S. (2003). Genetic control of Drosophila nerve cord development. Curr Opin Neurobiol *13*, 8-15.

Smibert, P., Miura, P., Westholm, J. O., Shenker, S., May, G., Duff, M. O., Zhang, D., Eads, B. D., Carlson, J., Brown, J. B., Eisman, R. C., Andrews, J., Kaufman, T., Cherbas, P., Celniker, S. E., Graveley, B. R., and Lai, E. C. (2012). Global patterns of tissue-specific alternative polyadenylation in Drosophila. Cell Rep *1*, 277-289.

Song, H., Goetze, S., Bischof, J., Spichiger-Haeusermann, C., Kuster, M., Brunner, E., and Basler, K. (2010). Coop functions as a corepressor of Pangolin and antagonizes Wingless signaling. Genes Dev *24*, 881-886.

Song, Y., and Lu, B. (2011). Regulation of cell growth by Notch signaling and its differential requirement in normal vs. tumor-forming stem cells in Drosophila. Genes Dev *25*, 2644-2658.

Song, Y., and Lu, B. (2012). Interaction of Notch signaling modulator Numb with alpha-Adaptin regulates endocytosis of Notch pathway components and cell fate determination of neural stem cells. J Biol Chem *287*, 17716-17728.

Sonoda, J., and Wharton, R. P. (2001). Drosophila Brain Tumor is a translational repressor. Genes Dev *15*, 762-773.

Sousa-Nunes, R., Chia, W., and Somers, W. G. (2009). Protein phosphatase 4 mediates localization of the Miranda complex during Drosophila neuroblast asymmetric divisions. Genes Dev *23*, 359-372.

Sousa-Nunes, R., Yee, L. L., and Gould, A. P. (2011). Fat cells reactivate quiescent neuroblasts via TOR and glial insulin relays in Drosophila. Nature *471*, 508-512.

Southall, T. D., and Brand, A. H. (2009). Neural stem cell transcriptional networks highlight genes essential for nervous system development. EMBO J *28*, 3799-3807.

Spana, E. P., and Doe, C. Q. (1995). The prospero transcription factor is asymmetrically localized to the cell cortex during neuroblast mitosis in Drosophila. Development *121*, 3187-3195.

Spana, E. P., Kopczynski, C., Goodman, C. S., and Doe, C. Q. (1995). Asymmetric localization of numb autonomously determines sibling neuron identity in the Drosophila CNS. Development *121*, 3489-3494.

Spradling, A., Fuller, M. T., Braun, R. E., and Yoshida, S. (2011). Germline stem cells. Cold Spring Harb Perspect Biol *3*, a002642.

Srivastava, M., and Pollard, H. B. (1999). Molecular dissection of nucleolin's role in growth and cell proliferation: new insights. FASEB J *13*, 1911-1922.

Technau, G. M., Berger, C., and Urbach, R. (2006). Generation of cell diversity and segmental pattern in the embryonic central nervous system of Drosophila. Dev Dyn *235*, 861-869.

Thiel, G., and Cibelli, G. (2002). Regulation of life and death by the zinc finger transcription factor Egr-1. J Cell Physiol *193*, 287-292.

Tirouvanziam, R., Davidson, C. J., Lipsick, J. S., and Herzenberg, L. A. (2004). Fluorescence-activated cell sorting (FACS) of Drosophila hemocytes reveals important functional similarities to mammalian leukocytes. Proc Natl Acad Sci U S A *101*, 2912-2917.

Trapnell, C., Pachter, L., and Salzberg, S. L. (2009). TopHat: discovering splice junctions with RNA-Seq. Bioinformatics *25*, 1105-1111.

Trapnell, C., Williams, B. A., Pertea, G., Mortazavi, A., Kwan, G., van Baren, M. J., Salzberg, S. L., Wold, B. J., and Pachter, L. (2010). Transcript assembly and quantification by RNA-Seq reveals unannotated transcripts and isoform switching during cell differentiation. Nat Biotechnol *28*, 511-515.

Urbach, R., and Technau, G. M. (2003). Molecular markers for identified neuroblasts in the developing brain of Drosophila. Development *130*, 3621-3637.

Uv, A. E., Harrison, E. J., and Bray, S. J. (1997). Tissue-specific splicing and functions of the Drosophila transcription factor Grainyhead. Mol Cell Biol *17*, 6727-6735.

Varnum-Finney, B., Xu, L., Brashem-Stein, C., Nourigat, C., Flowers, D., Bakkour, S., Pear, W. S., and Bernstein, I. D. (2000). Pluripotent, cytokine-dependent, hematopoietic stem cells are immortalized by constitutive Notch1 signaling. Nat Med *6*, 1278-1281.

Wagner, K. D., Wagner, N., Vidal, V. P., Schley, G., Wilhelm, D., Schedl, A., Englert, C., and Scholz, H. (2002). The Wilms' tumor gene Wt1 is required for normal development of the retina. EMBO J *21*, 1398-1405.

Wang, H., Somers, G. W., Bashirullah, A., Heberlein, U., Yu, F., and Chia, W. (2006). Aurora-A acts as a tumor suppressor and regulates self-renewal of Drosophila neuroblasts. Genes Dev *20*, 3453-3463.

Weng, M., Golden, K. L., and Lee, C. Y. (2010). dFezf/Earmuff maintains the restricted developmental potential of intermediate neural progenitors in Drosophila. Dev Cell *18*, 126-135.

Wirtz-Peitz, F., Nishimura, T., and Knoblich, J. A. (2008). Linking cell cycle to asymmetric division: Aurora-A phosphorylates the Par complex to regulate Numb localization. Cell *135*, 161-173.

Wodarz, A., Ramrath, A., Grimm, A., and Knust, E. (2000). Drosophila atypical protein kinase C associates with Bazooka and controls polarity of epithelia and neuroblasts. J Cell Biol *150*, 1361-1374.

Wodarz, A., Ramrath, A., Kuchinke, U., and Knust, E. (1999). Bazooka provides an apical cue for Inscuteable localization in Drosophila neuroblasts. Nature *402*, 544-547.

Wu, P. S., Egger, B., and Brand, A. H. (2008). Asymmetric stem cell division: lessons from Drosophila. Semin Cell Dev Biol *19*, 283-293.

Xiao, Q., Komori, H., and Lee, C. Y. (2012). klumpfuss distinguishes stem cells from progenitor cells during asymmetric neuroblast division. Development *139*, 2670-2680.

Yang, X., Bahri, S., Klein, T., and Chia, W. (1997). Klumpfuss, a putative Drosophila zinc finger transcription factor, acts to differentiate between the identities of two secondary precursor cells within one neuroblast lineage. Genes Dev *11*, 1396-1408.

Yoshiura, S., Ohta, N., and Matsuzaki, F. (2012). Tre1 GPCR signaling orients stem cell divisions in the Drosophila central nervous system. Dev Cell *22*, 79-91.

Yu, F., Morin, X., Cai, Y., Yang, X., and Chia, W. (2000). Analysis of partner of inscuteable, a novel player of Drosophila asymmetric divisions, reveals two distinct steps in inscuteable apical localization. Cell *100*, 399-409.

Zacharioudaki, E., Magadi, S. S., and Delidakis, C. (2012). bHLH-O proteins are crucial for Drosophila neuroblast self-renewal and mediate Notch-induced overproliferation. Development *139*, 1258-1269.

Zhu, S., Barshow, S., Wildonger, J., Jan, L. Y., and Jan, Y. N. (2011). Ets transcription factor Pointed promotes the generation of intermediate neural progenitors in Drosophila larval brains. Proc Natl Acad Sci U S A *108*, 20615-20620.

Zhu, S., Lin, S., Kao, C. F., Awasaki, T., Chiang, A. S., and Lee, T. (2006). Gradients of the Drosophila Chinmo BTB-zinc finger protein govern neuronal temporal identity. Cell *127*, 409-422.

Zhu, S., Wildonger, J., Barshow, S., Younger, S., Huang, Y., and Lee, T. (2012). The bHLH Repressor Deadpan Regulates the Self-renewal and Specification of Drosophila Larval Neural Stem Cells Independently of Notch. PLoS One *7*, e46724.

8 CONTRIBUTIONS

Single cell collection (Figure 4), unsorted cell culture stainings (Figure 7), live-imaging experiments of unsorted and sorted NBs (Figure 8), analysis of *klu* MARCM clones (Figure 20) and inhibition of PCD experiment in *klu* knock down background (Figure 21) were done by Christian Berger. Leo Otsuki, who was a summer student in the lab, helped with the collection of material for deep sequencing of NBs and neurons. Bioinformatic analyses described in 4.2.9 and 4.2.11 was done by Thomas R. Burkard. Maria Novatchkova generated the networks in Figures 10 and 11 (see 4.2.12), based on published networks from Neumuller, *et. al* (2011). Jonas Steinmann produced the shmiR line against *klu* (see 4.2.13) and generated the network for NB self-renewal based on published Drosophila microarray data (Figure 12, 5.4.6). Suzanne van der Horst assisted in the generation of over-expression contructs (4.2.14) while she was a master student in the lab. Anne-Sophie Laurenson from Heinrich Reichert's lab performed transplantation experiments and investigated micrometastasis in ovaries (Figure 16). Sara Farina-Lopez assisted in the generation of all transgenic stocks. The author contributed the other experiments in this study.

This work was published (Berger *et al.*, 2012) and the data has been deposited in NCBI GEO and are accessible through GEO series accession number GSE38764.

9 ACKNOWLEDGMENTS

Dear reader, you have read this far, congratulations! I hope it was an enjoyable read. The time has come to acknowledge people – I am pretty sure I forgot some of the people who were dear to me while I was doing my PhD. If you are one of them, feel free to complain :)

First and foremost, I would like to thank Juergen Knoblich, who has given me the opportunity to work in his lab and for all his support during the last four years.

Secondly, a big thanks to Christian Berger who has shared this project with me during the first couple years. I admire his positive personality and patience, and am grateful that he always had time to answer my questions, no matter how silly they might have been. Thank you for many personal and scientific discussions over (mostly) coffee and tea, and for staying up until three am when we submitted our paper.

And now, in no particular order, Catarina Homem for loads of fun times while hanging out, having lunch, flipping flies and discussing science with me and for reading my thesis; my gym buddy, the lovely and super smart Elif Eroglu; Suzanne van der Horst, the best master student ever; Christoph Jueschke for helping me write the Zusammenfassung even though I am a native Deutsch speaker; Leo Otsuki, the best summer student ever; Gerald Schmauss und Thomas Lendl for spending SO MANY hours FACSing with me and discussing whether this cell population we think we see might actually just be in our heads; Ryan Conder, I still wonder why every discussion we had turned into something naughty; and everybody else in the Knoblich lab and institute who made life here easy and pleasurable.

Now on to the non-work related people. Natuerlich meine Eltern, meine liebe Mama und mein lieber Papa, und meine Schwester Andrea plus brother in law, Oli – danke fuer eure Unterstuetzung! Mal schauen ob ihr bei meinem naechsten Job versteht was ich eigentlich mache und nicht nur wisst, dass ich Fruchtfliegenlarven kille :). Und last but not least, Peter Koester. Worte koennen nicht beschreiben wie dankbar ich bin, dass du die letzten vier Jahre an meiner Seite warst.

10 CURRICULUM VITAE

PERSONAL DETAILS

Name	Heike Harzer
Date of birth	11th of October, 1983
Place of birth	Saalfeld (Saale), Germany
Nationality	German

ACADEMIC EDUCATION AND RESEARCH EXPERIENCE

Nov 2008 – present	Pre-doctoral studies at the Research Institute of Molecular Biotechnology (IMBA) in Vienna, Austria in the laboratory of Dr. Juergen A. Knoblich
July 2008 – Oct 2008	Technical assistant at the Fritz-Leibniz Institute (FLI) in Jena, Germany in the laboratory of Dr. Alessandro Cellerino
Oct 2007 – Dec 2007	Technical assistant at AgResearch Grasslands in Palmerston North, New Zealand in the laboratory of Dr. Bruce Veit
June 2006 – April 2007	Master thesis at AgResearch Grasslands in Palmerston North, New Zealand in the laboratory of Dr. Susanne Rasmussen, under supervision by Dr. Linda Johnson *Titel: Characterization of a novel endophyte non-ribosomal peptide synthetase (NRPS) gene from Epichloe festucae and its role in endophyte-grass symbiosis.*
Feb 2006 – May 2006	Practical training at AgResearch Grasslands in Palmerston North, New Zealand in the laboratory of Dr. Susanne Rasmussen *Titel: Establishment of a qPCR assay for quantification of mycorrhiza in* Lolium perenne.
Nov 2005 – June 2008	Diplomstudium 'Biochemistry and Molecular Biology' at the Friedrich-Schiller University in Jena, Germany
Oct 2002 – Oct 2005	Vordiplom 'Biochemistry and Molecular Biology' at the Friedrich-Schiller University in Jena, Germany

SCIENTIFIC PUBLICATIONS

2012 Berger, C., Harzer, H., Burkard, T. R., Steinmann, J., van der Horst, S., Laurenson, A. S., Novatchkova, M., Reichert, H., and Knoblich, J. A. (2012). FACS purification and transcriptome analysis of drosophila neural stem cells reveals a role for Klumpfuss in self-renewal. Cell Rep *2*, 407-418.

SCIENTIFIC POSTERS

2012 Title: *FACS purification and transcriptome analysis of* Drosophila *neural stem cells reveals a role for Klumpfuss in self-renewal.*
IMP-IMBA Annual recess, Vienna, Austria.

2011 Titel: *Genome-wide analysis of self-renewal in* Drosophila melanogaster *larval neuroblasts.*
EuroSystem 3rd annual Consortium meeting, Prague, Czech Republic.

2009 Titel: *Genome-wide analysis of self-renewal in* Drosophila *neuroblasts.*
21st European Drosophila research conference (EDRC), Nice, France

Titel: *Identification of novel factors involved in stem cell maintenance in the fruitfly* Drosophila melanogaster*.*
EuroSystem 1st annual Consortium meeting, Cambridge, Great Britain.

11 APPENDIX

Table 2. Alternativley spliced genes

test_id	gene_id	gene	value_NB	value_neuron	log2_foldChange	p_value
FBtr0076544	FBgn0000116	Argk	146,023	199,314	-287,308	0.000770561
FBtr0076546	FBgn0000116	Argk	209,182	405,492	427,684	1.40E-02
FBtr0079085	FBgn0000228	Bsg25D	0	40,733	1.79769e+308	0.000195482
FBtr0302567	FBgn0000228	Bsg25D	477,056	932,345	-235,522	0.00118827
FBtr0070064	FBgn0000316	cin	0	285,898	1.79769e+308	3.62E-01
FBtr0070065	FBgn0000316	cin	177,516	479,257	-521,101	2.92E-05
FBtr0083056	FBgn0001219	Hsc70-4	479,544	80,251	406,479	5.98E+00
FBtr0083057	FBgn0001219	Hsc70-4	15556.8	1559.11	-331,875	0
FBtr0085175	FBgn0002441	l(3)mbt	105,606	570,577	-421,012	1.54E-03
FBtr0085176	FBgn0002441	l(3)mbt	0	12,747	1.79769e+308	9.98E-01
FBtr0075627	FBgn0002778	mnd	156,548	31,402	-56,396	4.11E-07
FBtr0114529	FBgn0002778	mnd	0	665,334	1.79769e+308	0.000240413
FBtr0079821	FBgn0002973	numb	0.884532	355,108	53,272	6.63E+00
FBtr0079822	FBgn0002973	numb	314,055	178,454	-41,374	4.27E-02
FBtr0073422	FBgn0003360	sesB	130,134	44,171	-488,075	7.18E-04
FBtr0073423	FBgn0003360	sesB	131,699	111,819	-355,801	4.00E-01
FBtr0073424	FBgn0003360	sesB	0	131,816	1.79769e+308	0.00014326
FBtr0088100	FBgn0003396	shn	813,812	0.335076	-460,213	1.06E-01
FBtr0330620	FBgn0003396	shn	0.255453	905,571	51,477	8.30E-01
FBtr0085211	FBgn0004387	Klp98A	222,595	172,096	-369,314	2.61E-02
FBtr0304671	FBgn0004387	Klp98A	0.364545	187,913	568,783	0.000116287
FBtr0082803	FBgn0004587	B52	30,837	126,767	203,944	0.00425805
FBtr0082804	FBgn0004587	B52	11,527	249,021	443,318	0.00140724
FBtr0308197	FBgn0004587	B52	765,408	144,933	-240,085	0.000945924
FBtr0083641	FBgn0004652	fru	266,604	0.43522	-593,681	2.50E-04
FBtr0083646	FBgn0004652	fru	757,367	0.154066	-561,937	0.00105213
FBtr0083647	FBgn0004652	fru	144,637	0.305587	-556,471	1.64E-01
FBtr0083649	FBgn0004652	fru	0	210,439	1.79769e+308	0.000592775
FBtr0083650	FBgn0004652	fru	87,466	0.695915	-365,174	9.53E-01
FBtr0089342	FBgn0005630	lola	379,908	661,798	-252,119	0.000434332
FBtr0089349	FBgn0005630	lola	677,232	897,179	-291,618	0.00350805
FBtr0089353	FBgn0005630	lola	106,884	298,695	480,456	4.82E-04
FBtr0089355	FBgn0005630	lola	174,322	293,663	407,434	1.89E-03
FBtr0089357	FBgn0005630	lola	986,703	245,009	-200,978	0.00365838
FBtr0089364	FBgn0005630	lola	46,513	35,984	295,165	0.000272183
FBtr0084511	FBgn0005674	Aats-glupro	413,303	346,396	-357,671	0.000138038
FBtr0084512	FBgn0005674	Aats-glupro	0	115,027	1.79769e+308	4.03E+00
FBtr0089186	FBgn0010217	ATPsyn-beta	4464.88	297,476	-390,778	0
FBtr0089187	FBgn0010217	ATPsyn-beta	190,305	967,568	566,798	0.00272113
FBtr0077662	FBgn0015600	toc	0.893864	237,794	473,351	1.57E-01
FBtr0077665	FBgn0015600	toc	0.705691	249,963	514,653	0.000250935
FBtr0110903	FBgn0015600	toc	478,702	28,474	-407,141	1.26E-03
FBtr0084503	FBgn0015795	Rab7	208,445	372,558	-248,413	0.00045643
FBtr0308612	FBgn0015795	Rab7	0	93,995	1.79769e+308	0.00111266

test_id	gene_id	gene	value_NB	value_neuron	log2_foldChange	p_value
FBtr0089486	FBgn0016917	Stat92E	410,946	323,385	297,623	0.0006035
FBtr0100457	FBgn0016917	Stat92E	286,909	381,487	-291,089	0.000131105
FBtr0082162	FBgn0024330	MED6	175,716	0.778026	-449,728	0.000256705
FBtr0301872	FBgn0024330	MED6	0	574,022	1.79769e+308	0.000721161
FBtr0089768	FBgn0026239	gukh	143,184	590,578	-45,996	4.61E-04
FBtr0100317	FBgn0026239	gukh	0	21,702	1.79769e+308	1.27E+00
FBtr0112924	FBgn0026239	gukh	48.59	552,212	-313,737	7.15E-01
FBtr0074010	FBgn0026428	HDAC6	0	407,803	1.79769e+308	0.000123488
FBtr0330405	FBgn0026428	HDAC6	936,569	917,877	-335,101	5.84E-01
FBtr0089950	FBgn0026620	tacc	112,719	869,201	294,696	0.000686918
FBtr0302614	FBgn0026620	tacc	182,384	339,171	-574,882	7.46E-07
FBtr0302615	FBgn0026620	tacc	234,035	0.392965	-589,618	4.75E-02
FBtr0086679	FBgn0027835	Dp1	0	577,839	1.79769e+308	2.91E+00
FBtr0086683	FBgn0027835	Dp1	201,667	132,256	-393,057	9.89E-02
FBtr0085357	FBgn0027873	Cpsf100	186,166	110,822	-407,028	4.65E-03
FBtr0085358	FBgn0027873	Cpsf100	0	123,218	1.79769e+308	4.53E+00
FBtr0071404	FBgn0028341	l(1)G0232	637,036	152,885	-205,892	0.00343698
FBtr0071405	FBgn0028341	l(1)G0232	228,894	224,848	-334,765	1.92E+00
FBtr0071407	FBgn0028341	l(1)G0232	0	527,201	1.79769e+308	1.18E+00
FBtr0085374	FBgn0028671	Vha100-1	108.47	193,079	-249,003	0.00114103
FBtr0085376	FBgn0028671	Vha100-1	443,406	486,183	34,548	0.000296606
FBtr0085381	FBgn0028671	Vha100-1	0	718,869	1.79769e+308	0.000104452
FBtr0301650	FBgn0028671	Vha100-1	0	367,477	1.79769e+308	0.000814897
FBtr0070908	FBgn0029870	Marf	0	225,944	1.79769e+308	0.00154745
FBtr0070910	FBgn0029870	Marf	144,597	126,141	-351,893	1.57E-02
FBtr0073790	FBgn0030479	Rbp1-like	435,431	746,217	-254,478	0.000532394
FBtr0304001	FBgn0030479	Rbp1-like	126,391	147,052	354,035	3.71E-01
FBtr0074733	FBgn0031037	CG14207	230,487	316,841	-286,286	9.36E+00
FBtr0074734	FBgn0031037	CG14207	318,774	486,478	393,177	0.000995273
FBtr0077190	FBgn0031174	CG1486	563,354	911,568	-262,762	0.000166199
FBtr0077191	FBgn0031174	CG1486	138,304	204,993	388,966	0.0023392
FBtr0089749	FBgn0031450	Hrs	0	959,208	1.79769e+308	2.89E+00
FBtr0089750	FBgn0031450	Hrs	140,279	117,916	-357,247	1.19E-01
FBtr0079641	FBgn0031990	CG8552	669,965	141,151	-224,685	0.00158974
FBtr0302595	FBgn0031990	CG8552	0	201,939	1.79769e+308	0.000404365
FBtr0081325	FBgn0032815	CG10462	632,329	0.495472	-699,573	1.26E-02
FBtr0331243	FBgn0032815	CG10462	0	221,085	1.79769e+308	0.00228889
FBtr0081338	FBgn0032849	mRpS18B	0	132,467	1.79769e+308	0.000395636
FBtr0081339	FBgn0032849	mRpS18B	272,664	349,672	-628,498	2.48E-06
FBtr0088956	FBgn0033188	CG1600	0.526304	475,772	649,823	0.000243942
FBtr0088957	FBgn0033188	CG1600	360,952	264,115	-377,257	1.89E-01
FBtr0088834	FBgn0033226	CG1882	568,347	635,784	-316,016	1.07E+00
FBtr0088835	FBgn0033226	CG1882	185,719	249,082	-289,843	0.0013682
FBtr0088837	FBgn0033226	CG1882	0	520,609	1.79769e+308	0.000512667
FBtr0302596	FBgn0033766	CG8771	0	109,461	1.79769e+308	8.77E-01
FBtr0306684	FBgn0033766	CG8771	272,444	101,506	-474,632	1.33E-02
FBtr0073175	FBgn0035473	mge	0	162,445	1.79769e+308	8.04E+00
FBtr0073176	FBgn0035473	mge	488,101	521,357	-322,684	9.69E-01
FBtr0273367	FBgn0035842	CG7504	259,746	502,358	-237,031	0.000793257

test_id	gene_id	gene	value_NB	value_neuron	log2_foldChange	p_value
FBtr0273368	FBgn0035842	CG7504	0	571,321	1.79769e+308	5.67E+00
FBtr0075956	FBgn0036286	CG10616	958,086	176,281	-244,228	0.000665114
FBtr0308896	FBgn0036286	CG10616	0	816,092	1.79769e+308	0.000465082
FBtr0075942	FBgn0036316	CG10960	943,434	178,045	-240,568	0.00106885
FBtr0075943	FBgn0036316	CG10960	0	581,357	1.79769e+308	0.000937203
FBtr0075326	FBgn0036662	CG9706	396,433	745,552	-24,107	0.00134616
FBtr0075327	FBgn0036662	CG9706	0	507,772	1.79769e+308	0.00152204
FBtr0074850	FBgn0036958	CG17233	313,137	0.121879	-468,327	0.00190173
FBtr0074851	FBgn0036958	CG17233	0	364,774	1.79769e+308	9.77E-02
FBtr0078216	FBgn0037007	CG5059	145,367	308,511	-223,631	0.00231408
FBtr0078218	FBgn0037007	CG5059	0	499,034	1.79769e+308	7.39E-01
FBtr0078777	FBgn0037299	CG1115	221,086	154,613	-383,788	6.46E-03
FBtr0305001	FBgn0037299	CG1115	0	859,125	1.79769e+308	0.000391893
FBtr0081824	FBgn0037533	CD98hc	984,987	146,401	-607,211	9.79E-05
FBtr0331344	FBgn0037533	CD98hc	737,955	717,422	328,122	0.000269434
FBtr0082329	FBgn0037855	CG6621	39,738	360,144	317,998	0.00100869
FBtr0302935	FBgn0037855	CG6621	62,582	870,598	-284,567	8.37E+00
FBtr0082360	FBgn0037890	CG17734	528,623	104,642	-56,587	1.35E-07
FBtr0082361	FBgn0037890	CG17734	0	562,587	1.79769e+308	0.00447997
FBtr0083000	FBgn0038271	CG3731	927,785	432,913	-442,164	2.13E-02
FBtr0083001	FBgn0038271	CG3731	0	34,441	1.79769e+308	1.06E+00
FBtr0085785	FBgn0039844	CG1607	28,655	268,728	322,928	0.00112314
FBtr0085786	FBgn0039844	CG1607	265,601	193,799	-377,663	2.78E-01
FBtr0089221	FBgn0039929	CG11076	257.87	260,628	-330,658	2.16E+00
FBtr0309864	FBgn0039929	CG11076	0	644,787	1.79769e+308	0.00185676
FBtr0076460	FBgn0040305	MTF-1	0	287,299	1.79769e+308	0.000312187
FBtr0113323	FBgn0040305	MTF-1	184,934	396,821	-222,045	0.0016862
FBtr0078693	FBgn0041191	Rheb	114,369	285,527	-2,002	0.00458035
FBtr0078694	FBgn0041191	Rheb	0	193,085	1.79769e+308	0.000125368
FBtr0072381	FBgn0050420	Atf-2	698,853	0.766573	-318,849	0.00183355
FBtr0072382	FBgn0050420	Atf-2	30,177	808,606	474,391	2.37E-01
FBtr0082452	FBgn0051363	Jupiter	644,672	579,046	-347,682	3.17E+00
FBtr0082453	FBgn0051363	Jupiter	653,068	131,759	433,452	3.65E+00
FBtr0082454	FBgn0051363	Jupiter	0	409,343	1.79769e+308	0.00132123
FBtr0082456	FBgn0051363	Jupiter	267,607	590.01	446,255	3.50E-03
FBtr0082457	FBgn0051363	Jupiter	322,194	615,788	425,643	0.000751189
FBtr0079038	FBgn0053113	Rtnl1	111,206	0.1253	-647,171	0.00053798
FBtr0079041	FBgn0053113	Rtnl1	139,936	0.479781	-818,818	1.69E-03
FBtr0301541	FBgn0053113	Rtnl1	0	612,634	1.79769e+308	1.77E+00
FBtr0302035	FBgn0053558	mim	0	413,056	1.79769e+308	7.58E-01
FBtr0302577	FBgn0053558	mim	121,608	459,261	-472,677	4.60E-06
FBtr0302578	FBgn0053558	mim	0	148,637	1.79769e+308	4.73E-01
FBtr0306614	FBgn0053558	mim	528,014	201,343	-471,285	2.78E-06
FBtr0111239	FBgn0086683	Spf45	115.19	100,596	-351,737	5.69E-01
FBtr0111241	FBgn0086683	Spf45	0	402,703	1.79769e+308	1.04E+00
FBtr0082626	FBgn0086687	desat1	256,817	251,323	-335,312	7.36E-01
FBtr0082630	FBgn0086687	desat1	457,597	344,789	291,356	0.00402526
FBtr0088716	FBgn0086784	stmA	914,158	212,088	-210,778	0.00317698
FBtr0301639	FBgn0086784	stmA	0.38678	174,687	549,711	0.00130857

test_id	gene_id	gene	value_NB	value_neuron	log2_foldChange	p_value
FBtr0083265	FBgn0250823	gish	0	357,895	1.79769e+308	1.22E-01
FBtr0301304	FBgn0250823	gish	81,489	0.386944	-439,641	0.00353713
FBtr0299648	FBgn0259174	Nedd4	0	272,632	1.79769e+308	0.000350221
FBtr0300520	FBgn0259174	Nedd4	790,487	104,158	-292,396	4.40E+00
FBtr0299754	FBgn0259221	CG42321	133,783	0.743815	-41,688	3.48E+00
FBtr0303100	FBgn0259221	CG42321	0.801709	984,171	361,776	0.00192446
FBtr0083765	FBgn0260003	Dys	52,345	0.394771	-372,896	5.70E-01
FBtr0083766	FBgn0260003	Dys	0.913926	515,545	581,788	5.01E-03
FBtr0110915	FBgn0260003	Dys	0.231534	Oct-65	552,349	0.00010938
FBtr0110919	FBgn0260003	Dys	0.451148	552,122	361,332	0.000489433
FBtr0301482	FBgn0261642	mbl	300,275	30,492	-329,978	6.64E-02
FBtr0306602	FBgn0261642	mbl	264,928	123,204	221,738	0.00284083
FBtr0306603	FBgn0261642	mbl	345,125	195,667	250,321	0.00130229
FBtr0306604	FBgn0261642	mbl	0.680502	118,764	412,535	0.00193661
FBtr0080727	FBgn0261882	l(2)35Bc	715,832	143,966	-563,582	3.45E-02
FBtr0303561	FBgn0261882	l(2)35Bc	0	486,393	1.79769e+308	0.00290191
FBtr0087245	FBgn0262166	calypso	861,397	208,728	-204,505	0.0032351
FBtr0087246	FBgn0262166	calypso	0	110,289	1.79769e+308	6.53E+00
FBtr0075634	FBgn0262707	CTPsyn	410,885	377,315	-34,449	2.14E+00
FBtr0075635	FBgn0262707	CTPsyn	80,179	551,959	278,327	0.00100223
FBtr0075636	FBgn0262707	CTPsyn	0	326,176	1.79769e+308	0.00334102
FBtr0080418	FBgn0263598	Vha68-2	336,292	108,443	-827,664	0
FBtr0305551	FBgn0263598	Vha68-2	0	35,192	1.79769e+308	0.000200948

Table containing alternatively spliced genes with at least two differentially expressed isoforms between NBs and neurons.

Table 3. 3'UTR enrichment in NBs and neurons

FBgn_r5.44_FB2012_02	gene	log2FoldChange
FBgn0004595	pros	-2.654785408
FBgn0000210	br	-3.798292126
FBgn0010113	hdc	-3.133432001
FBgn0010300	brat	-1.998238228
FBgn0015609	CadN	-4.152600967
FBgn0027339	jim	-4.150376604
FBgn0261710	nocte	-1.111867121
FBgn0000568	Eip75B	-3.294120455
FBgn0037636	CG9821	-1.815857623
FBgn0004198	ct	-2.478401054
FBgn0260400	elav	-3.695463818
FBgn0033313	Cirl	-2.151685594
FBgn0262737	mub	-1.962230317
FBgn0033636	tou	-1.615497948
FBgn0261617	nej	-1.429846851
FBgn0010575	sbb	-1.846052051
FBgn0036398	CG9007	-1.867925792
FBgn0262582	cic	-3.346443293
FBgn0085436	Not1	-0.843141548
FBgn0002921	Atpalpha	-1.018776628
FBgn0020309	crol	-2.150415204
FBgn0004656	fs(1)h	-1.102914939
FBgn0026160	tna	-2.946965914
FBgn0029939	CG9650	-4.574135165
FBgn0263072	CG43347	-4.377329774
FBgn0263865	Smr	-1.490004312
FBgn0262739	AGO1	-1.440816754
FBgn0025726	unc-13	-2.918479476
FBgn0003165	pum	-2.204610588
FBgn0052423	shep	-3.139385309
FBgn0085430	CG34401	-2.581027784
FBgn0261238	Alh	-2.324949142
FBgn0259246	brp	-3.94098531
FBgn0011259	Sema-1a	-3.356618865
FBgn0052529	CG32529	-1.711599462
FBgn0086655	jing	-2.645775249
FBgn0003435	sm	-3.634158804
FBgn0052676	CG32676	-3.261915598
FBgn0086758	chinmo	-2.629721133
FBgn0003415	skd	-2.170266772
FBgn0010905	Spn	-2.991127718
FBgn0015558	tty	-2.34695466
FBgn0000581	E(Pc)	-1.496454265
FBgn0262614	pyd	-1.527628882
FBgn0261444	CG3638	-1.882803349
FBgn0000273	Pka-C1	-2.707715936
FBgn0013948	Eip93F	-1.123098619

FBgn_r5.44_FB2012_02	gene	log2FoldChange
FBgn0035106	rno	-2.195208887
FBgn0004875	enc	-0.68410447
FBgn0028509	cenG1A	-2.216622296
FBgn0259240	Ten-a	-3.058739366
FBgn0085432	pan	-3.455571477
FBgn0086899	tlk	-0.872679659
FBgn0024277	trio	-2.371384212
FBgn0053558	mim	-0.991992269
FBgn0052767	CG32767	-2.609612847
FBgn0000464	Lar	-3.19929558
FBgn0004880	scrt	-4.418814888
FBgn0263995	cpo	-3.908320203
FBgn0052062	A2bp1	-2.618506244
FBgn0026375	RhoGAPp190	-2.124392577
FBgn0003301	rut	-2.752051656
FBgn0051992	gw	-1.089380706
FBgn0004369	Ptp99A	-2.183339307
FBgn0085450	Snoo	-2.724103161
FBgn0035142	hipk	-0.675196312
FBgn0026083	tyf	-0.428041435
FBgn0019968	Khc-73	-2.867739035
FBgn0010473	tutl	-4.587010592
FBgn0011817	nmo	-1.958535595
FBgn0016797	fz2	-3.105425938
FBgn0010313	corto	-0.742983306
FBgn0051163	SKIP	-2.897200593
FBgn0005427	ewg	-2.882232612
FBgn0000179	bi	-3.174392679
FBgn0035424	CG11505	-0.823029882
FBgn0036165	chrb	-2.134506345
FBgn0036451	CG9425	-0.981103262
FBgn0039186	CG5746	-1.652644084
FBgn0259745	wech	-1.048999441
FBgn0004907	14-3-3zeta	-0.067529264
FBgn0001624	dlg1	-1.047868781
FBgn0001122	G-oalpha47A	-2.770999217
FBgn0011666	msi	-0.422504497
FBgn0259214	PMCA	-1.539951192
FBgn0029979	CG10777	-1.083976485
FBgn0261642	mbl	-0.627547251
FBgn0261934	dikar	-0.977300265
FBgn0013759	CASK	-2.700151819
FBgn0023407	B4	-2.102562271
FBgn0003502	Btk29A	-3.368148959
FBgn0037705	mura	-2.32173257
FBgn0011764	Dsp1	-1.010119003
FBgn0041605	cpx	-3.913040423
FBgn0023095	caps	-4.73296329
FBgn0086675	fne	-3.346232541

FBgn_r5.44_FB2012_02	gene	log2FoldChange
FBgn0043362	bchs	-2.997199282
FBgn0263749	CG43674	-1.229430255
FBgn0259109	CG42251	-4.561805073
FBgn0029006	lack	-1.397155104
FBgn0025741	plexA	-1.447915242
FBgn0041111	lilli	-1.398733149
FBgn0015542	sima	-1.428266979
FBgn0015774	NetB	-4.57266523
FBgn0010762	simj	-1.533185047
FBgn0036576	CG5151	-2.600133665
FBgn0026869	Thd1	-2.665062337
FBgn0023531	CG32809	-2.969662594
FBgn0264270	Sxl	-1.429782752
FBgn0032957	CG2225	-3.375680555
FBgn0260970	CG42593	-1.441824475
FBgn0261793	Trf2	-0.732542852
FBgn0261873	sdt	-3.393814884
FBgn0262684	CG43154	-1.616506303
FBgn0027492	wdb	-0.7357024
FBgn0053547	Rim	-3.863000064
FBgn0001105	Gbeta13F	-0.740148796
FBgn0032479	CG16974	-0.869223405
FBgn0035481	CG12605	-4.030720977
FBgn0014870	Psi	-0.779310096
FBgn0030400	CG11138	-1.823197989
FBgn0003175	px	-1.961711372
FBgn0261811	pico	-3.407857129
FBgn0044323	Cka	-1.320423551
FBgn0026313	X11L	-2.426299557
FBgn0033212	CG1399	-2.649160713
FBgn0002968	Nrg	-0.686274925
FBgn0260003	Dys	-2.852669863
FBgn0031294	IA-2	-3.861449394
FBgn0040505	Alk	-4.340403162
FBgn0000259	CkIIbeta	-0.445602889
FBgn0035016	CG4612	-2.994210551
FBgn0036518	RhoGAP71E	-1.311722719
FBgn0040395	Unc-76	-2.300284369
FBgn0262742	Fas1	-3.800925887
FBgn0033159	Dscam	-4.354099572
FBgn0031090	Rab35	-1.212923349
FBgn0004370	Ptp10D	-3.41478735
FBgn0250823	gish	-1.073531427
FBgn0051641	stai	-2.990716137
FBgn0030049	Trf4-1	-1.2179435
FBgn0262740	CG11727	-2.601616042
FBgn0264006	CG43749	-3.653061013
FBgn0004876	cdi	-1.805649414
FBgn0039920	CG11360	-1.967306902

FBgn_r5.44_FB2012_02	gene	log2FoldChange
FBgn0000382	csw	-3.044053661
FBgn0003392	shi	-1.066112393
FBgn0031424	VGlut	-4.339340385
FBgn0037525	CG17816	-4.021220791
FBgn0030243	CG2186	-1.020438998
FBgn0000611	exd	-1.347656767
FBgn0052264	CG32264	-2.067268259
FBgn0082582	tmod	-2.244587332
FBgn0004395	unk	-1.677130214
FBgn0036374	Spt20	-1.345498437
FBgn0021873	Gef26	-1.175199415
FBgn0025936	Eph	-1.74658924
FBgn0043070	MESK2	-2.401560063
FBgn0046704	Liprin-alpha	-1.239143941
FBgn0041092	tai	-1.211113268
FBgn0264001	bru-3	-3.880800257
FBgn0030249	CG11203	-4.60907515
FBgn0038975	Nrx-1	-4.387532053
FBgn0085447	sif	-2.447854711
FBgn0020412	JIL-1	-0.597136189
FBgn0003380	Sh	-3.809698691
FBgn0004921	Ggamma1	-0.700094808
FBgn0013334	Sap47	-1.191847851
FBgn0003721	Tm1	-1.091164695
FBgn0030758	CanA-14F	-3.472218945
FBgn0013576	l(3)82Fd	-1.73341124
FBgn0019650	toy	-2.54580416
FBgn0010352	Nc73EF	-0.234884523
FBgn0026059	Mhcl	-1.167799081
FBgn0020767	Spred	-1.771337838
FBgn0015399	kek1	-3.065766503
FBgn0263257	cngl	-3.776335026
FBgn0023388	Dap160	-1.762771978
FBgn0053113	Rtnl1	-0.846746151
FBgn0000479	dnc	-3.700151131
FBgn0004611	Plc21C	-1.872805357
FBgn0005536	Mbs	-0.238278087
FBgn0085413	CG34384	-3.758119181
FBgn0029834	CG5937	-4.721089406
FBgn0037153	olf413	-1.657780255
FBgn0022382	Pka-R2	-3.557056938
FBgn0259110	mmd	-3.562044804
FBgn0022987	qkr54B	-0.9669555
FBgn0002413	dco	-0.341654105
FBgn0000546	EcR	-1.552207991
FBgn0004435	Galpha49B	-1.558817049
FBgn0028341	l(1)G0232	-1.385663861
FBgn0003138	Ptp61F	-0.279738973
FBgn0003310	S	-1.314784962

FBgn_r5.44_FB2012_02	gene	log2FoldChange
FBgn0040153	l(1)G0469	-2.647433809
FBgn0014001	Pak	-0.794242442
FBgn0005640	Eip63E	-2.161617393
FBgn0001235	hth	-0.479016139
FBgn0011747	Ank	-0.638836731
FBgn0029814	CG15765	-3.953186037
FBgn0038659	endoA	-1.325986624
FBgn0013799	Deaf1	-2.030806002
FBgn0011305	Rsf1	-0.790122709
FBgn0035903	CG6765	-2.438922393
FBgn0042135	CG18812	-1.960358115
FBgn0000173	ben	-0.338467801
FBgn0086372	lap	-1.842446473
FBgn0263111	cac	-2.480675101
FBgn0040068	vav	-1.670178618
FBgn0039927	CG11155	-3.759997545
FBgn0259481	Mob2	-0.490524546
FBgn0015278	Pi3K68D	-1.05381341
FBgn0015754	Lis-1	-0.976425854
FBgn0038504	Sur-8	-0.893541727
FBgn0262573	orb2	-1.865151849
FBgn0033739	Dyb	-2.719876687
FBgn0004624	CaMKII	-1.612945472
FBgn0020245	ttv	-2.908366535
FBgn0259927	CG42450	-4.047510149
FBgn0000567	Eip74EF	-3.519128802
FBgn0031374	CG7337	-1.278797281
FBgn0028582	lqf	-1.71946063
FBgn0028703	Nhe3	-1.851263411
FBgn0259743	RhoGEF3	-0.056227073
FBgn0017418	ari-1	-0.951934036
FBgn0041210	HDAC4	-1.980626946
FBgn0040397	CG3655	-1.440547484
FBgn0262907	rdx	-1.093793193
FBgn0031736	CG11030	-0.64193948
FBgn0026086	Adar	-1.740081217
FBgn0023526	CG2865	-1.692654137
FBgn0261239	Hr39	-1.891986236
FBgn0037949	CG17360	-2.458628859
FBgn0016126	CaMKI	-1.540907512
FBgn0040324	Ephrin	-1.719595114
FBgn0038890	CG7956	-1.241858754
FBgn0015806	S6k	-0.244530747
FBgn0052016	CG32016	-0.986547287
FBgn0030505	NFAT	-0.851093426
FBgn0011826	Pp2B-14D	-0.689132489
FBgn0033166	Eaf	-0.521103404
FBgn0259174	Nedd4	-0.404929283
FBgn0262468	vib	-0.933036857

FBgn_r5.44_FB2012_02	gene	log2FoldChange
FBgn0086674	Tango13	-1.04151478
FBgn0031150	bves	-1.814194477
FBgn0003134	Pp1alpha-96A	-0.664475603
FBgn0024941	RSG7	-4.157700831
FBgn0035688	CG10289	-0.315665909
FBgn0030421	CG3812	-2.377422144
FBgn0011656	Mef2	-2.671724862
FBgn0263355	CG31688	-2.959309183
FBgn0264090	CG43759	-1.236617098
FBgn0030508	CG15760	-4.24623419
FBgn0260990	yata	-0.337551999
FBgn0028408	Drep-2	-3.907726068
FBgn0039928	cals	-0.956833216
FBgn0261822	Bsg	-0.230568868
FBgn0003169	put	-1.052509349
FBgn0032946	nrv3	-3.848113915
FBgn0027101	Dyrk3	-1.217927112
FBgn0003218	rdgB	-2.196094053
FBgn0031414	eys	-4.178411431
FBgn0259150	CG42265	-2.183290058
FBgn0000286	Cf2	-2.494385784
FBgn0028863	CG4587	-4.207906422
FBgn0039209	CG13624	-0.345666929
FBgn0037736	CG12950	-2.392303826
FBgn0039584	beat-VI	-4.235489885
FBgn0016076	vri	-0.51854175
FBgn0040340	TRAM	-0.490420698
FBgn0262735	Imp	-1.377652335
FBgn0030182	CG15311	-4.05970565
FBgn0000242	Bx	-2.816986948
FBgn0014467	CrebB-17A	-0.566585823
FBgn0262115	CG17683	-0.603281577
FBgn0053207	pxb	-2.485966348
FBgn0000303	Cha	-4.209347429
FBgn0017558	Pdk	-1.463680403
FBgn0005564	Shal	-3.922823436
FBgn0052333	CG32333	-4.664522653
FBgn0259225	Pde1c	-3.298928843
FBgn0024811	Crk	-0.230717099
FBgn0031897	CG13784	-2.068607482
FBgn0261703	gce	-3.820029732
FBgn0263097	Glut4EF	-3.410662656
FBgn0262509	nrm	-3.162832213
FBgn0040765	luna	-4.194384713
FBgn0012034	AcCoAS	-0.533348451
FBgn0005694	Aef1	-0.069271186
FBgn0035285	CG12025	-0.72109966
FBgn0085385	CG34356	-3.94642713
FBgn0036494	Toll-6	-3.713703149

FBgn_r5.44_FB2012_02	gene	log2FoldChange
FBgn0031116	CG1695	-4.117838059
FBgn0041004	CG17715	-0.69047726
FBgn0036446	CG9384	-0.575738876
FBgn0034304	CG5742	-1.095754331
FBgn0040206	krz	-0.375601285
FBgn0086779	step	-0.698158676
FBgn0083963	CG34127	-3.715799753
FBgn0029504	CHES-1-like	-1.338973743
FBgn0259171	Pde9	-2.115469248
FBgn0000711	flw	-0.010534345
FBgn0020762	Atet	-1.108103345
FBgn0261262	CG42613	-3.975891306
FBgn0003429	slo	-3.730681496
FBgn0261549	rdgA	-2.909251277
FBgn0030090	fend	-1.76295911
FBgn0038740	CG4562	-4.528163665
FBgn0037321	CG1172	-0.520092342
FBgn0262866	S6kII	-0.293438856
FBgn0031885	Mnn1	-0.972805707
FBgn0042696	NfI	-3.502128608
FBgn0085421	Epac	-4.477338706
FBgn0259111	Ndae1	-3.96482154
FBgn0053481	dpr7	-3.722921472
FBgn0010105	comm	-3.481016808
FBgn0033958	CG12858	-3.46098772
FBgn0086677	jeb	-3.719452058
FBgn0032943	Tsp39D	-1.436837197
FBgn0037212	nAcRα-80B	-3.164868024
FBgn0085390	Dgk	-4.768482403
FBgn0261285	Ppcs	-0.668376034
FBgn0036844	Mkp3	-2.856203525
FBgn0036789	AlCR2	-4.421415431
FBgn0042185	CG18769	-1.411742305
FBgn0037521	CG2993	-3.72038161
FBgn0028369	kirre	-3.561321664
FBgn0004882	orb	-0.82741122
FBgn0052850	CG32850	-1.378746587
FBgn0263775	Hr4	-3.057529945
FBgn0016694	Pdp1	-1.459669094
FBgn0263353	CG11000	-2.951762383
FBgn0261569	CG42683	-3.344723976
FBgn0028433	Ggamma30A	-3.705079184
FBgn0011206	bol	-1.539637776
FBgn0263220	Hk	-3.484242783
FBgn0035756	unc-13-4A	-4.256453789
FBgn0010263	Rbp9	-2.161343384
FBgn0000448	Hr46	-3.053663751
FBgn0259677	CG42346	-3.332851319
FBgn0004635	rho	-3.593094173

FBgn_r5.44_FB2012_02	gene	log2FoldChange
FBgn0261548	CG42666	-2.942177069
FBgn0013995	Calx	-2.944873622
FBgn0028397	Tob	-4.01712325
FBgn0031258	CG4297	-4.336322397
FBgn0019985	mGluRA	-2.83977952
FBgn0032901	sky	-0.63519501
FBgn0034312	CG10916	-1.510849351
FBgn0051324	CG31324	-3.144314175
FBgn0083228	Frq2	-3.441132269
FBgn0051687	CG31687	-0.66472818
FBgn0023441	fus	-2.023386866
FBgn0004865	Eip78C	-2.129458819
FBgn0037213	CG12581	-1.821464577
FBgn0032502	CG15639	-3.442956459
FBgn0001325	Kr	-3.680002418
FBgn0259219	CG42319	-0.094775363

Table containing 40 genes with an extended 3'UTR that are expressed higher in NBs and 357 that are up-regulated in neurons. 3'UTR extension is not NB or neuron specific.